

INTERNAL CORROSION DIRECT ASSESSMENT OF GAS TRANSMISSION AND STORAGE LINES

Final Report 18.06484-200

Prepared for

Research and Special Programs Administration
Office of Pipeline Safety (OPS)
Contract No. DTRS5603T0001

Prepared by

Narasi Sridhar, Ben Thacker, Amit Kale, and Chris Waldhart
Southwest Research Institute®

Oliver Moghissi and Deanna Burwell
CC Technologies

December 28, 2004



SOUTHWEST RESEARCH INSTITUTE®
SAN ANTONIO HOUSTON WASHINGTON, DC

INTERNAL CORROSION DIRECT ASSESSMENT OF GAS TRANSMISSION AND STORAGE LINES

Final Report 18.06484-200

Prepared for

Research and Special Programs Administration
Office of Pipeline Safety (OPS)
Contract No. DTRS5603T0001

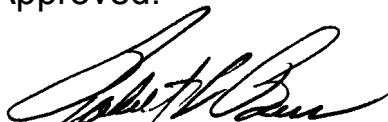
Prepared by

Narasi Sridhar, Ben Thacker, Amit Kale, and Chris Waldhart
Southwest Research Institute®

Oliver Moghissi and Deanna Burwell
CC Technologies

December 28, 2004

Approved:



Dr. Robert L. Bass, Vice President
Mechanical and Materials Engineering Division

TABLE OF CONTENTS

	<i>Page</i>
ACKNOWLEDGMENTS	xi
EXECUTIVE SUMMARY	xii
1.0 DRY GAS ICDA VALIDATION	1-1
1.1 Introduction.....	1-1
1.2 Validation Categories.....	1-2
1.3 Data Uncertainties.....	1-2
1.3.1 Source Map Uncertainties.....	1-3
1.3.2 Sampling and Measurement Error	1-3
1.3.3 Interpolation Process.....	1-3
1.3.4 In-Line Inspection (ILI)	1-4
1.4 ICDA Validation – Pipeline A.....	1-4
1.4.1 Summary	1-4
1.4.2 Step 1: Pre-Assessment (Pipeline A)	1-7
1.4.3 Step 2: Calculations and Initial ICDA Site Selections (Pipeline A).....	1-9
1.4.4 Step 3: Detailed Examination, Additional Site Selections (Pipeline A) ..	1-12
1.4.5 Step 4: Post-Assessment (Pipeline A).....	1-13
1.5 ICDA Validation – Pipeline B	1-13
1.5.1 Summary	1-13
1.5.2 Step 1: Pre-Assessment (Pipeline B)	1-15
1.5.3 Step 2: Calculations and Initial ICDA Site Selections (Pipeline B)	1-15
1.5.4 Step 3: Detailed Examination, Additional Site Selections (Pipeline B) ..	1-16
1.5.5 Step 4: Post-Assessment (Pipeline B).....	1-17
1.6 ICDA Validation – Pipeline C	1-18
1.6.1 Summary	1-18
1.6.2 Step 1: Pre-Assessment (Pipeline C)	1-21
1.6.3 Step 2: Calculations and Initial ICDA Site Selections (Pipeline C)	1-22
1.6.4 Step 3: Detailed Examination, Additional Site Selections (Pipeline C) ..	1-29
1.6.5 Step 4: Post-Assessment (Pipeline C).....	1-31
1.7 Pipeline D.....	1-39
1.7.1 Summary	1-39
1.7.2 Step 1: Pre-Assessment (Pipeline D)	1-41
1.7.3 Step 2: Calculations and Initial ICDA Site Selections (Pipeline D).....	1-43
1.7.4 Step 3: Detailed Examination, Additional Site Selections (Pipeline D) ..	1-46
1.7.5 Step 4: Post-Assessment (Pipeline D).....	1-46
2.0 WET GAS ICDA METHODOLOGY	2-1
2.1 Proposed Approach.....	2-1
2.2 Other Factors Affecting Corrosion	2-4
2.2.1 Liquid Hydrocarbons	2-4
2.2.2 Corrosion Inhibition.....	2-4

TABLE OF CONTENTS (Continued)

	<i>Page</i>
2.2.3 Bacteria and Biocides	2-5
2.2.4 Solids.....	2-5
2.2.5 Other Products	2-6
2.3 Example Application with Comparison to ILI Data	2-6
2.3.1 Pre-Assessment	2-6
2.3.2 Indirect Examination.....	2-9
2.3.3 Direct Examination and Comparison.....	2-11
2.3.4 Post-Assessment	2-14
 3.0 PROBABILISTIC ANALYSIS OF ICDA LOCATIONS	 3-1
3.1 Introduction.....	3-1
3.2 Sources of Uncertainty.....	3-2
3.2.1 Flow Modeling Uncertainties	3-2
3.3 Proposed Methodology	3-3
3.3.1 Water Accumulation	3-3
3.3.2 Corrosion Rate Model.....	3-4
3.4 Probabilistic Model.....	3-6
3.4.1 Corrosion Damage	3-6
3.5 Input Uncertainties.....	3-7
3.6 Mapping Uncertainty	3-7
3.7 Inspection Updating	3-8
3.7.1 Example 1: Determination of Critical Location Prior to Inspections	3-9
3.7.2 Example 2: Updating Corrosion Modeling with Inspection Data	3-11
3.8 Sensitivity Analysis	3-13
3.9 Discussion	3-16
3.9.1 Multiphase Fluid Dynamics Calculation	3-17
 4.0 CONCLUSIONS AND RECOMMENDATIONS	 4-1
 5.0 REFERENCES	 5-1

LIST OF FIGURES

<i>Figure</i>	<i>Page</i>
1-1 Pipeline A – Set I of IV. Combined inclination and elevation profile with anomalies and critical angles shown (1 ft = 0.305 m, 1 mi. = 1.609 km).....	1-10
1-2 Pipeline A – Set II of IV. Combined inclination and elevation profile with anomalies and critical angles shown (1 ft = 0.305 m, 1 mi. = 1.609 km).....	1-10
1-3 Pipeline A – Set III of IV. Combined inclination and elevation profile with anomalies and critical angles shown (1 ft = 0.305 m, 1 mi. = 1.609 km).....	1-11
1-4 Pipeline A – Set IV of IV. Combined inclination and elevation profile with anomalies and critical angles shown (1 ft = 0.305 m, 1 mi. = 1.609 km).....	1-11
1-5 Pipeline B. Combined inclination and elevation profile with anomalies and critical angles shown (1 ft = 0.305 m, 1 mi. = 1.609 km). Note that periods of stagnant flow suggests a range of critical angles extending from zero.....	1-14
1-6 Pipeline C. Anomaly orientation vs. 1) % depth of wall thickness, 2) anomaly length.....	1-21
1-7 Pipeline C with GIS elevation data. Region 1: ICDA predictions versus ILI anomalies.	1-24
1-8 Pipeline C with USGS elevation data. Region 1: ICDA predictions versus ILI anomalies. SLC indicates ILI internal anomalies oriented on the sides of the pipeline, TLC on the top, and BLC on the bottom.	1-24
1-9 Pipeline C with GIS elevation data. Region 2: ICDA predictions versus ILI anomalies.	1-25
1-10 Pipeline C with USGS elevation data. Region 2: ICDA predictions versus ILI anomalies. SLC indicates ILI internal anomalies oriented on the sides of the pipeline, TLC on the top, and BLC on the bottom.	1-25
1-11 Pipeline C with GIS elevation data. Region 3: ICDA predictions versus ILI anomalies.	1-26
1-12 Pipeline C with USGS elevation data. Region 3: ICDA predictions versus ILI anomalies. SLC indicates ILI internal anomalies oriented on the sides of the pipeline, TLC on the top, and BLC on the bottom.	1-26
1-13 Pipeline C with GIS elevation data. Region 4: ICDA predictions versus ILI anomalies.	1-27

LIST OF FIGURES (Continued)

<i>Figure</i>	<i>Page</i>
1-14 Pipeline C with USGS elevation data. Region 4: ICDA predictions versus ILI anomalies. SLC indicates ILI internal anomalies oriented on the sides of the pipeline, TLC on the top, and BLC on the bottom.	1-27
1-15 Pipeline C. GIS resurvey, Region 1.	1-28
1-16 Pipeline C. GIS resurvey, Region 2.	1-28
1-17 Pipeline C. GIS resurvey, Region 4.	1-29
1-18 a (left), b (top right), and c (bottom right). Pipeline C. MP 0.69: Actual 1st inclination greater than the critical inclination angle in Region 1. Site is a false creek crossing. This angle was found on a walk of the line and was not identified in either USGS topographical data or the GIS surveys. Section inspected by UT: Low point to 45 degrees inclination, as shown. Arrows indicate direction of gas flow in Region 1.	1-32
1-19 Pipeline C. MP 0.69: The actual 1 st inclination greater than the critical inclination angle in Region 1. View of the excavation site after refilling (gravel covers excavation site).	1-34
1-20 Pipeline C. MP 1.10 Double creek crossing: Second inclination greater than the critical inclination angle in Region 1 (in USGS and GIS analyses of Pipeline C this is considered the first because MP 0.69 was missed). It is thought that there is a single low point under the island at center, which was inaccessible. Underneath the island is also where the ILI internal anomalies identified in this area are thought to be located. The excavation was performed on the incline on the downstream side after the second creek, as shown. Arrows indicate direction of gas flow in Region 1.	1-35
1-21 (left). Pipeline C. MP 1.10: From island: close-up view of excavation site after the second creek crossing in Region 1; above and to the left of drainage pipe; gravel patch marks the spot. Excavation site is downstream of low point. It is also downstream of MP 1.10 ILI internal anomalies, which were thought to be associated with the low point (underneath the island between the two creeks in a difficult to access location). Arrow indicates direction of gas flow in Region 1.	1-36
1-22 (right) Pipeline C. MP 1.10: Sketch of likely pipeline profile under double creek crossing. Arrow indicates Region 1 gas flow direction.	1-36

LIST OF FIGURES (Continued)

<i>Figure</i>	<i>Page</i>
1-23 Pipeline C. MP 1.2: Top left and right: Bell hole further downstream on the incline after the first location predicted using USGS and GIS data; bottom part of this dig location is at a bend to greater inclination angle. Arrows indicate direction of gas flow in Region 1. Bottom left: Pipeline C. MP 1.2: Sketch of pipeline profile. Arrow indicates Region 1 gas flow direction.....	1-37
1-24 Pipeline C. MP 1.2: Close ups of the two UT locations shown in Figure 17G. Upper location UT'd is shown on the left. Lower location is on the right. Field bend from gradual to steeper inclination can be seen at UT location in the right-hand picture. Arrows indicate Region 1 gas flow direction.	1-37
1-25 Pipeline C. MP 5.923: Location not predicted by ICDA dry gas model. Several ILI anomalies associated with this location. Direct examination and inspection revealed 10% depth of wall thickness internal anomalies found along the bottom of the line via ultrasonic transmission. Arrows indicate Region 1 gas flow direction. Lower left: Pipeline C. MP 5.923: Sketch of pipeline profile. Arrows indicates Region 1 gas flow direction.	1-38
1-26 Pipeline D. ICDA regions based in inlet locations, uni-directional flow.	1-42
1-27 Pipeline D. Regions 1 and 2: ICDA predictions versus ILI anomalies.....	1-44
1-28 Pipeline D. Regions 3, 4, 5, 6, and 7: ICDA predictions versus ILI anomalies. Note location of historic leak at MP 9.5.	1-44
1-29 Pipeline D. Regions 8, 9, and 10: ICDA predictions versus ILI anomalies. ...	1-45
1-30 Pipeline D. Region 11: ICDA predictions versus ILI anomalies.....	1-45
2-1 Flow regimes expected in west gas systems include stratified, slug, and annular flow.	2-1
2-2 Example flow regime map for 24-inch I.D. horizontal pipe after Taitel and Dukler (1976).....	2-2
2-3 A schematic approach to classifying segments of a pipeline according to flow regimes.....	2-3
2-4 A simplified flow chart to classifying flow regimes.....	2-3

LIST OF FIGURES (Continued)

<i>Figure</i>	<i>Page</i>
2-5 Elevation profile with regions defined by well line inputs. Green triangles at 1.00 wall thickness location are primary WG-ICDA indications. Triangles at 0.90 wall thickness location are secondary indications.	2-10
2-6 Trunk line alpha is divided into 10 regions (5 each for gas injection and withdrawal). ILI anomalies (>20%) are plotted by size according to the right hand axis. First priority ICDA indications are marked at 100% wall thickness (i.e., '1'), and second priority are marked at 0.8.....	2-12
2-7 Cutout of trunk line alpha at MP 0.456.....	2-13
2-8 Deposits on pipe at MP 0.456. Top section of pipe on left hand photo is top-of-pipe.....	2-13
2-9 Cleaned pipe at MP 0.456. Top section of pipe on left hand photo is top-of-pipe.....	2-13
2-10 Comparison of ILI internal corrosion anomalies with actual examination of the pipe surface. ILI anomaly depth of zero indications that internal corrosion was not identified.....	2-14
3-1 OLGA-S calculations of water hold-up fraction as a function of different water loading (as superficial water velocity) and pipe inclination angles.....	3-3
3-2 Uncertainty in inclination and critical angle.....	3-6
3-3 Probability of water formation along pipe length with highest probability observed at location 971.	3-10
3-4 Probability of Corrosion depth exceeding critical depth along pipe length assuming water is present at all locations.	3-10
3-5 Total probability of corrosion exceeding critical depth along pipe length.	3-11
3-6 Sensitivity of the calculated probability of water hold-up given all other uncertainties in the parameters to the mean value of gas pressure.	3-14
3-7 Sensitivity of the calculated probability of water hold-up given all other uncertainties in the parameters to the mean value of gas temperature.	3-15

LIST OF FIGURES (Continued)

<i>Figure</i>	<i>Page</i>
3-8 Sensitivity of calculated probability of water holdup to standard deviation in pressure (i.e., width of assumed pressure distribution) given all other uncertainties.	3-15
3-9 Sensitivity of the calculated probability of water hold-up given all other uncertainties in the parameters to the mean value of pipe angle.	3-16
3-10 The simplified pipe segment used to perform detailed fluid dynamics calculation of water flow.....	3-17
3-11 Liquid water buildup on the bottom 10 percent of pipe cross section in the upslope from the water and gas entry point indicating that water location point a significant distance from the bottom of a critical angle.....	3-18

LIST OF TABLES

<i>Table</i>		<i>Page</i>
1-1	Criteria For Inclusion In ICDA Of Dry Gas Pipelines Process Validation ..	1-2
1-2	Pipeline A: Flow Rates and Critical Angles (using Low Pressure, 500 Psi = 3.45 MPa).....	1-5
1-3	Pipeline A: ICDA Regions.....	1-5
1-4	Summary: Results for Pipelines A, B, C, and D	1-6
1-5	Pipeline A: ILI Tool-Identified Internal Anomalies – Correlation with Sites Selected by ICDA Method	1-6
1-6	Pipeline A: Percentage of Tool-Identified Internal Anomalies Predicted by ICDA	1-7
1-7	Pre-Assessment of Feasibility: Pipelines A, B, C, And D	1-8
1-8	Pipeline A: Sites Selected for Detailed Examination by The ICDA Method	1-12
1-9	Pipeline A: Estimated Horizontal Uncertainties; Provided in Miles (Km)..	1-14
1-10	Pipeline B: Percentage of Tool-Identified 50-100% Depth Internal Anomalies Predicted by Dry Gas ICDA	1-15
1-11	Pipeline B: Flow Rates and Critical Angles (Using Low Pressure, 500 Psi = 3.5 MPa).....	1-16
1-12	Pipeline B: Sites Selected for Detailed Examination by The ICDA Method	1-16
1-13	Pipeline B: 50-100% Depth Inspection Tool-Identified Anomalies – Comparison with Sites Identified by ICDA Method	1-17
1-14	Pipeline B: Estimated Horizontal Uncertainties; Provided in Miles (Km)..	1-18
1-15	Pipeline C <i>Using Hand-Held GIS Field Data</i> : Percentage of Tool-Identified Internal Anomalies Predicted by ICDA, by Percentage Depth	1-20
1-16	Pipeline C <i>Using Hand-Held GIS Field Data</i> : Percentage of Tool-Identified Internal Anomalies Predicted by ICDA, by Length	1-20

LIST OF TABLES (Continued)

<i>Table</i>	<i>Page</i>
1-17 Pipeline C Using Hand-Held GIS Field Data: Percentage of Tool-Identified Internal Anomaly Groups Predicted by ICDA, by Percentage Depth	1-20
1-18 Pipeline C Using Computerized USGS Data: Percentage of Tool Identified Internal Anomalies Predicted by ICDA, by Percentage Depth	1-20
1-19 Pipeline C Using Computerized USGS Data: Percentage of Tool-Identified Internal Anomalies Predicted by ICDA, by Length	1-20
1-20 Pipeline C Using Computerized USGS Data: Percentage of Tool-Identified Internal Anomaly Groups Predicted by ICDA, by Percentage Depth.....	1-21
1-21 Pipeline C Using Computerized USGS Data: Percentage of Tool-Identified Internal Anomaly Groups Predicted by ICDA, by Anomaly Orientation (4-To8 O-Clock BLC; 10 To-2 O-Clock TLC; 2-To-4 And 8-To-10 O-Clock SLC)	1-22
1-22 Pipeline C: Region Definitions	1-22
1-23 Pipeline C: Flow Rates.....	1-23
1-24 Pipeline C: Calculated Critical Angles	1-23
1-25 Pipeline C Using Hand-Held GIS Field Data: Sites Selected For Detailed Examination By The ICDA Method	1-30
1-26 Pipeline C Using Computerized USGS Data: Sites Selected for Detailed Examination by The ICDA Method.....	1-31
1-27 Pipeline C: ILI Tool Anomalies – Correlation with Sites Selected by ICDA Method	1-33
1-28 Pipeline C: Estimated Horizontal Uncertainties	1-39
1-29 Pipeline D: Summary of Results A) for Anomalies with >30% Percentage Depth of Wall Thickness and B) for Anomalies of > 1 Ft (0.305 M) Length	1-40
1-30 Pipeline D: Percentage of Tool-Identified Internal Anomalies Predicted by ICDA, by Percentage Depth of Wall Thickness	1-40

LIST OF TABLES (Continued)

<i>Table</i>	<i>Page</i>
1-31 Pipeline D: Percentage of Tool-Identified Internal Anomalies Predicted by ICDA, by Anomaly Length (1. >30% Depth Of Wall Thickness, and 2. >15% Depth Internal Anomalies Considered)	1-41
1-32 Pipeline D: 2001-2002 Gas Analysis Statistics.....	1-41
1-33 Pipeline D: Maximum Flow Rates and Critical Angles.....	1-43
1-34 Pipeline D: Sites Selected for Detailed Examination by The ICDA Method	1-46
1-35 Pipeline D: ILI Tool Anomalies of > 30% Depth of Wall Thickness – Correlation with Sites Selected by ICDA Method.....	1-47
1-36 Pipeline D: Roughly Estimated Horizontal Uncertainties	1-48
2-1 WG-ICDA Region Definition.....	2-7
2-2 First Priority Sites as Determined by The WG-ICDA Method. STF is Stratified Flow, and SLG is Slug Flow	2-7
2-3 Recent Pigging History	2-8
2-4 First Priority Sites as Determined by The WG-ICDA Method. STF is Stratified Flow, and SLG is Slug Flow	2-10
2-5 Locations of Excavation Based on ILI Anomalies. Locations where No Internal Diameter Anomalies were Identified were Excavation for Other Reasons (e.g., External Diameter Anomalies). Locations with Internal Corrosion were Cut Out and Examined	2-14
3-1 Typical Wet Gas Pipeline Flow Parameters.....	3-4
3-2 Typical Wet Gas Pipeline Corrosion Growth Parameters.....	3-7
3-3 Updating of Model Weights Given Assumed Observations Corresponding to Input Component Models	3-12
3-4 Inspection Locations Along Pipeline	3-13

ACKNOWLEDGMENTS

The authors thank the Office of Pipeline Safety, Pipeline Research Council International, Interstate Natural Gas Association of America, Duke Energy, Southern California Gas, Gulf South Pipeline Company, LP, Dominion Transmission Company, and Texas Gas Transmission, LLC, for their support. The authors also thank Lori Salas for her assistance in preparing the report. Neither CC Technologies, Southwest Research Institute[®], members of these companies, nor any person acting on their behalf:

- a. Makes any warranty or representation, expressed or implied, with respect to the accuracy, completeness, or usefulness of the information contained in this paper, or that the use of any apparatus, methods, or process disclosed in this paper may not infringe upon privately owned rights; or
- b. Assumes any liability with respect to the use of, or for damages resulting from the use of, any information, apparatus, method, or process disclosed in this paper.

EXECUTIVE SUMMARY

The total cost of corrosion of all pipelines through internal corrosion has been estimated to range from US\$ 50 million to US\$ 100 million per year. Mechanical and geometrical constraints preclude the use of inline inspection (pigging) in a large portion of pipelines. Further, internal corrosion is often difficult to detect because pipe interiors are not easily accessible. Tools for performing detailed examination of pipe corrosion require excavation and are not economical to perform on the entire pipeline. Therefore, it is necessary to identify likely locations of internal corrosion in pipelines, so that the detailed examination methods can be deployed more effectively. An Internal Corrosion Direct Assessment (ICDA) method was previously developed. The method consists of four iterative steps: (i) obtain operating, geographical, and historical information regarding a pipeline and determine whether ICDA can be performed for this pipeline, (ii) use this information to perform flow modeling to obtain critical pipeline inclination angles for water accumulation, and compare the critical angles to the actual pipeline inclination profile to determine the locations where water or other corrosive electrolytes are likely to accumulate, (iii) perform detailed examinations of these locations, and (iv) use the results of the detailed examinations to determine further assessment. The method is presently applicable to dry gas pipelines.

The objectives of the current project were to validate the method using field data and develop or extend the method to wet gas lines using a combination of probabilistic method and flow modeling.

Validation of The Dry Gas ICDA Method

Validation of the Internal Corrosion Direct Assessment (ICDA) methodology for dry gas lines was performed using in-line inspection data from four pipelines. Analyses were performed on data from on-land surveys using Global Positioning System (GPS) instrumentation and incorporated in Geographic Information Systems (GIS) and United States Geological Survey (USGS) three-dimensional positioning data. In the case of USGS data, constant pipeline depth of cover was assumed, unless specific information of pipeline depth (e.g., using pipeline current mapper or other tools) was available.

USGS topographical data were used in analyzing the first pipeline, Pipeline A. Eighty-five percent of internal wall loss indications detected by ILI coincided with ICDA locations. Another 5 percent of the sites may have been identified by ICDA had pipe elevation profiles been known more accurately, including the presence of road or stream crossings not shown on elevation maps. The location of a historic leak was also predicted. In the second pipeline, Pipeline B, which utilized field GIS measurements, ICDA correlated with 78 percent of ILI-indicated internal anomalies having >50% depth of wall thickness. This pipe was extensively corroded.

The third pipeline, Pipeline C, was known to have corrosion at the top of the pipeline in contradiction to ICDA model premises. Some correlation between ICDA and ILI was still shown. Pipeline C was analyzed two ways: 1) using computerized USGS topographical data, and 2) using GIS field measured vertical and horizontal positioning data. Although the GIS data

used actual depth of cover information in the elevation profile, three problems were encountered during this particular GIS survey: (1) tool resolution was not sufficient for dry gas ICDA at some locations, (2) during the line walk some significant inclinations were overlooked, and (3) the pipeline locator could not detect pipe at certain locations because the pipe was buried deep (presumed to be greater than 20 feet in one case). The USGS topographical map missed some engineered inclinations where pipeline elevation change would not have correlated with surface features. Fifty-three percent of individual internal anomalies with greater than 30 percent depth of wall thickness were predicted for Pipeline C using the computerized USGS data, while only 16 percent of the internal anomalies were predicted using the GIS field data. In addition to the USGS and GIS analyses, direct examinations (digs and ultrasonic testing) were performed on Pipeline C to obtain some information about ILI call-outs and distance uncertainties and to develop an understanding of practical challenges in applying dry gas ICDA.

The fourth pipeline, Pipeline D, utilized USGS data for pipeline elevation profile. ICDA predicted corrosion sites correlated with 87 percent of ILI-indicated internal anomalies with greater than 30 percent depth of wall thickness. The location of a known historic internal corrosion leak was also predicted using ICDA on Pipeline D.

Standardization of The Dry Gas ICDA Method

The dry gas ICDA method is being standardized as NACE RP 0104. The standard will be issued in 2005. At present, most of the negatives have been resolved. Additional flow calculations were performed to satisfy one negative and extend the method's applicability to lower pressure distribution systems.

Probabilistic Analysis of Internal Corrosion

Although the current validation work has shown that the approach used for dry gas ICDA is appropriate, several issues have been identified. Resolving these issues would greatly increase the confidence in the application of ICDA. The uncertainties in the ICDA method include:

1. Uncertainties in pipeline elevation profiles: This variable has proven to be a critical factor in the success of ICDA. Improvements in the resolution of pipeline elevation measurements and data alignment are needed. For example, low-resolution GPS surveys are not sufficient for ICDA purposes, although they may suffice for pipeline location. Accurate records of pipeline layout would also identify "hidden" elevation changes that do not correlate with surface topographical features.
2. Uncertainties in detailed examination methods: Uncertainties in ILI or other non-destructive examination techniques need to be considered. These include uncertainties in position of ILI tools as well as the indication type (corrosion or other defects)
3. Uncertainties in flow modeling: In addition to uncertainties in flow parameters (i.e. flow rates, pressures, flow direction, etc.), there are model uncertainties. The current flow modeling assumes that a sharp transition in flow regime (and therefore water hold-up) occurs at certain values of Froude number. Such an assumption may be

valid only for low input liquid volumes. Large volumes of input liquid may smear such a sharp transition.

4. Uncertainties in locating detailed examination along a pipe inclination: After identifying a site of potential water accumulation, it is necessary to determine how far from the lowest elevation to examine the pipe. The simplified flow modeling used to locate the water accumulation site is not adequate to determine the length of pipe to be examined. Detailed computation fluid dynamics calculations were performed using FLUENT to examine this issue.
5. Uncertainties in corrosion models: Many corrosion models exist to predict the corrosion rate as a function of gas and water chemistry.

One method of quantifying the effect of these uncertainties is to conduct a probabilistic assessment of water hold-up locations. Such a probabilistic assessment may help prioritize locations for detailed examination. An example of a probabilistic ICDA assessment is described in this report. This methodology can be used for both the dry and wet gas ICDA. The probabilistic model also enables one to conduct sensitivity analyses. The probabilistic model has been programmed in to a spreadsheet using an efficient algorithm for reliability estimation.

Wet Gas ICDA Methodology

Results of an example WG-ICDA application and comparison to ILI data indicated that the prioritization of corrosion likelihood was consistent with the damage found by ILI and inspections at excavation sites.

- The dominant factor used for internal corrosion prioritization was the onset of slugging (i.e., liquid accumulation) at the bottom of a significant incline. Other factors were either not significant or could not be determined by historical data.
- The WG-ICDA process identified that extensive internal corrosion existed in the pipeline.
- Locations predicted by WG-ICDA to have the highest likelihood of corrosion were verified by ILI anomalies and/or inspections at excavation sites. In one case, a location of significant corrosion was identified by excavation and inspection despite being missed by ILI.
- Quantitative comparison of WG-ICDA performance and ILI was not possible because of large uncertainties in both the WG-ICDA influencing factors and the ILI anomalies.

Recommendations

- Although the principle behind the ICDA method has been shown to be valid, many uncertainties remain in its implementation. One of the greatest uncertainties is the pipeline elevation profile. ICDA requires more accurate GIS data and pipe depth information.

- The probabilistic aspects of the ICDA should be pursued further because of the great number of uncertainties in the input parameters and models. The WG-ICDA method has shown promise, but needs to be further developed and validated. Here too, the probabilistic assessment should be combined with the basic method to quantitatively account for the uncertainties and discrepancies between prediction and observation.
- Detailed examination of ICDA locations requires knowledge of length of pipe to be examined. Detailed flow modeling that would predict the extent of water hold up in any ICDA regions is recommended. Results from such flow modeling should then be abstracted into a more simplified estimation.

1.0 DRY GAS ICDA VALIDATION

1.1 Introduction

Mechanical and geometrical constraints preclude the use of inline inspection in a large portion of pipelines. Further, internal corrosion is often difficult to detect because pipe interiors are not easily accessible. Direct examination methods for detecting pipe wall thickness changes due to internal corrosion, such as ultrasonic transmission (UT) and radiography, exist. However, these require excavation and cleaning of the pipe surface prior to measurements, making a full-line inspection impractical. Corrosion monitoring tools, such as Field Signature Method (FSM) probe, are seeing increasing use, but these require excavation of the pipe and installation in location of suspected internal corrosion. Due to these limitations, it was necessary to utilize a new approach to identify likely locations of internal corrosion in pipelines, so that these direct examination methods can be more effectively deployed.

An Internal Corrosion Direct Assessment (ICDA) method was previously developed for dry gas pipelines that may experience short term upsets of water (or other electrolyte). ICDA is a four-step process based on the principle that for dry gas pipelines liquid collects at local low points in the pipeline (i.e., upstream of inclinations), and that it is at these locations that internal corrosion is most likely to occur. Detailed examinations of locations along certain pipelines where an electrolyte (such as water) first accumulates therefore provides information about the remaining length of pipe (Moghissi et al., 2002a,b).

The ICDA process consists of: 1) Pre-Assessment, 2) Indirect Inspection, 3) Detailed Examination, and 4) Post-Assessment. In the Pre-Assessment step, historical data is collected, the feasibility of applying ICDA to a given pipeline is determined, and ICDA regions on the pipe are defined. Calculations of the inclination profile and flow modeling for liquid hold-up are performed and integrated to select sites where electrolyte is expected to accumulate in the Indirect Inspection step. The flow modeling identifies the point past which liquid carry-over is not expected, termed the critical angle. During the Detailed Examination step, pipe at selected sites is excavated and examined for internal corrosion. The presence of significant internal corrosion triggers additional sites for examination. If no corrosion is identified it may be concluded that downstream corrosion is unlikely and can be confirmed by two additional digs. The Post-Assessment step analyzes data collected in the previous steps to assess the effectiveness of the ICDA process and to determine reassessment intervals (Moghissi et al., 2003). The 4-step process of ICDA is expounded in the draft NACE 'Internal Corrosion Direct Assessment (ICDA) Methodology for Pipelines Carrying Normally Dry Natural Gas' Recommended Procedure (NACE International, 2005) still under review at the time this paper was written. ICDA process may not be practical for some pipelines even when they meet the other requirements for ICDA under the pre-assessment step. In cases where there are closely spaced liquid inputs or a large number of critical inclination changes, the ICDA procedure would call for numerous excavations and inspections. The economics of such a large number of excavation and the associated permitting difficulties may render the application of ICDA impractical for these cases.

This chapter presents the results of field validation of the dry-gas ICDA methodology. The validation compares ICDA process results with in-line inspection (ILI) data for four pipelines. One limitation for implementation of ICDA is accuracy in the elevation profile. For the purpose of validation, the area of excavation was made wider than normally would be practical. This is, in part, because of the uncertainty with aligning elevation data with ILI location. For ICDA implementation, the area of excavation is expected to be smaller, and improvements in locating and elevation measurements are expected to result in greater confidence for selecting excavation locations.

In a typical model validation, the model predictions are compared to experimental observations for determining the accuracy of the model. The ICDA is a process, which incorporates a flow model. Therefore, validation does not merely involve comparison of the predictions of the flow model with observed water accumulation sites. The ICDA process includes identification of initial sites most likely to accumulate water and additional sites upstream and downstream of these initial sites. The validation compares all these locations identified by the ICDA process against observations by ILI and other examination methods.

1.2 Validation Categories

Each pipeline example was assigned a rank according to the extensiveness of provided operating history and the availability of ILI and detailed examination data. The purpose of the ranking was to screen pipelines for inclusion in the ICDA Process Validation. Only pipelines that achieved rankings of I or II were included in the validation. The criteria for inclusion of pipelines in the validation are shown in Table 1-1.

Table 1-1. Criteria For Inclusion In ICDA Of Dry Gas Pipelines Process Validation

Rank	Category	ILI	Operating History	Detailed Examination	Confidence in Validation
I	Ideal	Applicable & Recent	Yes	Yes	High
II	Good	Any Time Period	Yes	No	Moderate
III	Acceptable	No	Some	Some	Fair
IV	Poor	No	Some	No	Poor
V	Unacceptable	No	No	No	None

1.3 Data Uncertainties

It is important to bear in mind when interpreting and selecting sites based on the calculated inclination profile that some uncertainties exist. For each pipeline in the ICDA Process Validation, one of two resources was used to determine the pipeline elevation and inclination profiles: 1) USGS maps, or 2) GPS measurements incorporated in a GIS database. USGS maps and GPS data are used to find elevations and distances along pipeline lengths. USGS maps may be employed in hard copy or computer file form, depending on what

is available. GPS measurements are performed by individual pipeline operators. Pipe depth measurements may be used in combination with GPS to augment the analysis. Use of these resources and the resources themselves include some uncertainties. These uncertainties arise from three main sources: 1) uncertainty from the source map (USGS only), 2) sampling and measurement error, and 3) the interpolation process. A fourth uncertainty also exists, unique to the ICDA Process Validation. As inclination profiles are compared with ILI data in the validation, problems of alignment with and accuracy of the in-line inspection data must also be considered.

1.3.1 Source Map Uncertainties

USGS maps used in this survey utilized The United States National Map Accuracy Standards (NMAS). The NMAS prescribe bounds for horizontal and vertical accuracy. No more than ten percent of horizontal (distance) data points should be in error by more than ~forty feet on USGS maps used in the ICDA validation of the two pipelines discussed in this paper. NMAS standards (NMAS, 1947) also state that no greater than ten percent of vertical (elevation) data points should be in error by “more than one-half the contour interval.” The maximum contour interval of the USGS maps used for this paper is ten feet.

1.3.2 Sampling and Measurement Error

The most significant GPS measurement considerations are instrument and operator-generated uncertainties. The instrument itself may not have adequate accuracy and precision to provide meaningful information for ICDA. Additionally, if GPS sampling is not sufficient to capture all significant inclinations, ICDA is not expected to be successful. Another source of vertical uncertainty is the assumption of constant pipe depth. USGS maps and GPS surface measurements that are not supplemented by pipe depth measurements may not represent the true inclination profiles. Particularly at features (i.e., road crossings, gas inlets/ outlets), pipe depth is not always constant. In this regard, the External Corrosion Direct Assessment (ECDA) data may in some cases permit better vertical pipe information (NACE International, 2003). Lastly, gross errors may occur with the manual measurement and transfer of information from GPS instruments or from USGS maps on which the pipelines have been traced to data files for analysis.

1.3.3 The Interpolation Process

One source of interpolation process uncertainty in using hard-copies of USGS maps comes from the fact that the elevation contour interval is set at a certain value (i.e., 3 m), and fine contours in-between are not captured. Likewise, in using GIS sufficient data must be collected, with adequate precision and accuracy, to discern (by interpolation between data points) inclination angles of importance to ICDA. It is conceivable that information from finer contours may reveal significant inclinations that would not appear on typical USGS maps or result from standard GIS surveys. An advantage of computerized USGS maps is that finer changes in

elevation and distance may be detected. Accordingly, a careful GIS survey, using the appropriate instruments and executed with an understanding of requirements of ICDA in mind, will resolve important inclination angles that would otherwise be missed.

Another type of interpolation process uncertainty occurs when elevations and distances are read from USGS maps upon which pipelines have been traced. In such cases, distances and elevations are manually interpolated between features (i.e., roads) common to those indicated in company stationing data files (or ILI odometer files, in the case of the validation); distance and elevation measurements from the USGS maps are then aligned with company data by these features. Uncertainty increases with distance between features used for alignment.

1.3.4 In-line Inspection (ILI)

The location error associated with in-line inspection tools is usually given as $\pm 0.5\%$ to $\pm 1\%$ of the distance recorded by the tool from a known reference point depending on the instrument and pipeline conditions. ILI location uncertainty has three main sources: clock resolution and accuracy, odometer wheel slippage or malfunction, and blunt errors. 1) Above ground markers (AGM) are used to reduce the chaining distance from a known point to any ILI anomaly. The closer together the AGM's are the better the tolerance on location. Most AGM's function by synchronizing clocks in the multiple AGM's deployed with the clock inside the ILI tool. Synchronization discrepancies can occur causing the AGM location to be misrepresented in the ILI reported. When AGM's malfunction and cannot be identified in the ILI data the absolute location error will increase, as the distance between usable AGM chaining references will increase and probably double. 2) On low friction pipe surfaces, around bends, in dirty pipelines, and during speed excursions odometer wheel slippage or malfunction can occur affecting recorded ILI distance. Most ILI tools are equipped with at least two to three odometers and on-board signal processing in an attempt to overcome these problems. 3) A last consideration are errors that may occur during data entry or interpretation of ILI data.

1.4 ICDA Validation - Pipeline A

1.4.1 Summary

Pipeline A had been in service since 1954. Pipe nominal diameter was 20 in. (51 cm), wall thickness 0.281 in. (0.7 cm). Operating pressure ranged 500 to 975 psi (3.45 to 6.7 MPa). For modeling purposes, the temperature was assumed a constant 60° F (15.6° C). Flow rates are shown in Table 1-2; these ranged up to 134.6 MMSCFD ($159 \times 10^3 \text{ m}^3/\text{h}$). The pipe had multiple inlets, as detailed in Table 1-3. The only outlets were the beginning and end of the line. Gas flow in the pipe has been in both south and north directions, sometimes both in the same day. Split flow was frequent and reportedly occurred typically at milepost (MP) 48.80 (78.5 km), with $\frac{1}{4}$ of the gas generally flowing south and $\frac{3}{4}$ flowing north. Although gas quality data from 1997 show the gas as dry, it is known that MPa 48.80 (78.5 km) was a location of frequent liquid upsets.

Table 1-2. Pipeline A: Flow Rates and Critical Angles
(using Low Pressure, 500 Psi = 3.45 MPa)

FLOWING NORTH:			
<i>Beginning of ICDA Region no.:</i>	<i>Location, mi. (km)</i>	<i>Maximum Flow Rate, MMSCFD (10³ x m³/h)</i>	<i>Critical Angle for Region (degrees)</i>
South			
1	24.27 (39.1)	115 (136)	4
2	28.66 (46.1)	117.2 (138)	4
6	39.74 (64)	117.3 (138)	4
7	41.01 (66)	123.9 (146)	5
North			
FLOWING SOUTH:			
<i>Beginning of ICDA Region no.:</i>	<i>Location, mi. (km)</i>	<i>Maximum Flow Rate, MMSCFD (10³ x m³/h)</i>	<i>Critical Angle for Region (degrees)</i>
North			
9	44.36 (71.4)	125.6 (148)	5
	44.35 (71.4)	125.7 (148)	5
11	41.01 (66)	132.3 (156)	6
12	39.74 (64)	132.5 (156)	6
16	28.66 (46.1)	134.6 (159)	6
South			

ILI data were collected in 1997. Direct inspection and examination information from this period were also provided, along with repair data for some sites. Additionally provided were locations of some corrosion monitoring coupons and gas quality information for some years. Distance and elevation were obtained from hard copies of USGS maps; the pipe depth was assumed constant.

Table 1-3. Pipeline A: ICDA Regions

<i>South to North Gas Flow Direction</i>				<i>North to South Gas Flow Direction</i>			
<i>Region</i>	<i>Start mi. (km)</i>	<i>Start MP Description</i>	<i>End mi. (km)</i>	<i>Region</i>	<i>Start mi. (km)</i>	<i>Start MP Description</i>	<i>End mi. (km)</i>
1	24.29 (39.1)	historical input	28.66 (46.1)	9	44.35 (71.4)	current input	41.15 (66.2)
2	28.66 (46.1)	Line B tie-in	31.66 (51)	10	41.15 (66.2)	historical input	41.01 (66)
3	31.66 (51)	historical input	35.24 (56.7)	11	41.01 (66)	current input	39.74 (64)
4	35.24 (56.7)	historical input	35.67 (57.4)	12	39.74 (64)	current input	35.67 (57.4)
5	35.67 (57.4)	historical input	39.74 (64)	13	35.67 (57.4)	historical input	35.24 (56.7)
6	39.74 (64)	current input	41.01 (66)	14	35.24 (56.7)	historical input	31.66 (51)
7	41.01 (66)	current input	41.15 (66.2)	15	31.66 (51)	historical input	28.66 (46.1)
8	41.15 (66.2)	historical input	44.35 (71.4)	16	28.66 (46.1)	Line B tie-in	24.29 (39.1)

Recent ILI, some detailed examination, all required and much recommended data (NACE International, 2005) were provided for Pipeline A. Therefore, Pipeline A was considered an excellent candidate for ICDA Validation, ranked Category I (Ideal).

The ICDA Method predicted locations of internal corrosion in Pipeline A that correlated with the ILI internal corrosion anomalies. As shown in Table 1-4, 85% of anomalies identified by ILI were predicted by the ICDA method. An additional 5% might also be predicted by ICDA, as these were associated with roads, and pipe depth information was not available, as indicated in Table 1-5. 80% of anomalies with depth 30-39% of wall thickness were predicted by ICDA (see Table 1-6). The location of a historic leak was also predicted by ICDA. The total length of pipe evaluated by ICDA was 20.1 miles (32.3 km), located

between MPs 24.29 (39.1 km) and 44.35 (71.4 km). It should be noted that the uncertainty in ILI with respect to detection, identification, and sizing of anomalies decreases the correlation. The level of correlation between ICDA and actual internal corrosion defects is therefore expected to be higher.

Table 1-4. Summary: Results for Pipelines A, B, C, and D

<i>Example</i>	<i>Total Number of Sites Examined</i>	<i>% of Total Pipe Length Examined</i>	<i>Percentage Internal Anomalies Predicted by Dry Gas ICDA *</i>	<i>for Internal Anomalies having % Depth of Wall Thickness</i>
A (USGS)	36	<15	85	>20
B (GIS)	17	<16	79	>50
C (GIS)**	26	<4	16	>30
C (USGS)**	27	<9	53	>30
D (USGS)	69	<11	87***	>30

* Assumes full circumference of pipe examined.

** The analysis on Pipeline C was performed 2 ways: once using GIS elevation data and once using USGS elevation data.

*** Assumes +/- 200 ft (61 m) horizontal uncertainty.

Table 1-5. Pipeline A: ILI Tool-Identified Internal Anomalies – Correlation with Sites Selected by ICDA Method

Location of Internal Anomaly, mi. (km)	Region nos.	% Depth	Length, in. (cm)	Orientation (o-clock)	Predicted by ICDA?	Notes
24.294 (39.1)	1&16	22	0.3 (0.8)	5	Yes.	
24.294 (39.1)	1&16	25	0.6 (1.5)	7	Yes.	
24.299 (39.11)	1&16	23	0.7 (1.8)	4	Yes.	
24.299 (39.11)	1&16	21	1.7 (4.3)	5	Yes.	
24.299 (39.11)	1&16	22	1.8 (4.6)	5	Yes.	
24.299 (39.11)	1&16	21	0.4 (1)	5	Yes.	
25.259 (40.65)	1&16	22	1.3 (3.3)	5	No.	
25.26 (40.65)	1&16	24	1.1 (2.8)	5	No.	
27.774 (44.7)	1&16	20	3.4 (8.6)	4	Yes.	
27.774 (44.7)	1&16	21	0.8 (2)	4	Yes.	
29.305 (47.16)	2&15	40	4.4 (11.2)	6	No.	
29.39 (47.3)	2&15	35	6.8 (17.3)	5	No.	
29.466 (47.42)	2&15	24	1.4 (3.6)	6	No.	Highway crossing.
32.376 (52.1)	3&14	25	0.4 (1)	3	No.	Road crossing.
36.733 (59.12)	5&12	24	0.3 (0.8)	5	Yes.	
36.757 (59.15)	5&12	25	0.4 (1)	5	Yes.	
36.757 (59.15)	5&12	21	0.3 (0.8)	5	Yes.	
36.757 (59.15)	5&12	32	1.7 (4.3)	5	Yes.	
36.757 (59.15)	5&12	21	0.4 (1)	5	Yes.	
36.757 (59.15)	5&12	24	0.5 (1.3)	5	Yes.	
39.785 (64.03)	6&11	23	2.1 (5.3)	7	Yes.	
39.785 (64.03)	6&11	28	2.9 (7.4)	7	Yes.	
39.785 (64.03)	6&11	21	0.4 (1)	6	Yes.	
39.785 (64.03)	6&11	21	2.5 (6.4)	5	Yes.	
39.785 (64.03)	6&11	21	2.9 (7.4)	8	Yes.	
39.785 (64.03)	6&11	21	0.4 (1)	5	Yes.	
39.785 (64.03)	6&11	30	2.5 (6.4)	8	Yes.	
39.785 (64.03)	6&11	21	0.5 (1.3)	5	Yes.	
39.785 (64.03)	6&11	45	6.6 (16.8)	8	Yes.	
39.786 (64.03)	6&11	21	1.8 (4.6)	5	Yes.	
39.786 (64.03)	6&11	38	3.2 (8.1)	8	Yes.	
39.786 (64.03)	6&11	22	3.9 (9.9)	5	Yes.	
39.786 (64.03)	6&11	31	3 (7.6)	8	Yes.	
39.786 (64.03)	6&11	23	0.4 (1)	8	Yes.	
39.786 (64.03)	6&11	22	0.5 (1.3)	5	Yes.	
39.786 (64.03)	6&11	29	0.5 (1.3)	7	Yes.	
39.786 (64.03)	6&11	23	0.4 (1)	8	Yes.	
39.787 (64.03)	6&11	20	4.9 (12.4)	6	Yes.	
44.197 (71.13)	8&9	23	1.6 (4.1)	7	Yes.	
44.197 (71.13)	8&9	20	1.2 (3)	7	Yes.	

Table 1-6. Pipeline A: Percentage of Tool-Identified Internal Anomalies Predicted by ICDA

Percentage of Internal Anomalies Predicted, by Percent Depth:			
% Depth	<i>Number of Anomalies</i>	<i>Number of Anomalies Predicted</i>	<i>% of Anomalies Predicted</i>
20-29	33	29	87.9
30-39	5	4	80.0
40-49	2	1	50.0
TOTAL	40	34	85.0

Percentage of Internal Anomalies Predicted, by Defect Length:			
Length, in. (cm)	<i>Number of Anomalies</i>	<i>Number of Anomalies Predicted</i>	<i>% of Anomalies Predicted</i>
0 - 6 (0-15)	38	33	86.8
6-12 (15-30)	2	1	50.0
TOTAL	40	34	85.0

1.4.2 Step 1: Pre-Assessment (Pipeline A)

1.4.2.1 Collected Data and Feasibility Assessment

As pigging smears out the liquid, there is legitimate concern that it could impact internal corrosion in ways not predicted by ICDA. Pipeline A was subjected to occasional maintenance pigging (theoretically twice a year; in reality less frequently, depending on flow). An internal leak that occurred in 1997 was thought to be due to the fact that maintenance pigging had not been frequent in recent years. There was no history of internal corrosion in the pipeline prior to 1987; internal corrosion appears to have occurred between 1987 and 1997, the ten years immediately prior to the 1997 ILI run. The repair data supplied by the operator indicate that some portions of pipe between MP 39.79 (64 km) and MP 48.16 (77.5 km) were coated with a black, sooty material. Some material was also found with cut-away and cleaning of pipe at MP 35.24 (56.7 km) and at MP 48.81 (78.6 km), with removal of stuck cleaning tools from these locations. Brushes and cups of the cleaning tools removed from these two locations were described as being “packed with black grainy material,” and twenty to twenty-five gallons of this material was removed from the line at each location. In the case of MP 35.24 (56.7 km), it appears the material did not travel as far downstream as MP 35.67 (57.4 km), since no excess of foreign material was observed at milepost 35.67 (57.4 km).

1997 gas quality data for the transmission pipeline indicate water content of 2 to 6 lb/MMSCF (32 to 96 mg/m³), suggesting nominally dry gas conditions, but liquid upsets were known to have occurred. Carbon dioxide and hydrogen sulfide levels are also shown in the 1997 gas quality reports. Measurements at several locations along the pipe length indicate 1.1 to 2.25% CO₂, and 0 to 5.5 ppm H₂S. Additionally, information suggests there may at some point have been some glycol carry-over from one of the inputs.

The collected data were sorted for criteria specified in the draft NACE standard (NACE International, 2005). Results of the Feasibility Assessment were favorable. Pipeline A passed twelve of the thirteen criteria. It was unknown if the frequency of pigging was less than the

frequency of upsets, as the precise frequency of upsets was not available. Feasibility Assessment results are shown in Table 1-7.

Table 1-7. Pre-Assessment of Feasibility: Pipelines A, B, C, And D

No.	Criteria	Pipeline A	Pipeline B	Pipeline C	Pipeline D
1	The pipeline does not normally contain any liquids, including glycols.	Pass	Pass	Pass	Pass
2	The pipeline has not been previously converted from a service for which ICDA is not applicable (i.e., crude oil, products).	Pass	Pass	Pass	Pass
3	The pipeline is uninhibited.	Pass	Unknown	Pass	Pass
4	The pipeline does not have an internal coating that is intended to provide corrosion protection.	Pass	Unknown	Pass	Pass
5	If pipeline has been pigged, significant volumes of liquid were not recovered in the pigging operation.	Pass	Unknown	Some recovered	Some recovered
6	The frequency of pigging is less than the frequency of upsets.	Unknown	Pass	Pass	Unknown
7	The maximum superficial gas velocity in the pipeline is 25 ft/s (7.6 m/s).	Pass	Fail (average 16.2 m/s)	Pass	Pass
8	Nominal pipe diameter is between 4 and 48 inches (0.1 to 1.2 m).	Pass	Pass	Pass	Pass
9	Pressures are maintained within the range 500 to 1100psi (3.4 to 7.6MPa).	Pass	Pass	Pass	Pass
10	There is a relatively constant temperature over the pipe length [i.e., ambient soil temperature and up to 130 degrees F (54 degrees Celsius) at compressor discharge].	Pass	Pass	Pass	Pass
11	History does not indicate any internal corrosion at top of pipeline.	Pass	Fail (some at top)	Fail (ILI indicates)	Isolated (<3% of ILI call-outs)
12	Pipelines are not subjected to regular (e.g., annual or more frequent basis) maintenance.	Pass	Unknown	Pass	Semi-annual batch treatment.
13	Pipelines that contain significant accumulations of solids, sludge, or scale should not be assessed by dry gas ICDA.	Pass	Unknown	Some found; significance undetermined.	Some found; significance undetermined.

1.4.2.2 ICDA Region Definition

Flow in the pipe had been bi-directional. For this reason, it was necessary to define ICDA regions for each direction. As indicated previously, the only outlets were at the beginning and end of the line; however, there were multiple inlets in between. Pressure was constant down the pipe length and therefore did not play a role in ICDA region definition. The flow rate, however, had changed at each current and historical inlet. Due to the flow rate differences, ICDA regions were defined based on historic and current inlet locations. The pipeline length to be evaluated by ICDA was divided into sixteen ICDA regions between MP 24.27 and MP 44.35 (39.1 to 71.4 km). ICDA Regions are shown in Table 1-3.

1.4.3 Step 2: Calculations and Initial ICDA Site Selections (Pipeline A)

1.4.3.1 ICDA Calculations

Table 1-2 contains maximum flow rates for the period 1997 to 1998; prior data was not available. Some of the ICDA Regions begin at historical inputs that were no longer in service by the year 1997 and are therefore not indicated in the table. Each calculation of the overall maximum flow rate for any pipeline length assumed 1) all gas was flowing in one direction (possible based on pipeline history), and 2) all inlets were at their maximum 1997-1998 flow rates. In reality, the pipeline experienced a variety of flow situations. The 1997-1998 flow information provided was assumed to be representative of typical flow between 1987 and 1997.

The low pressure 500 psi (3.5MPa) and the pipe inner diameter 19.44 in. (49.4 cm) were also used in the flow modeling to determine the angle past which liquid hold-up is not expected, or critical angle. The critical angles for each region are shown in Table 1-2.

The results of the flow modeling for the variety of conditions are shown in Table 1-2. The angles shown in the table were used to select sites for detailed examination of each region. The largest critical angles were 6 degrees for the North to South direction and 5 degrees for the South to North flow direction. It should be noted that small differences in diameters (due to different wall-thickness) present for short lengths of the pipeline were considered in the final analysis and found to be negligible in their effects on this pipeline.

The inclination profile was found using elevations and distances from hard-copies of USGS topographical quad maps.

1.4.3.2 Initial Site Selections

Flow modeling results were integrated with the inclination profile shown in Figures 1-1 through 1-4. These plots also show the elevation profile and ILI anomalies. As the flow in Pipeline A was bi-directional, the inclinations on the composite plots must be read two ways. For South to North ICDA Regions (1 to 8) the positive inclination angle should be used and the plot read from left to right. North to South regions (9 to 16) should be read from right to left using the negative inclination angles (i.e., -5.5' is actually 5.5'). In some cases (e.g., Regions 4 and 7) there were fewer than three low points associated with inclinations, so there were fewer (or no) sites to examine.

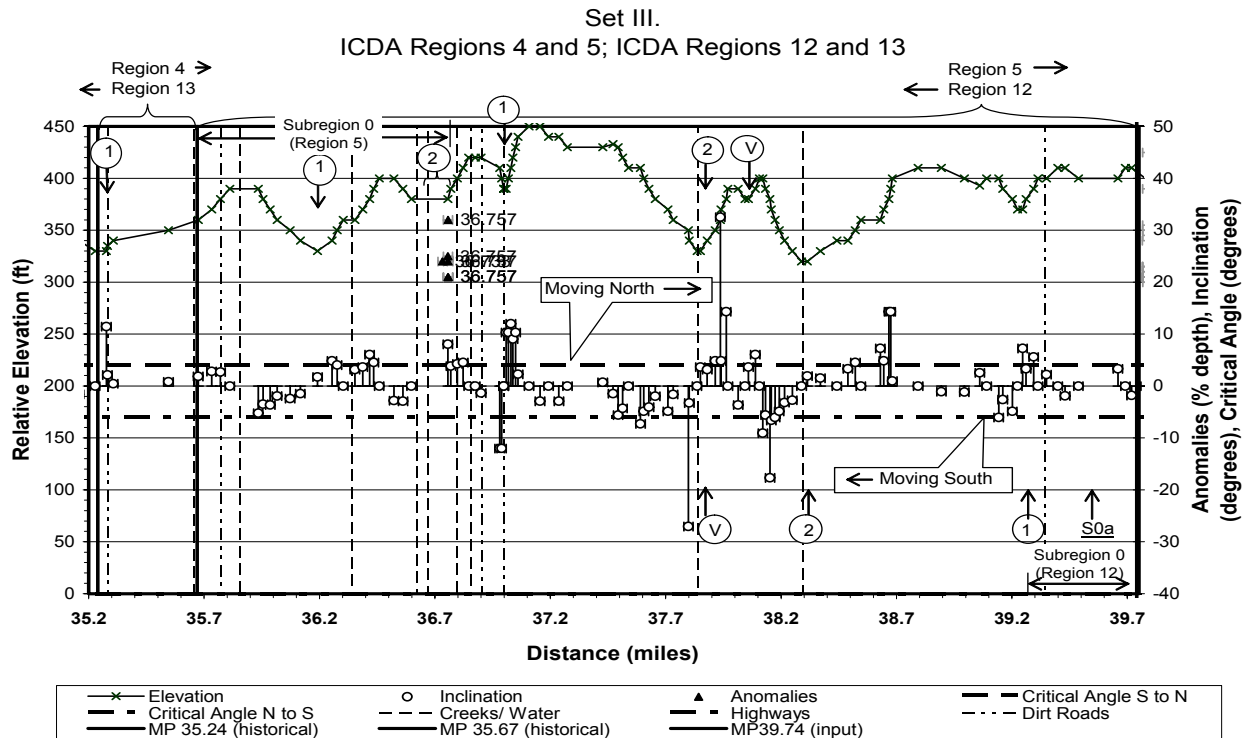


Figure 1-3. Pipeline A – Set III of IV. Combined inclination and elevation profile with anomalies and critical angles shown (1 ft = 0.305 m, 1 mi. = 1.609 km).

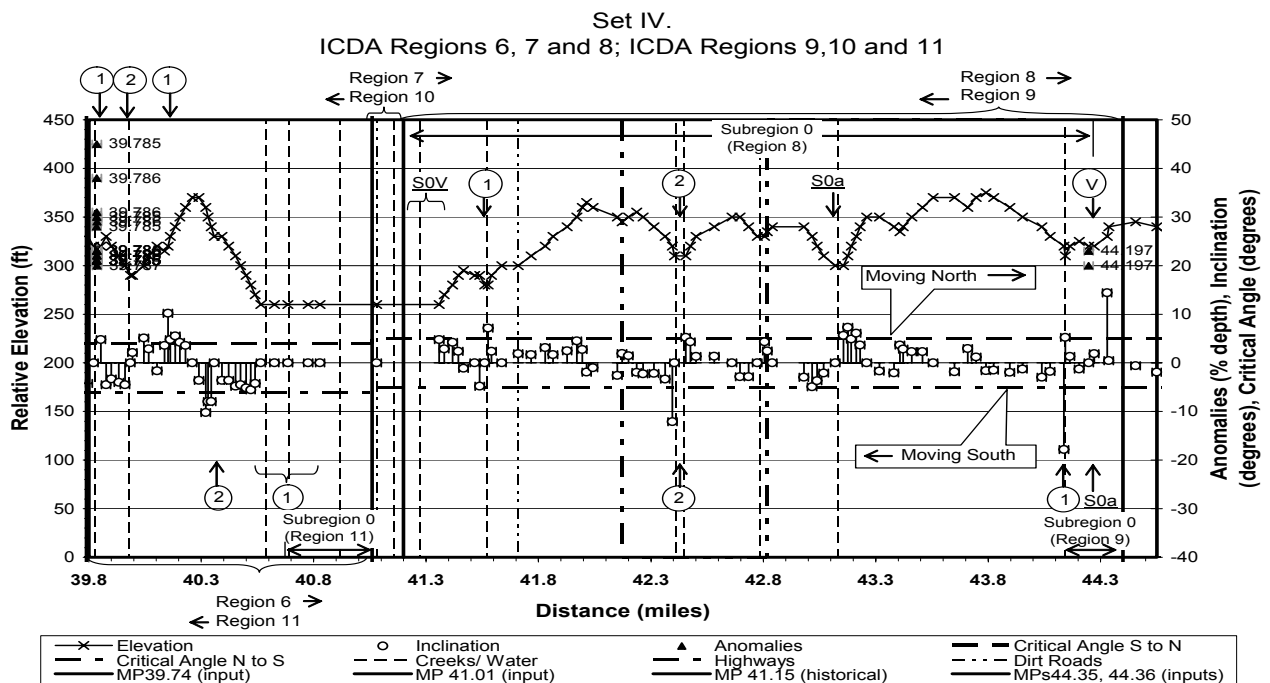


Figure 1-4. Pipeline A – Set IV of IV. Combined inclination and elevation profile with anomalies and critical angles shown (1 ft = 0.305 m, 1 mi. = 1.609 km).

1.4.4 Step 3: Detailed Examination, Additional Site Selections (Pipeline A)

The sites selected for Pipeline A are shown in Table 1-8. Pipeline A used the ICDA Process flow chart, Figure 1-3 in the draft NACE standard (NACE International, 2005). The set number and identification are provided to facilitate the correlation of Table 1-8 data with data in Figures 1-1 to 1-4. The “set number” corresponds with the plot the anomaly is shown on, and the “identification” shows the location of the anomaly within each set.

Table 1-8. Pipeline A: Sites Selected for Detailed Examination by The ICDA Method

Set #	Letter	Region no.	Subregion no.	Location, mi. (km)	Reason for Examination	Internal Anomaly?
I	1	1		24.338 (39.17)	1st site; 2nd largest inclination angle.	Yes.
I	1	1		27.846 (44.81)	2nd site; largest inclination angle.	Yes.
I	S1a	1	1	26.562 to 27.519 (42.75 to 44.29)	Next largest inclination angle in Subregion 1.	No.
I	S1V	1	1	25.62 to 25.86 (41.23 to 41.62)	Validation: Next largest inclination angle in Subregion 1.	No.
I	1	16		28.116 (45.25)	1st site; 2nd steepest inclination angle.	No.
I	2	16		26.562 to 25.947 (42.75 to 41.76)	2nd site; steepest inclination angle.	No.
II	1	2		29.01 (46.69) to 29.095 (46.82)	1st site with inclination > than critical.	No.
II	2	2		31.345 (50.44)	2nd site with inclination > than critical.	No.
II	V	2		31.656 (50.95)	Validation: inclination angle larger than previous.	No.
II	1	15		31.306 (50.38)	1st site; site with steepest inclination.	No.
II	2	15		30.801 to 30.613 (49.57 to 49.27)	2nd site; 2nd steepest inclination.	No.
II	1	3		32.161 (51.76)	1st site with inclination > than critical.	No.
II	2	3		32.574 (52.42)	2nd site with inclination > than critical.	No.
II	V	3		32.684 (52.60)	Validation: next site with inclination greater than critical.	No.
II	1	14		33.045 (53.18)	1st site with inclination > than critical.	No.
II	2	14		32.684 (52.60)	2nd site with inclination > than critical.	No.
II	S0a	14	0	33.984 (54.69)	Next largest inclination angle in Subregion 0.	No.
II	S0V	14	0	34.925 (56.21)	Validation: next largest inclination angle in Subregion 0.	No.
III	a	4		35.277 (56.77)	Only low point in Region 4.	No.
III	1	5		36.192 to 36.254 (58.25 to 58.35)	1st site with inclination > than critical.	No.
III	2	5		36.756 (59.15)	2nd site with inclination > than critical.	Yes.
III	1	5		36.998 (59.54)	Next site with inclination > than critical.	No.
III	2	5		37.84 (60.9)	Next site with inclination > than critical.	No.
III	V	5		38.058 (61.25)	Validation: next site with inclination greater than critical.	No.
III	1	12		39.224 (63.12)	1st site with inclination > than critical.	No.
III	2	12		38.296 to 38.157 (61.63 to 61.41)	2nd site with inclination > than critical.	No.
III	V	12		37.84 to 37.802 (60.90 to 60.84)	Validation: inclination angle larger than previous.	No.
III	S0a	12	0	39.488 (63.55)	Next largest inclination angle in Subregion 0.	No.
IV	1	6		39.804 (64.06)	1st site with inclination > than critical.	Yes.
IV	1	6		39.935 to 39.995 (64.27 to 64.37)	2nd site with inclination > than critical.	No.
IV	2	6		40.087 (64.51)	Next site with inclination > than critical.	No.
IV	1	11		40.515 to 40.490 (65.2 to 65.16)	1st site; 2nd steepest inclination angle.	No.
IV	2	11		40.308 (64.87)	2nd site; steepest inclination angle.	No.
IV	1	8		41.526 (66.83)	1st site with inclination > than critical.	No.
IV	2	8		42.399 (68.23)	2nd site with inclination > than critical.	No.
IV	V	8		44.221 (71.17)	Validation: inclination angle larger than previous.	Yes.
IV	S0a	8	0	43.107 (69.37)	Next largest inclination angle in Subregion 0.	No.
IV	S0V	8	0	41.308 (66.48)	Validation: next largest inclination angle in Subregion 0.	No.
IV	1	9		44.093 (70.96)	1st site with inclination > than critical.	No.
IV	2	9		42.346 (68.15)	2nd site with inclination > than critical.	No.
IV	S0a	9	0	44.197 (71.13)	Next largest inclination angle in Subregion 0.	Yes.

1.4.5 Step 4: Post-Assessment (Pipeline A)

1.4.5.1 Comparison of ILI with ICDA Results

As shown in Table 1-6, of the 40 ILI-identified internal anomalies 34, or 85%, were predicted by ICDA. Details of each individual anomaly are shown in Table 1-5. Percent depths, length, and orientations of anomalies are shown, with the regions they occurred in, whether they were predicted by ICDA, and any notes. Only anomalies greater than 20% depth of wall thickness were considered. All anomalies occurred in the bottom half of the pipe. Of the six anomalies that were not predicted by ICDA, two were located near highway or road crossings. It is expected that at these locations pipe depths will not necessarily follow the contour of ground elevations as pipe is frequently buried deeper in accommodation of roads and highways. GIS/pipeline depth measurements of adequate accuracy and precision would be necessary to determine the true pipe inclinations at these sites.

1.4.5.2 Uncertainties

Elevation uncertainties resulting from the use of hard-copy USGS maps are discussed in the Data Uncertainties section at the beginning of this report. The elevation contour interval for Pipeline A maps was ten feet. The company indicated that ILI data were well aligned with pipe distances, with a maximum of +/- 50 ft (15 m) error (Table 1-9). A possibility exists that the 1997 to 1998 flow rate data used in the analysis does not accurately represent all flow rates for the period 1987 to 1996. For instance, no flow rate data was available for known historical inlets. Despite the flow rate uncertainties, the results of the Pipeline A ICDA Process Validation were positive, which suggests the contribution of flow rate uncertainty was negligible or at least small.

1.5 ICDA Validation - Pipeline B

1.5.1 Summary

Pipeline B had an outer diameter of 20 in. (51 cm) with 0.250 in. (0.64 cm) wall thickness. Operating pressure ranged 500 (low average) to 810 (high) psi (3.5 to 5.6 MPa). Flow rate ranged 0 to 20MMSCFD (0 to 23.6×10^3 m³/h) and averaged 10MMSCFD (11.8×10^3 m³/h). Pipe flow was uni-directional, east to west. The pipeline had no in-line gas producers, nor were there any outlets aside from the line end. There were a few road crossings on the line, but no river crossings. Road crossings are shown in Figure 1-5, with internal anomaly details overlying elevation and inclination profiles. There were no historical leaks as the company knew of internal corrosion problems with the line. A smart pig run in 1987 found the line in relatively poor condition and in 1994 replacement of the corroded areas began.

Recent ILI data and operating history were available for Pipeline B. However, there was an absence of documented detailed examination information. The ICDA Validation ranking for Pipeline B was thus Category II (Good).

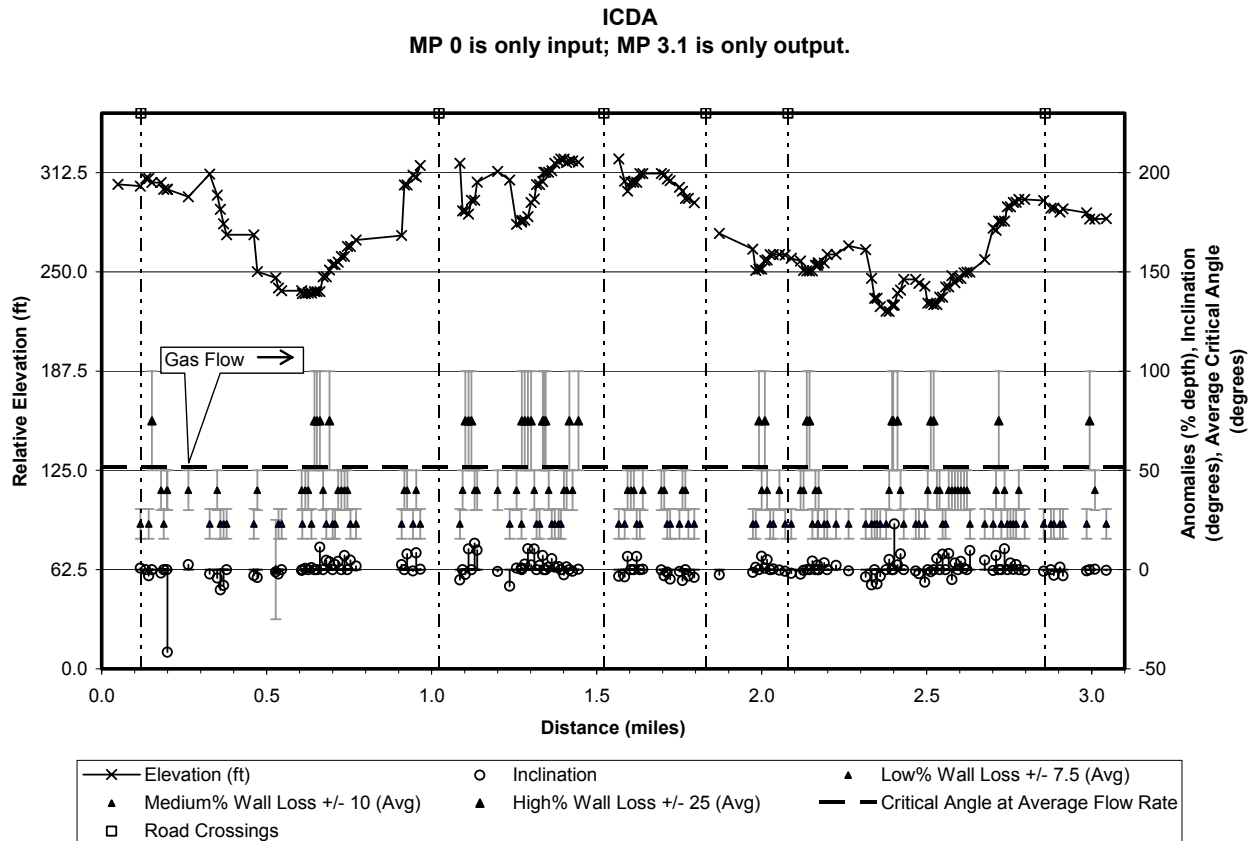


Figure 1-5. Pipeline B. Combined inclination and elevation profile with anomalies and critical angles shown (1 ft = 0.305 m, 1 mi. = 1.609 km). Note that periods of stagnant flow suggests a range of critical angles extending from zero.

Because of ubiquitous corrosion in the pipe only the most severe anomalies, those having >50% depth, were included in the validation. The ICDA Process predicted ~78% of 50-100% depth internal anomalies indicated by ILI (Table 1-4). Flow modeling showed that the critical angle well-exceeded all pipeline inclinations and on the first two detailed examinations >50% corrosion was found. Therefore, all inclinations connected with low points were recommended for detailed examination. The results are shown in Tables 1-9 and 1-10.

Table 1-9. Pipeline A: Estimated Horizontal Uncertainties; Provided in Miles (Km)

Region	National Map Accuracy Standards (NMAS)	ILI (Company Provided)	Interpolation (Root Mean Square Error)
1, 16	0.0126 (0.020)	0.019 (0.031)	0.034 (0.055)
2, 3, 14, 15	0.0126 (0.020)	0.019 (0.031)	0.035 (0.056)
4, 5, 12, 13	0.0126 (0.020)	0.019 (0.031)	0.02 (0.032)
6, 11	0.0126 (0.020)	0.019 (0.031)	0.02 (0.032)
7, 8, 9, 10	0.0126 (0.020)	0.019 (0.031)	0.017 (0.027)

Table 1-10. Pipeline B: Percentage of Tool-Identified 50-100% Depth Internal Anomalies Predicted by Dry Gas ICDA

Percentage of Internal Anomalies of 50-100% Depth Predicted:			
	<i>Number of Anomalies</i>	<i>Number of Anomalies Predicted</i>	<i>% of Anomalies Predicted</i>
Pipe Bottom Half only Examined.		17	60.7
Full Pipe Circumference Examined.		22	78.6
TOTAL		28	

1.5.2 Step 1: Pre-Assessment (Pipeline B)

1.5.2.1 Collected Data and Feasibility Assessment

Pipeline B met many of the ICDA Process criteria, as shown in Table 1-1. Two points were identified upon which it deviated. First, the maximum superficial velocity exceeded 25 ft/s (7.6 m/s). The maximum superficial velocity was found to be 53 ft/s (16.2 m/s) in the case of low average pressure, 500psi (3.5 MPa), and average flow rate of 10MMCFD (11.8×10^3 m³/h). Second, although most of the ILI-identified internal anomalies were located on the bottom of the pipe, some appear to have occurred at the top. Field inspections during repair/replacement of the most severely internally corroded areas revealed corrosion in the bottom quadrant of the line, as expected. Many other locations of defects attributed to internal corrosion were found to be caused by other mechanisms (e.g., external corrosion).

There was no history of hydrotesting on the pipeline. The pipeline was considered hydrocarbon wet, typically <7 lb/MMSCF (<112 mg/m³). As a last note, the presence of chlorides and irons was detected at a location downstream of the line.

1.5.2.2 ICDA Region Definition

Flow was uni-directional, from East to West, and there were no additional inlets or outlets. Therefore, there was only one region for this line.

1.5.3 Step 2: Calculations and Initial ICDA Site Selections (Pipeline B)

1.5.3.1 ICDA Calculations

Table 1-11 shows the data used in the flow modeling calculations, which in this case represent average flow, and the resultant critical angle. The inclination profile was created using company- provided elevation and distance data from a computerized USGS data source. Critical angle, inclination profile, elevation profile, and ILI-identified internal anomalies are plotted together in Figure 1-5.

**Table 1-11. Pipeline B: Flow Rates and Critical Angles
(Using Low Pressure, 500 Psi = 3.5 MPa)**

Inner Diameter = 19.5 inches (49.5cm)
 Temperature = 60 F (15.6 C)
 (Flow unidirectional. Low Flow Rate = 0)

<i>Direction</i>	<i>Typical Flow Rate, MMSCFD (Thousand standard m³/h)</i>	<i>Pressure, psi (MPa)</i>	<i>Critical Angle (degrees)</i>
West to East	422 (498)	500 (3.45)	53

1.5.3.2 Initial Site Selections

Because no inclination angles in the profile (Figure 1-5) were greater than the critical angle of 53°, those sites with the greatest inclination angles were the first to be examined in detail.

1.5.4 Step 3: Detailed Examination, Additional Site Selections (Pipeline B)

The order of inspections is shown in Table 1-12. Because inspections at the steepest two inclination angles, located at MP 2.377 (3.83 km) and MP 1.094 (1.76 km), revealed >50% internal corrosion at both sites all sites associated with low points were recommended for detailed examination. The order of site examinations was steepest (23°) to shallowest inclination angle. Fifty feet were added at the end of each excavation site to take into account data uncertainties.

Table 1-12. Pipeline B: Sites Selected for Detailed Examination by The ICDA Method

<i>Number</i>	<i>Start Mile- post (km)</i>	<i>End Mile- post (km)</i>	<i>Reason for Examination</i>	<i>50-100% Depth Internal Anomaly?</i>	<i>% Depth</i>	<i>Inclination Angle (°)</i>
1	2.377 (3.83)	2.402 (3.87)	Steepest inclination angle; low point.	Yes.	50-100	23
2	1.094 (1.76)	1.13 (1.82)	Next steepest critical angle upstream; low point.	Yes.	50-100	13.2
3	0.609 (0.98)	0.681 (1.1)	Next steepest critical angle upstream; low point.	Yes.	50-100	11.2
4	1.257 (2.02)	1.282 (2.06)	Next steepest critical angle upstream; low point.	Yes.	50-100	10.5
5	2.71 (4.36)	2.754 (4.43)	Next steepest critical angle upstream; low point.	Yes.	50-100	10.5
6	0.943 (1.52)	0.953 (1.53)	Low point.	No.	30-50	8.4
7	1.982 (3.19)	2 (3.22)	Low point.	Yes.	50-100	6.7
8	1.594 (2.57)	1.622 (2.61)	Low point.	No.	30-50	6.6
9	2.521 (4.06)	2.531 (4.07)	Low point.	Yes.	50-100	5.6
10	2.127 (3.42)	2.154 (3.47)	Low point.	Yes.	50-100	4.3
11	2.585 (4.16)	2.604 (4.19)	Low point.	No.	30-50	4.1
12	0.119 (0.19)	0.119 (0.19)	Low point.	No.	20-30	3.1
13	0.263 (0.42)	0.263 (0.42)	Low point.	No.	30-50	2.4
14	1.409 (2.27)	1.409 (2.27)	Low point.	Yes.	50-100	1.4
15	2.904 (4.67)	2.904 (4.67)	Low point.	No.	20-30	1.3
16	1.445 (2.33)	1.445 (2.33)	Appears to be low point; data gap follow s.	Yes if examined.	50-100	n/a
17	2.994 (4.82)	2.994 (4.82)	Appears to be low point; data gap follow s.	Yes if examined.	50-100	n/a

1.5.5 Step 4: Post-Assessment (Pipeline B)

1.5.5.1 Comparison of ILI with ICDA Results

The correlation of ILI-identified internal anomalies with detailed examined locations is shown in Table 1-13. Twenty eight anomalies exhibited >50% depth. If the full circumference of the pipe were evaluated ~78% of >50% depth anomalies would be predicted by ICDA (see Table 1-10). This data is also shown in Table 1-4.

Table 1-13. Pipeline B: 50-100% Depth Inspection Tool-Identified Anomalies – Comparison with Sites Identified by ICDA Method

Location of Internal Anomaly mi. (km)	Orientation	Identified by ICDA?	Distance from Low Point, ft (m)	Upstream or Downstream of Low point?	If on Slope, Inclination Angle (°)
0.153 (0.25)	3:00	No.	180 (54.9)		n/a
0.645 (1.04)	11:00	Yes. *			11.2
0.652 (1.05)	11:00	Yes. *			11.2
0.661 (1.06)	7:00	Yes.			11.2
0.69 (1.11)	6:00	Yes.	48 (14.6)	Downstream	4.6
1.102 (1.77)	9:00	Yes.			13.2
1.111 (1.79)	6:00	Yes.			13.2
1.121 (1.8)	6:00	Yes.		Downstream	13.2
1.273 (2.05)	3:00	Yes.			10.5
1.282 (2.06)	6:00	Yes.			10.5
1.292 (2.08)	8:00	Yes.	53 (16.2)	Downstream	10.5
1.301 (2.09)	6:00	Maybe. **	101 (30.8)	Downstream	10.5
1.336 (2.15)	6:00	No.		Downstream	7
1.34 (2.16)	5:00	No.		Downstream	7
1.345 (2.16)	5:00	No.		Downstream	7
1.418 (2.28)	6:00	Yes.			1.4
1.445 (2.33)	5:00	Maybe. ***			n/a
1.991 (3.2)	2:00	Yes. *			6.7
2.01 (3.23)	2:00	Yes. *		Downstream	6.7
2.136 (3.44)	5:00	Yes.			4.3
2.145 (3.45)	6:00	Yes.			4.3
2.395 (3.85)	2:00	Yes. *			23
2.399 (3.86)	4:00	Yes.		Downstream	23
2.412 (3.88)	5:00	Yes.	53 (16.2)	Downstream	23
2.513 (4.04)	7:00	No.	42 (12.8)	Upstream	5.6
2.521 (4.06)	7:00	Yes.			5.6
2.719 (4.38)	6:00	Yes.			10.5
2.994 (4.82)	5:00	Maybe. ***			n/a

* Corrosion will be identified only if full circumference of pipe is inspected for internal corrosion. 17% of tool-identified internal anomalies are on the top of the pipe.

** If the length of pipe under “Distance from Low point” is inspected for internal corrosion, this anomaly would be identified.

*** If the location is, as it appears, a low point (data gap directly after location).

1.5.5.2 Uncertainties

Estimated uncertainties are shown in Table 1-14. Computerized USGS maps were used for Pipeline B. Elevation uncertainties were expected to be within NMAS bounds for USGS maps. Pipe depth was not measured and was also a possible source of vertical uncertainty. ILI contribution to distance error was not expected to exceed +/- 50 ft (15 m). The history provides evidence the flow rate has been high enough for the critical angle to exceed the model bounds. Even at average flow rate, any liquid in the flow stream could have carried through to the end of the pipe, because, all inclinations were smaller than the critical angle under average flow conditions. However, because there were periods of stagnant conditions, some locations could have suffered localized corrosion despite being at inclinations lower than the critical inclination angle based on average flow rates. The extent of these stagnant periods is not known and contributed significantly to the uncertainties in ICDA identification of internal corrosion locations.

Table 1-14. Pipeline B: Estimated Horizontal Uncertainties; Provided in Miles (Km)

Region	National Map Accuracy Standards	ILI (Estimated)
1	0.0126 (0.02)	0.01 (0.016)

1.6 ICDA Validation - Pipeline C

1.6.1 Summary

Pipeline C was installed in the 1950's and has reportedly functioned as a dry natural gas pipeline. Pipe inner diameter generally ranged 19.25 to 21.12 inches (48.9 to 53.6 cm) and was 12.75 inches (32.4 cm) for some short lengths. 2001 operating pressure was reported as < 800 psig (5.52 MPa) ~0.5% of the time, 800-900 psig (5.52 to 6.21 MPa) ~28.5% of the time, and > 900 psig (6.21 MPa) ~71% of the time. Gas flow has been in both north and south directions and, reportedly, flow can be zero at both ends with the central portion of the line still feeding distribution and fed by producers. There is gas storage at the North end (MP 0). Both beginning (MP 0, 0 km) and end of the line have served as inlets. Producer locations were given as MP 18.041 (29.034 km) and MP 38.015 (61.179 km). The maximum flow rate in the year 2001 was 151.2 MMSCFD ($178 \times 10^3 \text{ m}^3/\text{h}$) for flow south to north (S → N) and 338.4 MMSCFD ($399.2 \times 10^3 \text{ m}^3/\text{h}$) north to south (N → S). Average flow rates were also provided: 86.4 MMSCFD ($101.9 \times 10^3 \text{ m}^3/\text{h}$) for S → N, and 134.4 MMSCFD ($158.5 \times 10^3 \text{ m}^3/\text{h}$) for N → S. No prior internal corrosion leaks or failures were reported for the line.

Recent (2003) ILI data, operating history, and detailed examination data were provided for Pipeline C. Therefore, Pipeline C is an ideal candidate for ICDA Validation and is ranked Category I (Ideal).

The ICDA analysis was performed between MP 0 (0 km) and MP 38.015 (61.179 km). Pipeline C elevation profile was analyzed two ways: 1) using computerized USGS horizontal

and vertical data, 2) using GIS field elevation and stationing measurements captured through a line survey performed by a company contractor. In the latter case, the actual pipeline depth of burial was considered for most locations. However, at some locations, the pipe could not be located by the pipeline mapper because it was buried quite deep (presumably greater than 20 feet). At these locations, pipeline elevation data is missing. Some subtle inclinations, a few of significance (see Figure 18) were missing from both USGS and GIS data sets. In a walk along the first few miles of the pipeline after the last GIS survey, a 45-degree inclination associated with an elbow (~MP 0.69; see Figures 18 through 21) was identified that had been missed. It is somewhat clear from Figure 21 why this location was missed as the ground looks flat at this location (obscuring the changes in pipe inclination beneath). This highlights an important point, that there are higher demands placed on the GIS survey performed for ICDA than for many typical uses; and, pipe depth measurements may be important in some cases. It is clear that in the ICDA GIS survey, the data collection system used must have acceptable accuracy and precision for the analyst to discern all significant changes in pipe inclination, and a sufficient number of data points must be obtained particularly in areas with important elevation changes. There was so much error in this particular (Pipeline C) GIS survey, primarily due to quality of the instrument used, that interpreting the data was very difficult (Figures 1-7, 1-9, 1-11, and 1-13) and time consuming, and in the end rendered the accuracy/ precision of analysis dubious (see next paragraph). On the other hand, USGS data, while it may provide a good inclination profile of the pipeline and be useful for an initial analysis, may need in many cases to be supplemented by field information on pipeline elevations. Finally, no internal anomalies were found using ultrasonic transmission on the full circumference at the location that had been missed (~MP 0.69), nor had any internal anomalies been reported for this location by ILI. However, internal corrosion was found at ICDA sites downstream of this location (Figures 1-7 and 1-8). 45 degrees was clearly greater than the critical inclination angle of 16 degrees, and according to the dry gas ICDA method (NACE International, 2005) there should have been liquid accumulation there. Thus, the question is raised as to whether length of incline is significant in determining presence/extent of corrosion. The current dry gas ICDA method does not consider length of inclination in site selection; this question is important and merits further investigation.

Several more individual anomalies were identified using the USGS data than with the GIS field data. There were a total of 69 ILI individual internal anomaly call-outs in Pipeline C (one anomaly was excluded due to lack of stationing data in its vicinity) (Table 1-15). 53% of individual anomalies >30% depth were identified using the computerized USGS data (Table 1-18), and 21% of anomalies having >1 inch length were identified using the USGS data (Table 1-19). By contrast, only 16% of individual anomalies >30% depth were identified using the GIS field data (Table 1-15), while 14% of anomalies having >1 inch length were identified using the GIS field data (Table 1-16). 50% of internal anomaly groups were predicted using the USGS field data (Table 1-20), in comparison with 36% of internal anomaly groups (having >20% depth of wall thickness) predicted using the computerized GIS data (Table 1-17).

Table 1-15. Pipeline C *Using Hand-Held GIS Field Data*: Percentage of Tool-Identified Internal Anomalies Predicted by ICDA, by Percentage Depth

Percentage of Anomalies Predicted, by Percentage Depth:			
% Depth	<i>Number of Anomalies</i>	<i>Number of Anomalies Predicted</i>	<i>% of Anomalies Predicted</i>
20-29	50	4	8
30-39	19	3	16
40-100	0	n/a	n/a
TOTAL	69	7	10

Table 1-16. Pipeline C *Using Hand-Held GIS Field Data*: Percentage of Tool-Identified Internal Anomalies Predicted by ICDA, by Length

Percentage of Anomalies Predicted, by Length:			
<i>Length in (cm)</i>	<i>Number of Anomalies</i>	<i>Number of Anomalies Predicted</i>	<i>% of Anomalies Predicted</i>
<1 (<2.5)	55	5	9
1 - 3.4 (2.5 - 8.6)	14	2	14
>3.4 (>8.6)	0	n/a	n/a

Table 1-17. Pipeline C *Using Hand-Held GIS Field Data*: Percentage of Tool-Identified Internal Anomaly Groups Predicted by ICDA, by Percentage Depth

Percentage of Anomaly Groups Predicted, by Percentage Depth of Wall Thickness			
% Depth	<i>Number of Groups</i>	<i>Number of Groups Predicted</i>	<i>% of Groups Predicted</i>
20-39	14	5	36
40-100	0	n/a	n/a

Table 1-18. Pipeline C *Using Computerized USGS Data*: Percentage of Tool Identified Internal Anomalies Predicted by ICDA, by Percentage Depth

Percentage of Anomalies Predicted, by Percentage Depth of Wall Thickness:			
% Depth	<i>Number of Anomalies</i>	<i>Number of Anomalies Predicted</i>	<i>% of Anomalies Predicted</i>
20-29	50	16	32
30-39	19	10	53
40-100	0	n/a	n/a
TOTAL	69	26	38

Table 1-19. Pipeline C *Using Computerized USGS Data*: Percentage of Tool-Identified Internal Anomalies Predicted by ICDA, by Length

Percentage of Anomalies Predicted, by Length:			
<i>Length in (cm)</i>	<i>Number of Anomalies</i>	<i>Number of Anomalies Predicted</i>	<i>% of Anomalies Predicted</i>
<1 (<2.5)	55	23	42
1 - 3.4 (2.5 - 8.6)	14	3	21
>3.4 (>8.6)	0	n/a	n/a

Table 1-20. Pipeline C *Using Computerized USGS Data*: Percentage of Tool-Identified Internal Anomaly Groups Predicted by ICDA, by Percentage Depth

Percentage of Anomaly Groups Predicted, by Percentage Depth of Wall Thickness			
% Depth	Number of Groups	Number of Groups Predicted	% of Groups Predicted
20-39	14	7	50
40-100	0	n/a	n/a

1.6.2 Step 1: Pre-Assessment (Pipeline C)

1.6.2.1 Collected Data and Feasibility Assessment

Pipeline C met most of the ICDA Process feasibility requirements. However, ILI indicated internal anomalies on the top of the pipe suggesting (if these all represent internal corrosion at the top-of-the-line) the pipeline segment may *fail* the criterion of no internal corrosion on the top of the pipeline; in such case the ICDA dry gas model premise would be violated. Orientation of ILI internal indications versus % depth of wall thickness and versus length is shown in Figure 1-6, with 29% of individual internal anomalies on the top half of the line and most severe anomalies at the bottom of the line. As can be seen from this figure, most individual internal anomalies were at the bottom of the line. Orientation information considering groups of anomalies is shown in Table 1-21. Solids and sludge were found at locations inspected at the beginning and just beyond the end of the pipeline. The exact quantities of solids and sludge and what level of significance they represent are unknown. Likewise, the quantities and contributions of hydrocarbons and glycol found at these locations are unknown, although it is known that glycol was carried over from the dehydration system at times.

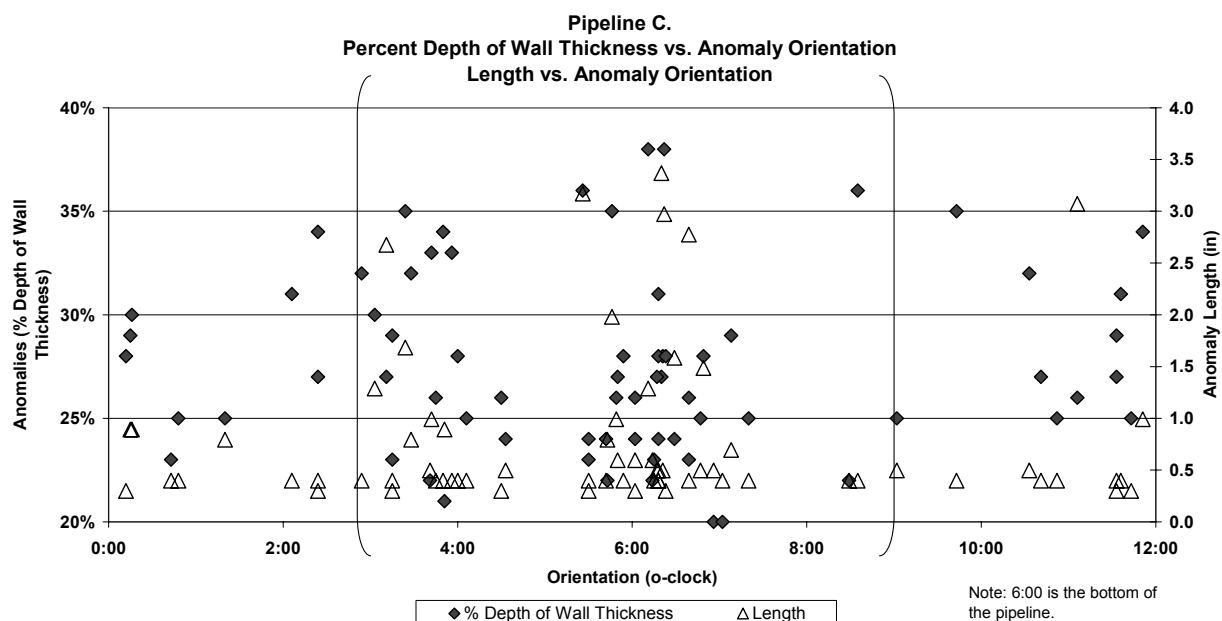


Figure 1-6. Pipeline C. Anomaly orientation vs. 1) % depth of wall thickness, 2) anomaly length.

Table 1-21. Pipeline C *Using Computerized USGS Data*: Percentage of Tool-Identified Internal Anomaly Groups Predicted by ICDA, by Anomaly Orientation (4-To8 O-Clock BLC; 10 To-2 O-Clock TLC; 2-To-4 And 8-To-10 O-Clock SLC)

	By Anomaly Orientation		
	Bottom-of-line (BLC)	Top-of-Line (TLC)	Side-of-Line (SLC)
No. of Anomaly Groups With This Orientation	5	5	5
No. of Anomaly Groups Predicted	2	3	2
% of Anomaly Groups Predicted	40%	60%	40%

The first pigging on the line occurred just prior to the ILI-tool inspection. There was one known large liquid upset in 2001, and glycol was observed at the end of the line following that upset. It is suspected that upsets occurred at other times, but additional data was not available. Some solids and liquid hydrocarbons were found in the pipeline during recent emptying of drip legs in the first twelve (12) miles and end (past MP 38, 61.2 km) portions of the pipeline. Any presence of solids near MP 18 (29 km) could not be identified as these drips were not part of the maintenance. Solids collected were found to be composed mainly of sand and iron; they also contained some glycol and sulfur. The line was found to be covered in places with fine silt, and the 2003 ILI report noted presence of possible scaling at some locations.

1.6.2.2 ICDA Region Definition

As flow in the pipe has been in two directions, it was necessary to define ICDA regions for each direction. Inlets were at the beginning (MP 0, 0 km) and near the end (MP 38.015, 61.179 km) of the line, and at MP 18.041 (29.034 km). The pressure was not reduced or increased for different parts of the pipeline and therefore did not play a role in ICDA region definition. ICDA regions were defined based on the inlets at MP 0 (0 km), MP 18.041 (29.034 km), and MP 38.015 (61.179 km). The pipeline was divided into four ICDA regions. ICDA Regions are shown in Table 1-22.

Table 1-22. Pipeline C: Region Definitions

<i>Region no.</i>	<i>Start miles (km)</i>	<i>Start Description</i>	<i>Flow Direction</i>	<i>End miles (km)</i>
1	0 (0)	inlet	N --> S	18.041 (29.034)
2	18.041 (29.034)	inlet	N --> S	38.015 (61.179)
3	38.015 (61.179)	inlet	S --> N	18.041 (29.034)
4	18.041 (29.034)	inlet	S --> N	0 (0)

1.6.3 Step 2: Calculations and Initial ICDA Site Selections (Pipeline C)

1.6.3.1 ICDA Calculations

For each flow direction, the company provided high and low pressures, as well as maximum, average, and low operating flow rates for the year 2001. Prior data were not available (See Table 1-23). It was assumed that the 2001 flow information provided is

representative of flow rates for the duration of the pipeline history. Velocity calculations to find the critical angles used the provided maximum flow rates and the low-average operating pressure of 800 psig (5.52 MPa). The results of the flow modeling calculations of critical angle for the variety of conditions are shown in Table 1-24. It should be noted that small differences in diameters for short lengths of the pipeline were considered in the final analysis and found to be negligible.

Table 1-23. Pipeline C: Flow Rates

	<i>Maximum</i> <i>MMSCFD (10³ m³/h)</i>	<i>Average</i> <i>MMSCFD (10³ m³/h)</i>	<i>Minimum</i> <i>MMSCFD (10³ m³/h)</i>
North to South	338.4 (399)	134.4 (159)	36 (42)
South to North	151.2 (178)	86.4 (102)	48 (57)

Table 1-24. Pipeline C: Calculated Critical Angles

Temperature = 60 F (16 C)

Low Average Operating Pressure = 800 psig (5.52 MPa)

<i>Direction</i>	<i>Maximum Flow Rate</i> <i>MMSCFD (10³ m³/h)</i>	<i>Pipe inner diameter</i> <i>inches (cm)</i>	<i>Critical Angle</i> <i>(degrees)</i>
North to South	338.4 (399)	21.12 (54)	16
North to South	338.4 (399)	19.25 (49)	25
South to North	151.2 (178)	21.12 (54)	4
South to North	151.2 (178)	19.25 (49)	5

The inclination profiles were calculated from the USGS data (as shown in Figures 1-8, 1-10, 1-12, and 1-14) and GIS ground survey data (as shown in Figures 1-7, 1-9, 1-11, and 1-13). There was also resurvey data available for some portions of Regions 1, 2, and 4 (See Figures 1-15, 1-16, and 1-17, respectively), although these were not considered in the GIS analysis (Site selections; Tables 1-15, 1-16, 1-17 and 1-25). The GIS survey data include pipe depth data at most locations. However, at some sites, the pipe could not be located due to deep burial (presumed to be greater than 20 feet deep).

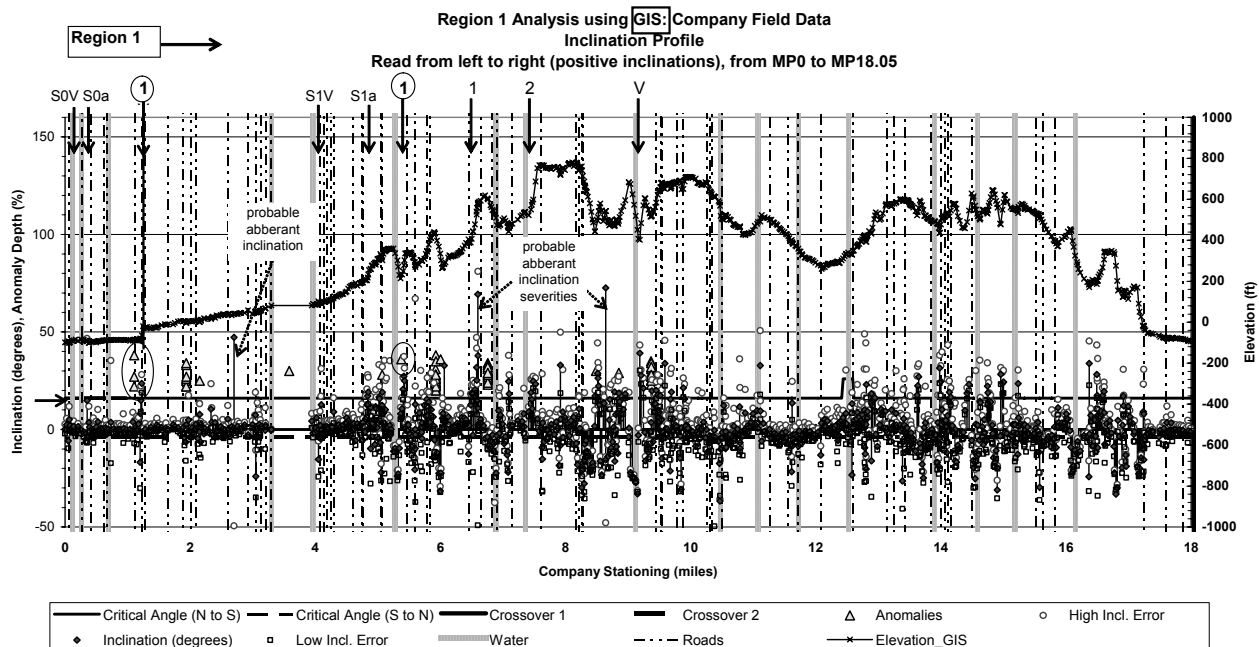


Figure 1-7. Pipeline C with GIS elevation data. Region 1: ICDA predictions versus ILI anomalies.

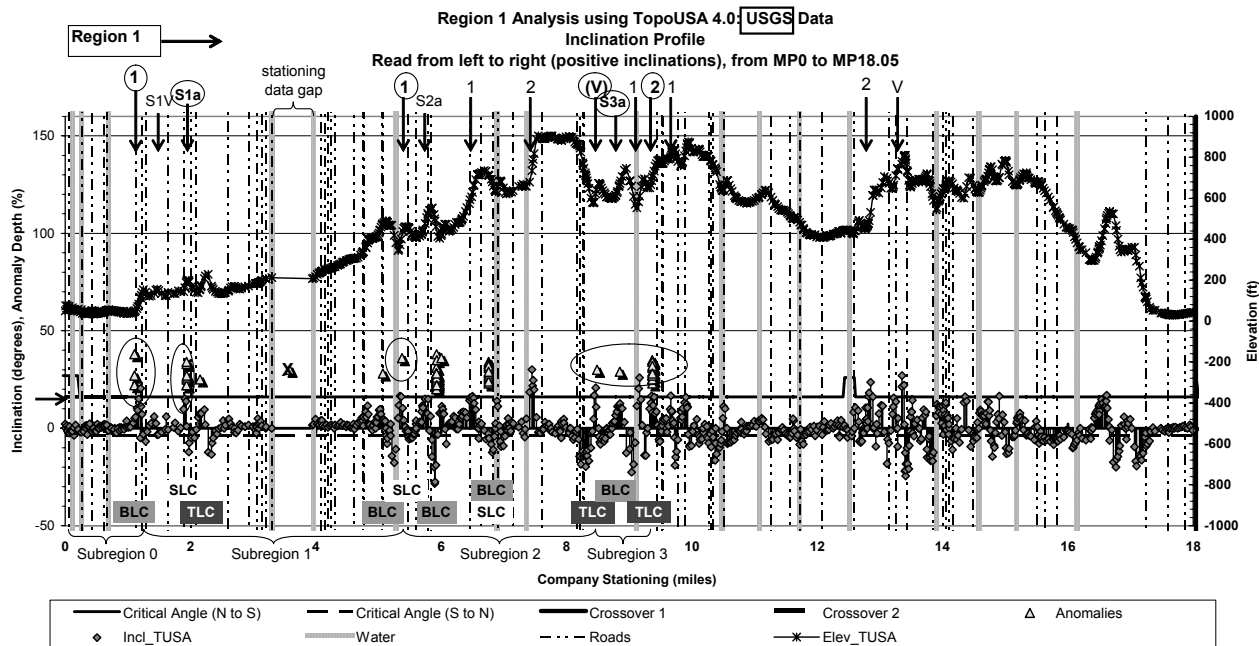


Figure 1-8. Pipeline C with USGS elevation data. Region 1: ICDA predictions versus ILI anomalies. SLC indicates ILI internal anomalies oriented on the sides of the pipeline, TLC on the top, and BLC on the bottom.

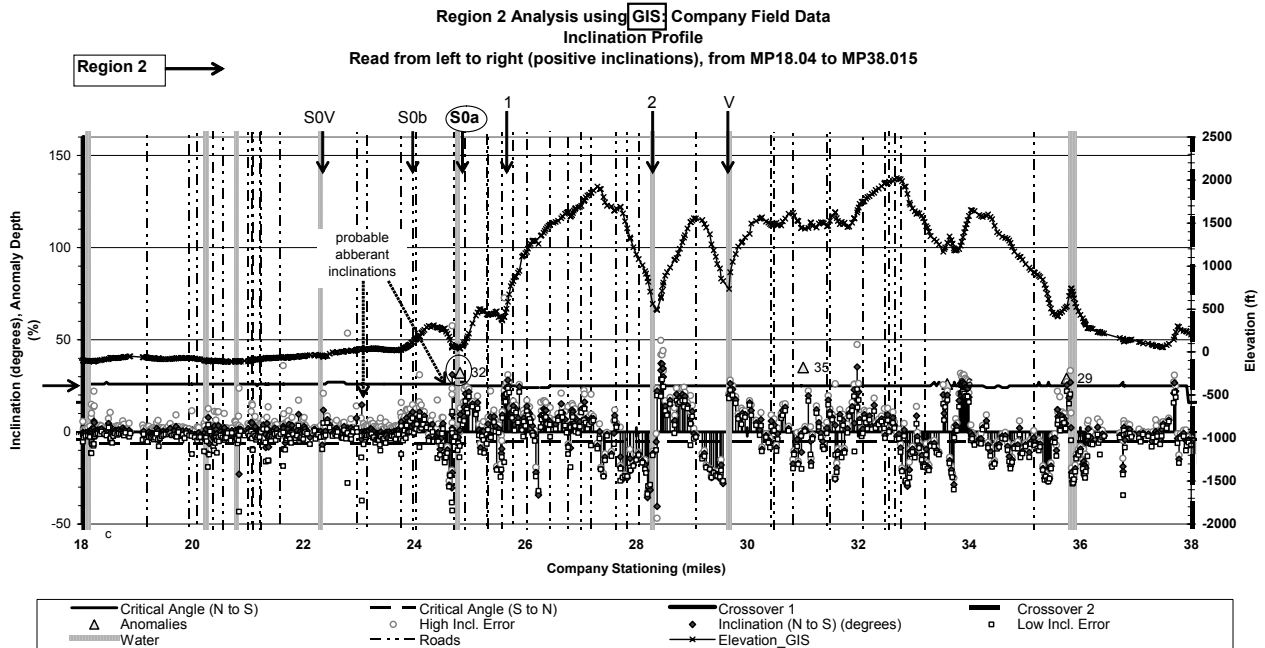


Figure 1-9. Pipeline C with GIS elevation data. Region 2: ICDA predictions versus ILI anomalies.

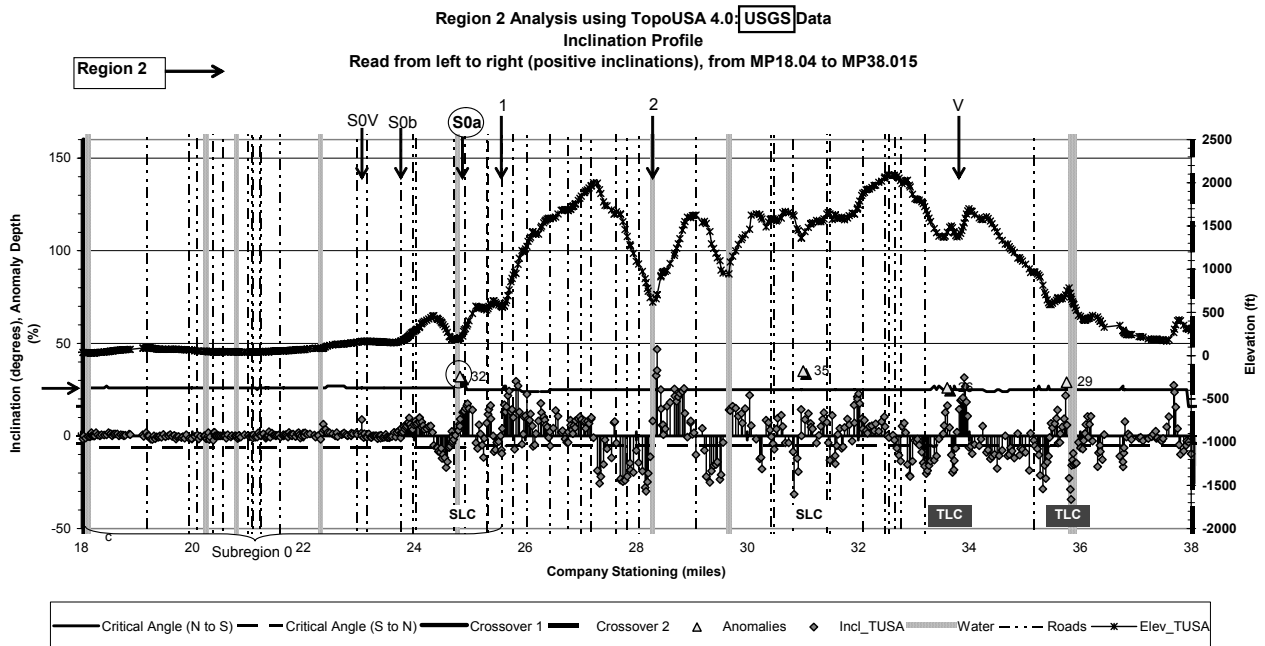


Figure 1-10. Pipeline C with USGS elevation data. Region 2: ICDA predictions versus ILI anomalies. SLC indicates ILI internal anomalies oriented on the sides of the pipeline, TLC on the top, and BLC on the bottom.

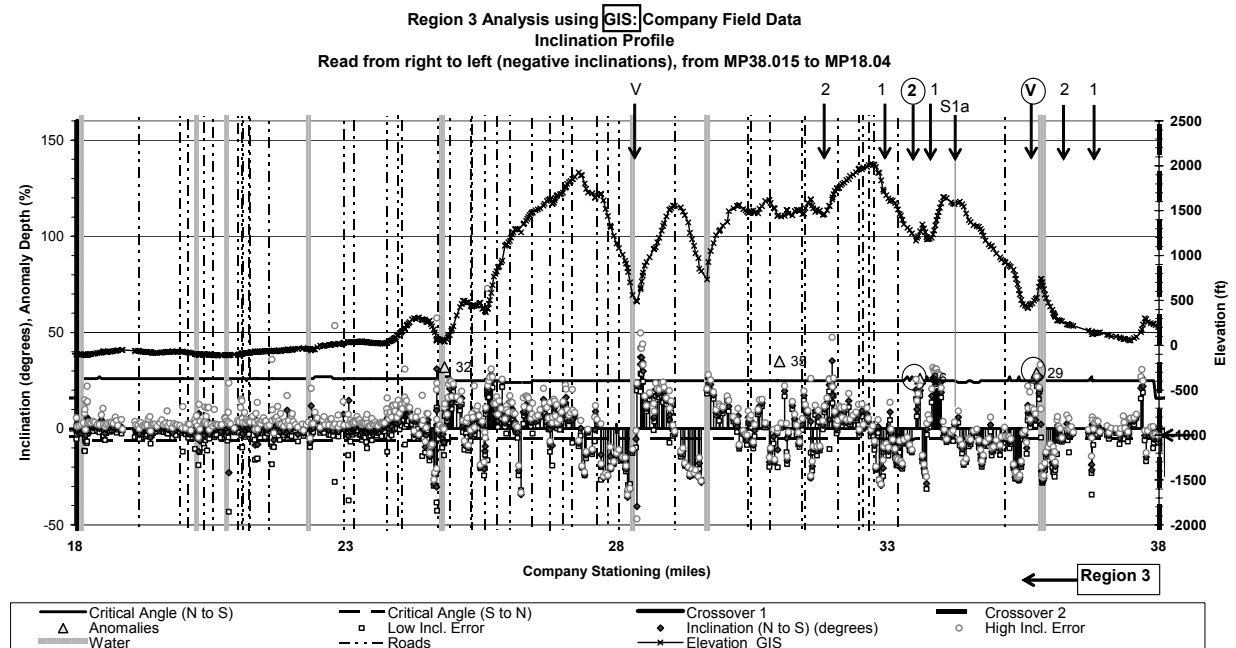


Figure 1-11. Pipeline C with GIS elevation data. Region 3: ICDA predictions versus ILI anomalies.

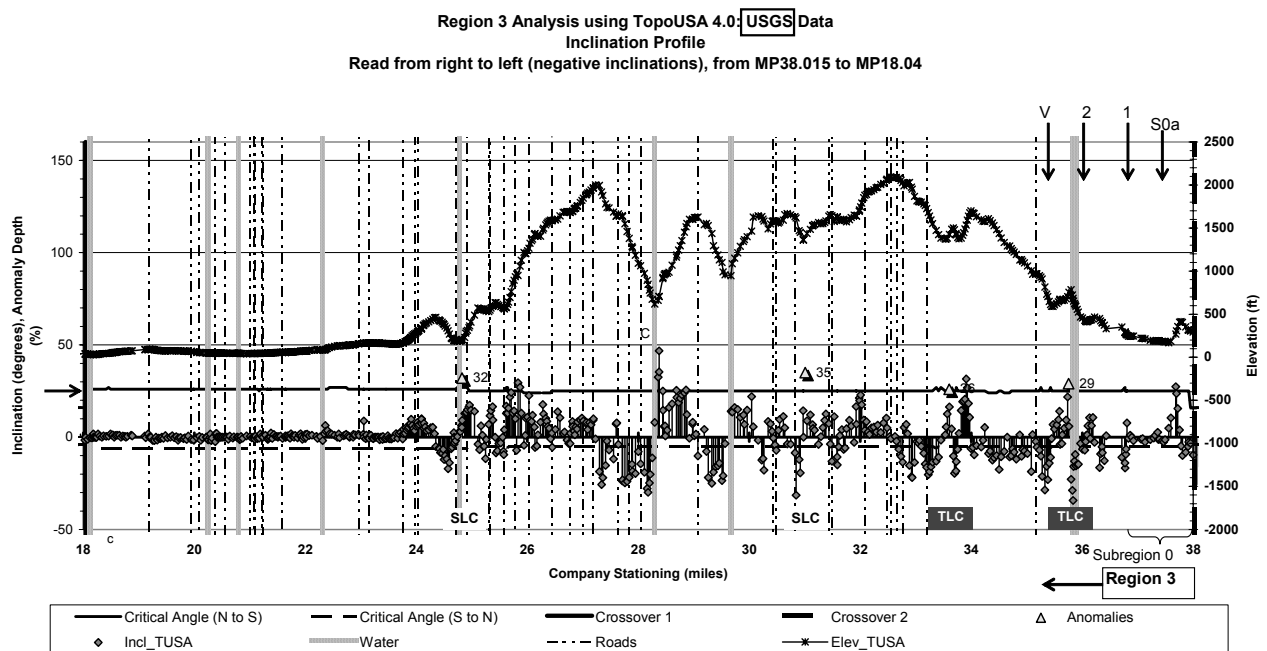
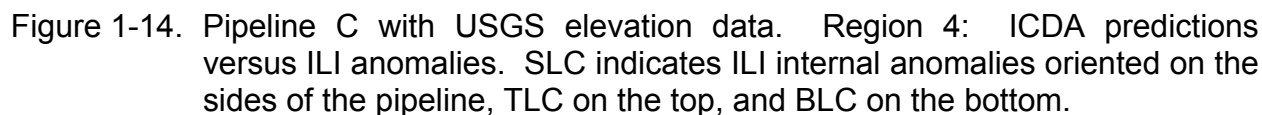
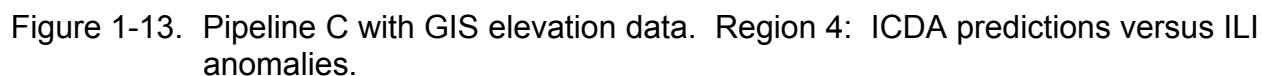


Figure 1-12. Pipeline C with USGS elevation data. Region 3: ICDA predictions versus ILI anomalies. SLC indicates ILI internal anomalies oriented on the sides of the pipeline, TLC on the top, and BLC on the bottom.



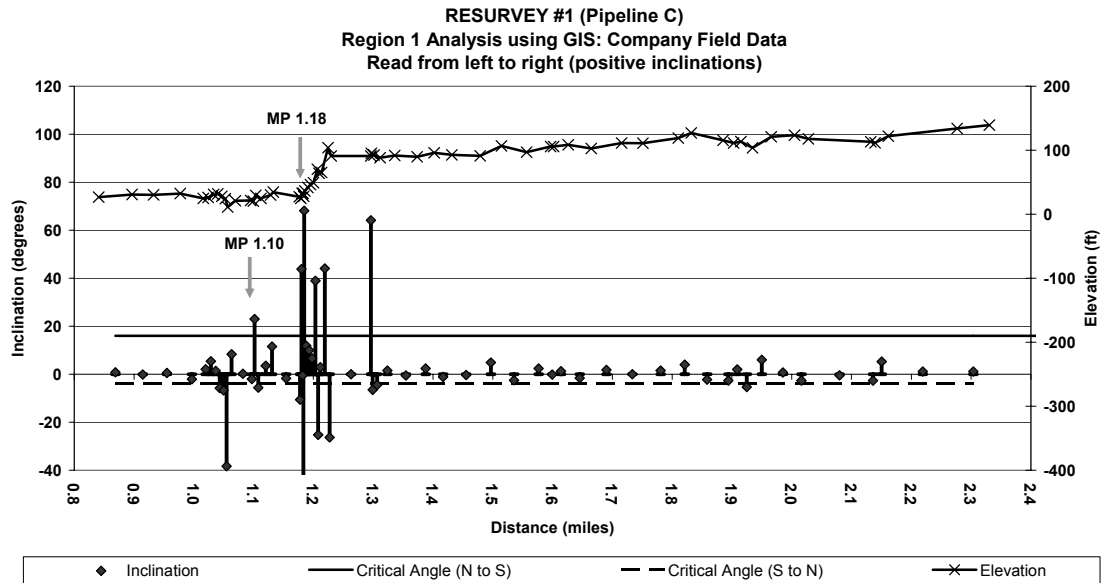


Figure 1-15. Pipeline C. GIS resurvey, Region 1.

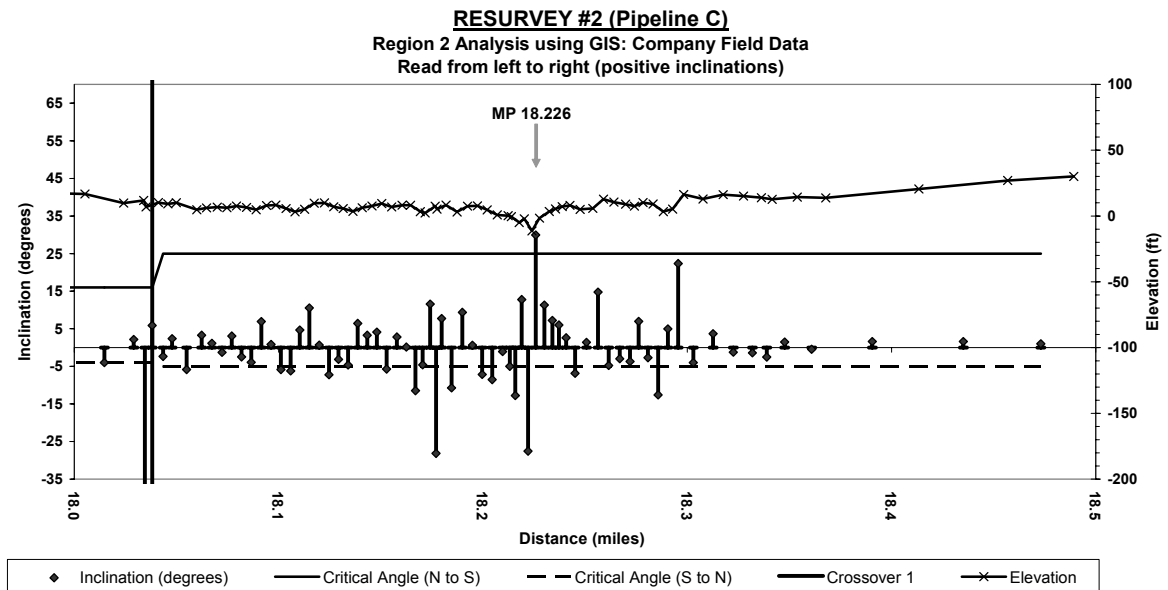


Figure 1-16. Pipeline C. GIS resurvey, Region 2.

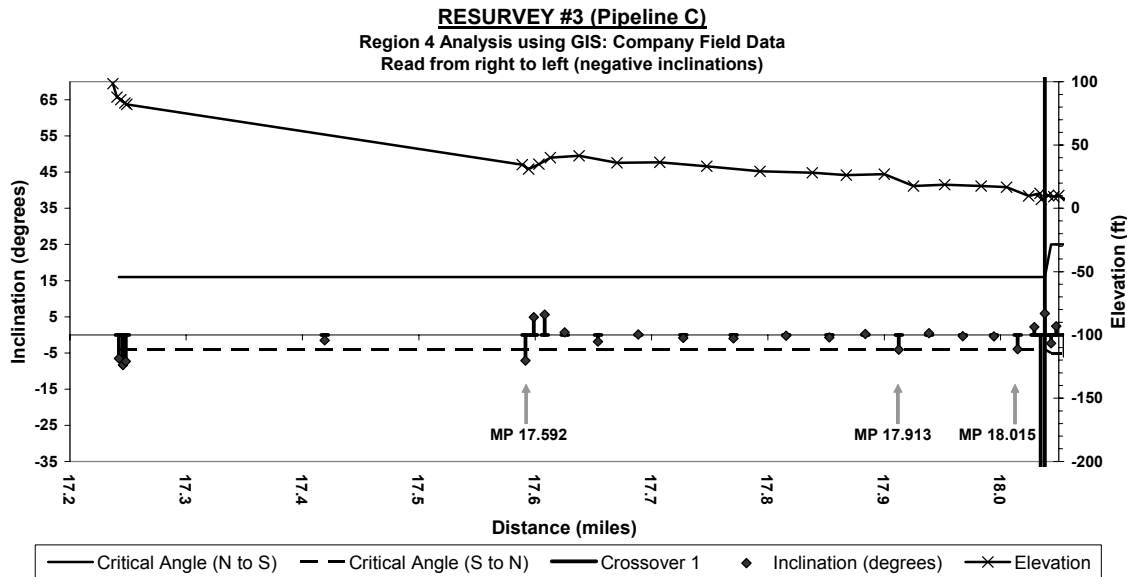


Figure 1-17. Pipeline C. GIS resurvey, Region 4.

1.6.3.2 Initial Site Selections

Flow modeling results are integrated with the inclination profile in Figures 1-7 through 1-14, which also show the elevation profile and ILI anomalies. Odd-numbered figures (Figures 1-7, 1-9, 1-11, and 1-13) shown on the top half of each page depict site selections based on the GIS inclination profile. On the bottom half of each page are the even-numbered figures (Figures 1-8, 1-10, 1-12, and 1-14), showing site selections for the same regions based on analysis of the USGS data. The plots are arranged this way so that the reader can compare results from selecting sites using the GIS data (above) with sites selected using the USGS data (below). It can be seen that results are similar, with more accurate site selection using the USGS data (note that problems with the GIS can be rectified in future surveys by better tool selection/ care with surveying). Because of the high error in the particular GIS tool used, the GIS plots are more complicated and difficult to read; shown is estimated low and high error inclinations for each point based on “sub-meter accuracy” *and* the actual calculated inclinations. Road and water crossings from the USGS data are shown on all eight figures. As the flow in Pipeline C was bi-directional, the inclinations on the composite plots must be read two ways. For North (MP 0) to South (MP 38) flow, ICDA Regions 1 and 2 (Figures 1-7 through 1-10), the positive inclination angle should be used and the plot read from left to right. South (MP 38) to North (MP 0) flow, ICDA Regions 3 and 4 (Figures 1-11 through 1-14) should be read from right to left using the negative inclination angles (i.e., -10 is actually 10°).

1.6.4 Step 3: Detailed Examination, Additional Site Selections (Pipeline C)

Pipeline C site selections are shown in Tables 1-25 and 1-26. Table 1-25 shows site selections using GIS data, while Table 1-26 shows site selections using USGS data. Twenty-six (26) sites were selected in the four regions using GIS data: nineteen (19) main sites

in regions, and seven (7) sites in subregions (Table 1-25). Twenty-seven (27) sites were selected in the four regions using USGS data: nineteen (19) main sites in regions, and eight (8) sites in subregions (Table 1-26). Because the GIS data had large apparent error margins, some assumptions were made in performing the GIS analysis, as follows. 1) The GIS analysis excluded apparently aberrant inclinations, where an aberrant inclination was defined as an inclination for which there were no error inclinations greater than the calculated inclination (if reading right to left, more negative) and/ or an inclination with very large error bars. 2) Three degrees was the smallest GIS angle considered significant in selecting ICDA sites for the Pipeline C analysis. 3) GIS measurement error calculations were based on reported “sub-meter” accuracy and are discussed in the “Uncertainties” section for Pipeline C, below. Site selection followed the recommended approach in draft standard (NACE International, 2005). The low error inclination angle (i.e., most negative if flow in North to South direction) was used to select the main region sites. Inclination angles calculated from given GIS coordinates were used in selection of subregion sites. The rationale was to be certain critical angle had been exceeded in the important region site selections; therefore the value representing the lowest inclination angle expected with sub-meter accuracy was used for these. Subregions were considered of secondary importance, and sub-meter accuracy bounds were not considered in their selections.

Table 1-25. Pipeline C Using Hand-Held GIS Field Data: Sites Selected For Detailed Examination By The ICDA Method

Region Number (n)	First or Second Iteration, or Validation?	SubRegion (S'n) and Order of Inspection (a, b, c...)	low error inclination angle (degrees)	inclination angle based exactly on GPS information (degrees)	location of inclination angle (miles)	location of inclination angle (km)	Notes
1	1		19		1.227	1.975	1st site with inclination > than critical.
1	1		19		5.425	8.731	2nd site with inclination > than critical.
1	1		19		6.576	10.583	Next site with inclination > than critical.
1	2		21		7.483	12.043	Next site with inclination > than critical.
1	V		30		9.187	14.785	Validation: inclination > than previous inclinations.
1		S0a		15	0.351	0.565	Largest angle in Subregion 0 (S0).
1		S0V		5	0.068	0.109	Validation: largest angle upstream previous angle in S0.
1		S1a	13	19	4.827	7.768	Largest angle in Subregion 1 (S1).
1		S1V	4	13	4.103	6.603	Validation: largest angle upstream previous angle in S1.
2	1		24	28	25.686	41.338	1st site; inclination 2nd greatest inclination in region.
2	2		28	37	28.464	45.808	2nd site; greatest inclination in region.
2	V		23	26	29.694	47.788	Validation: 3rd greatest inclination in region.
2		S0a		22	24.985	40.209	Largest angle in S0.
2		S0V		11	23.971	38.578	Validation: largest angle upstream previous angle in S0.
3	1		14		36.77	59.176	1st site with inclination > than critical.
3	2		17		36.1	58.097	2nd site with inclination > than critical.
3	V		25		35.446	57.045	Inclination > than previous inclinations.
3	1		25		33.722	54.270	Next site with inclination > than critical.
3	2		18		33.275	53.551	Next site with inclination > than critical.
3	1		29		32.885	52.923	Next site with inclination > than critical.
3	2		9		31.753	51.102	Next site with inclination > than critical.
3	V		47		28.375	45.665	Final Validation: inclination > than previous inclinations.
3		S1a		4	34.095	54.871	Only site in Subregion 1.
4	1		21		17.16	27.616	1st site with inclination > than critical.
4	2		13		16.962	27.298	2nd site with inclination > than critical.
4	V		28		16.816	27.063	Validation: inclination > than previous inclinations.

Table 1-26. Pipeline C *Using Computerized USGS Data*: Sites Selected for Detailed Examination by The ICDA Method

Region Number (n)	First or Second Iteration, or Validation?	SubRegion (S*n) and Order of Inspection (a, b, c...)	inclination angle based exactly on USGS information (degrees)	location of inclination angle (miles)	Notes	Internal Anomaly?	Critical Angle (degrees)
1	1		20	1.204	1st site with incl. > than critical.	Yes	16
1	1		16	5.362	2nd site with incl. > than critical.	Yes	16
1	1		16	6.521	Next site with incl. > than critical.	No	16
1	2		30	7.449	Next site with incl. > than critical.	No	16
1	V		21	8.467	Next site with incl. > than critical.	Yes	16
1	1		26	9.163	Next site with incl. > than critical.	No	16
1	2		17	9.369	Next site with incl. > than critical.	Yes	16
1	1		17	9.665	Next site with incl. > than critical.	No	16
1	2		24	12.851	Next site with incl. > than critical.	No	16
1	V		27	13.352	Next site with incl. > than critical.	No	16
1		S1a	15	1.931	Largest angle in Subregion 1.	Yes	16
1		S1V	6	1.42	Next largest angle upstream previous angle.	No	16
1		S2a	15	5.79	Largest angle in Subregion 2.	No	16
1		S3a	13	8.851	Largest angle in Subregion 3.	Yes	16
2	1		30	25.832	1st site with incl. > than critical.	No	25
2	2		47	28.376	2nd site with incl. > than critical.	No	25
2	V		32	33.908	Next site with incl. > than critical.	No	25
2		S0a	17	24.96	Largest angle in Subregion 0.	Yes	25
2		S0b	8	23.972	Next largest angle upstream previous angle.	No	25
2		S0V	5	22.433	Next largest angle upstream previous angle.	No	25
3	1		17	36.774	1st site with incl. > than critical.	No	5
3	2		34	35.835	2nd site with incl. > than critical.	No	5
3	V		29	35.327	Next site with incl. > than critical.	No	5
3		S0a	3	37.131	Largest angle in Subregion 0.	No	5
4	1		19	17.095	1st site with incl. > than critical.	No	4
4	2		20	16.764	2nd site with incl. > than critical.	No	4
4	V		25	13.411	Next site with incl. > than previous sites.	No	4

1.6.5 Step 4: Post-Assessment (Pipeline C)

1.6.5.1 Comparison of ILI with ICDA Results

Anomalies were considered to be predicted by ICDA if within ~50 ft (0.01 mi, or 0.016 km) of a model-predicted ICDA site (defined as length between low point and critical inclination angle). Table 1-27 shows correlations of ILI internal anomalies with ICDA predictions using both 1) GIS field data and 2) computerized USGS data. In addition, Tables 1-15 (GIS) and 1-18 (USGS) show the percentage of anomalies predicted by percentage depth of wall thickness, and Tables 1-16 (GIS) and 1-19 (USGS) by anomaly length. Tables 1-17 (GIS) and 1-20 (USGS) show the percentage of anomaly *groups* predicted, where an anomaly group is defined as a cluster of anomalies all within 0.02 mi. (0.032 km) of one another. Direct examinations were performed to verify some of the ILI information. Photos of some of those examinations are shown in Figures 1-18 through 1-25. All excavations were performed in Region 1, which has a critical inclination angle of 16 degrees.

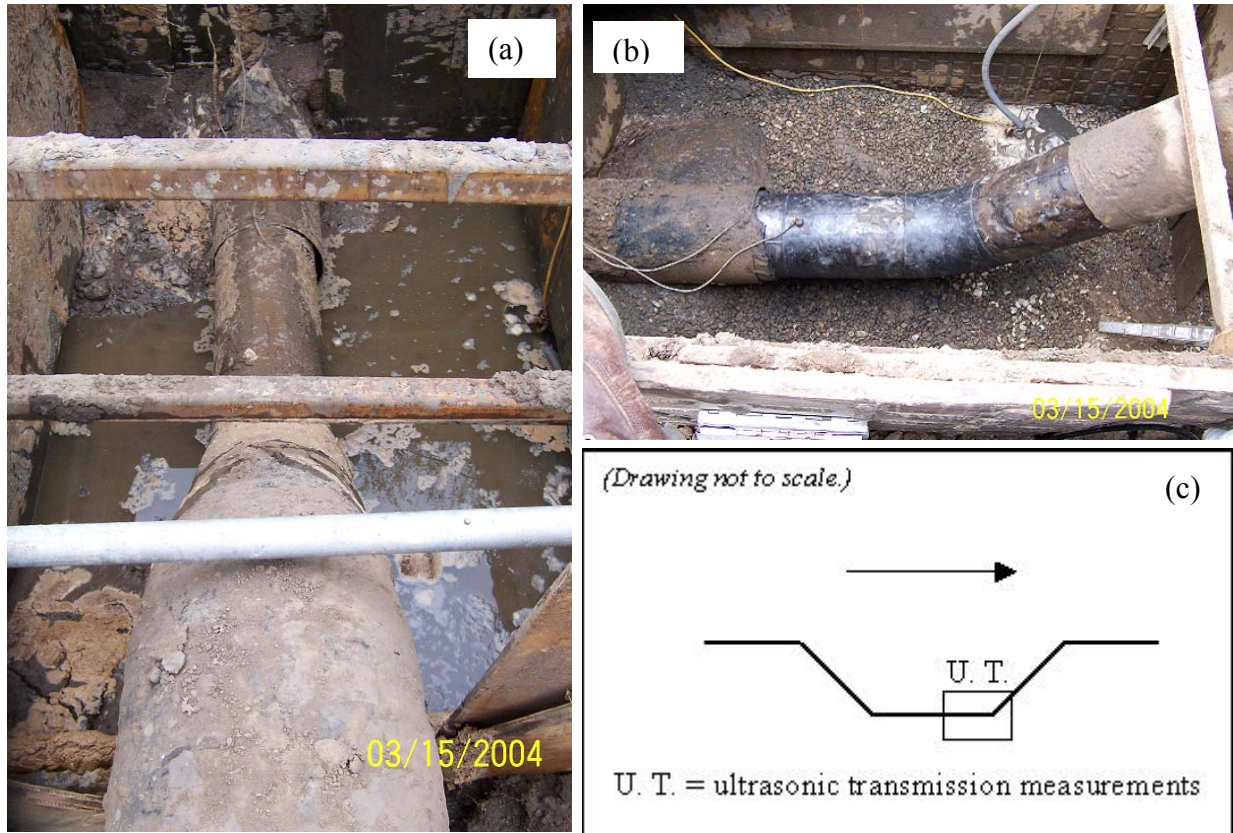


Figure 1-18. a (left), b (top right), and c (bottom right). Pipeline C. MP 0.69: Actual 1st inclination greater than the critical inclination angle in Region 1. Site is a false creek crossing. This angle was found on a walk of the line and was not identified in either USGS topographical data or the GIS surveys. Section inspected by UT: Low point to 45 degrees inclination, as shown. Arrows indicate direction of gas flow in Region 1.

Table 1-27. Pipeline C: ILI Tool Anomalies – Correlation with Sites Selected by ICDA Method

Location of Internal Anomaly (miles)	Location of Internal Anomaly (km)	Region nos.	% Depth	Length (in)	(cm)	Width (in)	(cm)	Orientation (0-clock)	Predicted using GIS Field data?	Predicted using Computerized USGS data?	Notes
1.105	1.778	1&4	38	1.3	3.3	3.0	7.6	6:11	Yes	Yes	Within 2 ft (0.61 m) of weld.
1.105	1.779	1&4	22	0.6	1.5	1.0	2.5	6:14	Yes	Yes	Within 2 ft (0.61 m) of weld.
1.105	1.779	1&4	27	0.6	1.5	0.6	1.6	5:50	Yes	Yes	Within 2 ft (0.61 m) of weld.
1.935	3.114	1&4	22	0.4	1.0	0.5	1.2	8:29	No	Yes	Within 2 ft (0.61 m) of weld.
1.935	3.114	1&4	25	0.5	1.3	0.5	1.3	9:02	No	Yes	Within 2 ft (0.61 m) of weld.
1.935	3.114	1&4	33	0.4	1.0	0.5	1.3	3:56	No	Yes	Within 2 ft (0.61 m) of weld.
1.935	3.114	1&4	34	0.4	1.0	0.4	1.1	3:50	No	Yes	Within 2 ft (0.61 m) of weld.
1.935	3.115	1&4	22	0.5	1.3	0.4	1.0	3:41	No	Yes	Within 2 ft (0.61 m) of weld.
1.936	3.115	1&4	26	0.4	1.0	0.4	1.1	3:45	No	Yes	Weld location
1.940	3.121	1&4	27	2.7	6.8	1.4	3.5	3:11	No	Yes	Within 1 ft (0.3 m) of ETS.
2.152	3.464	1&4	25	0.8	2.0	0.8	2.1	1:20	No	No	Within 2 ft (0.61 m) of weld.
5.068	8.157	1&4	28	0.5	1.3	1.3	3.3	6:21	No	No	
5.373	8.647	1&4	36	0.4	1.0	0.6	1.5	8:35	Yes	Yes	
5.922	9.530	1&4	31	0.4	1.0	0.3	0.8	6:18	No	No	
5.922	9.530	1&4	23	0.4	1.0	0.4	1.1	6:15	No	No	
5.922	9.531	1&4	21	0.9	2.3	0.5	1.3	3:51	No	No	
5.922	9.531	1&4	26	0.6	1.5	1.5	3.8	6:02	No	No	
5.922	9.531	1&4	24	0.3	0.8	0.7	1.7	6:02	No	No	
5.922	9.531	1&4	27	3.4	8.6	7.2	18.3	6:20	No	No	
5.922	9.531	1&4	27	0.5	1.3	0.3	0.7	6:17	No	No	
5.923	9.531	1&4	20	0.5	1.3	0.7	1.7	6:56	No	No	
5.923	9.532	1&4	23	2.8	7.0	1.9	4.9	6:39	No	No	
5.923	9.532	1&4	23	0.4	1.0	0.4	1.1	5:30	No	No	
5.923	9.532	1&4	24	0.4	1.0	0.5	1.3	5:42	No	No	
5.923	9.532	1&4	28	0.4	1.0	0.4	1.0	5:54	No	No	
5.923	9.532	1&4	24	0.3	0.8	0.3	0.7	5:30	No	No	
5.923	9.532	1&4	26	0.4	1.0	0.3	0.8	6:39	No	No	
5.923	9.533	1&4	24	0.4	1.0	0.3	0.7	6:18	No	No	
5.923	9.533	1&4	28	0.5	1.3	0.2	0.6	6:18	No	No	
5.923	9.533	1&4	25	0.5	1.3	0.8	1.9	6:47	No	No	
5.923	9.533	1&4	24	1.6	4.0	0.8	2.1	6:29	No	No	
5.924	9.533	1&4	25	0.4	1.0	0.4	1.1	7:20	No	No	
5.924	9.533	1&4	28	0.3	0.8	0.4	1.1	6:23	No	No	
5.924	9.533	1&4	20	0.4	1.0	0.7	1.7	7:02	No	No	
5.924	9.533	1&4	26	1.0	2.5	1.5	3.9	5:49	No	No	
5.924	9.534	1&4	28	1.5	3.8	2.3	5.9	6:49	No	No	
5.925	9.535	1&4	38	3.0	7.5	4.0	10.0	6:22	No	No	
5.927	9.539	1&4	22	0.8	2.0	0.6	1.4	5:43	No	No	
5.927	9.539	1&4	35	2.0	5.0	5.2	13.3	5:46	No	No	
6.002	9.660	1&4	36	3.2	8.1	6.0	15.4	5:26	No	No	Within 2 ft (0.61 m) of weld.
6.755	10.871	1&4	31	0.4	1.0	0.3	0.9	2:06	No	No	Within 2 ft (0.61 m) of weld.
6.755	10.871	1&4	23	0.3	0.8	0.5	1.3	3:15	No	No	Within 2 ft (0.61 m) of weld.
6.755	10.871	1&4	25	0.4	1.0	0.4	1.1	4:06	No	No	Within 2 ft (0.61 m) of weld.
6.755	10.871	1&4	26	0.3	0.8	0.4	1.1	4:30	No	No	Within 2 ft (0.61 m) of weld.
6.755	10.871	1&4	34	0.4	1.0	0.6	1.4	2:24	No	No	Within 2 ft (0.61 m) of weld.
6.755	10.871	1&4	27	0.3	0.8	0.4	1.1	2:24	No	No	Within 2 ft (0.61 m) of weld.
6.755	10.871	1&4	33	1.0	2.5	2.6	6.7	3:42	No	No	Within 2 ft (0.61 m) of weld.
6.755	10.871	1&4	24	0.5	1.3	0.5	1.3	4:33	No	No	Within 2 ft (0.61 m) of weld.
6.755	10.871	1&4	28	0.4	1.0	0.4	1.1	4:00	No	No	Within 2 ft (0.61 m) of weld.
6.755	10.871	1&4	32	0.4	1.0	0.3	0.8	2:54	No	No	Within 2 ft (0.61 m) of weld.
6.755	10.871	1&4	29	0.4	1.0	0.4	1.1	3:15	No	No	Within 2 ft (0.61 m) of weld.
8.486	13.657	1&4	30	0.9	2.3	1.4	3.6	0:16	No	Yes	
8.851	14.245	1&4	29	0.7	1.8	1.4	3.5	7:08	No	Yes	
9.368	15.076	1&4	35	0.4	1.0	0.5	1.3	9:43	No	Yes	
9.368	15.076	1&4	25	0.3	0.8	0.4	0.9	11:43	No	Yes	
9.368	15.076	1&4	25	0.4	1.0	0.3	0.9	10:52	No	Yes	
9.368	15.077	1&4	23	0.4	1.0	0.6	1.5	0:43	No	Yes	
9.368	15.077	1&4	27	0.3	0.8	0.3	0.8	11:33	No	Yes	
9.368	15.077	1&4	31	0.4	1.0	0.3	0.8	11:36	No	Yes	
9.368	15.077	1&4	25	0.4	1.0	0.4	1.0	0:48	No	Yes	
9.368	15.077	1&4	27	0.4	1.0	0.6	1.4	10:41	No	Yes	
9.368	15.077	1&4	29	0.4	1.0	0.3	0.7	11:33	No	Yes	
9.369	15.077	1&4	34	1.0	2.5	1.3	3.4	11:51	No	Yes	
9.369	15.078	1&4	32	0.5	1.3	0.3	0.8	10:33	No	Yes	
9.369	15.078	1&4	28	0.3	0.8	0.6	1.5	0:12	No	Yes	
24.824	39.950	2&3	32	0.8	2.0	1.5	3.9	3:28	Yes	Yes	
31.008	49.903	2&3	35	1.7	4.3	4.1	10.3	3:24	No	No	
33.603	54.080	2&3	26	3.1	7.8	7.5	19.1	11:06	Yes	No	
35.752	57.537	2&3	29	0.9	2.3	2.0	5.0	0:15	Yes	No	

Figures 1-18 and 1-19 were previously discussed (Pipeline C Summary, above). They depict excavation of MP 0.69, an upward-inclined elbow of 45 degrees, the first true site with inclination greater than the critical inclination angle though it was not identified in the USGS and GIS data sets; as indicated previously it was only observed later during a walk of the line. Full circumference ultrasonic transmission (UT) readings were conducted from the low point location to the beginning of the inclination and (see depiction in Figure 1-18(c)). As the ILI had suggested (no internal anomalies indicated), no internal corrosion was identified by UT at this location.



Figure 1-19. Pipeline C. MP 0.69: The actual 1st inclination greater than the critical inclination angle in Region 1. View of the excavation site after refilling (gravel covers excavation site).

Figures 1-20 through 1-22 show a double creek crossing at ~MP 1.10, the next inclination greater than critical. The exact pipeline profile under these creeks is unknown. Based on available information, the pipeline profile under the creeks looks something like that shown in the sketch in Figure 1-22, with the second creek slightly (~6 ft) higher than the first. There was thought to be only low point under the creeks, at about the location of the bisecting island. ILI internal anomalies are associated with the pipe under the island. It was not possible to excavate the creeks or island for the validation due to permitting and economic constraints; the location where anomalies were expected was thus not accessible for excavation. Instead, a location on the incline downstream of the second creek, past ILI anomaly indications, was inspected instead (as shown in Figures 1-20 and 1-21). As expected, no internal corrosion was found there.

The next site inspected was an increase in the inclination downstream from the previous site, at MP 1.2. Figures 1-23 and 1-24 depict the excavation; UT was performed at two locations and revealed no internal corrosion (ILI also did not show internal corrosion at this location).

The last excavation, at MP 5.923, was performed to verify ILI internal anomaly call-outs on a long downhill slope. These internal anomalies were not predicted by the dry gas ICDA model, and so this location was of interest. Internal corrosion of 10% depth of wall thickness was found along the bottom of the pipeline, which was subjected to complete circumference UT

as shown in Figure 1-25. These results may indicate a need to inspect low points to critical inclinations *in both directions* at sites (selected in Steps 2 and 3) for which there is a history of bidirectional flow.



Figure 1-20. Pipeline C. MP 1.10 Double creek crossing: Second inclination greater than the critical inclination angle in Region 1 (in USGS and GIS analyses of Pipeline C this is considered the first because MP 0.69 was missed). It is thought that there is a single low point under the island at center, which was inaccessible. Underneath the island is also where the ILI internal anomalies identified in this area are thought to be located. The excavation was performed on the incline on the downstream side after the second creek, as shown. Arrows indicate direction of gas flow in Region 1.



Figure 1-21. (left). Pipeline C. MP 1.10: From island: close-up view of excavation site after the second creek crossing in Region 1; above and to the left of drainage pipe; gravel patch marks the spot. Excavation site is downstream of low point. It is also downstream of MP 1.10 ILI internal anomalies, which were thought to be associated with the low point (underneath the island between the two creeks in a difficult to access location). Arrow indicates direction of gas flow in Region 1.

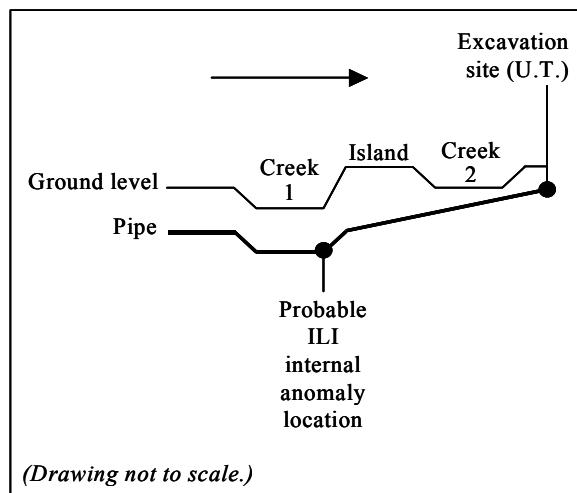


Figure 1-22. (right) Pipeline C. MP 1.10: Sketch of likely pipeline profile under double creek crossing. Arrow indicates Region 1 gas flow direction.

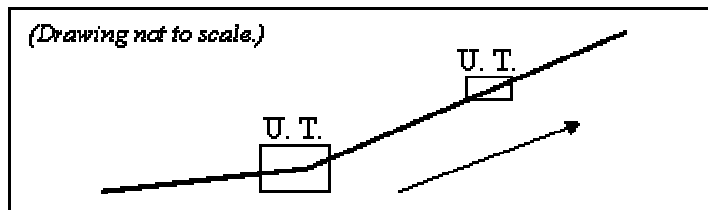


Figure 1-23. Pipeline C. MP 1.2: Top left and right: Bell hole further downstream on the incline after the first location predicted using USGS and GIS data; bottom part of this dig location is at a bend to greater inclination angle. Arrows indicate direction of gas flow in Region 1. Bottom left: Pipeline C. MP 1.2: Sketch of pipeline profile. Arrow indicates Region 1 gas flow direction.



Figure 1-24. Pipeline C. MP 1.2: Close ups of the two UT locations shown in Figure 17G. Upper location UT'd is shown on the left. Lower location is on the right. Field bend from gradual to steeper inclination can be seen at UT location in the right-hand picture. Arrows indicate Region 1 gas flow direction.

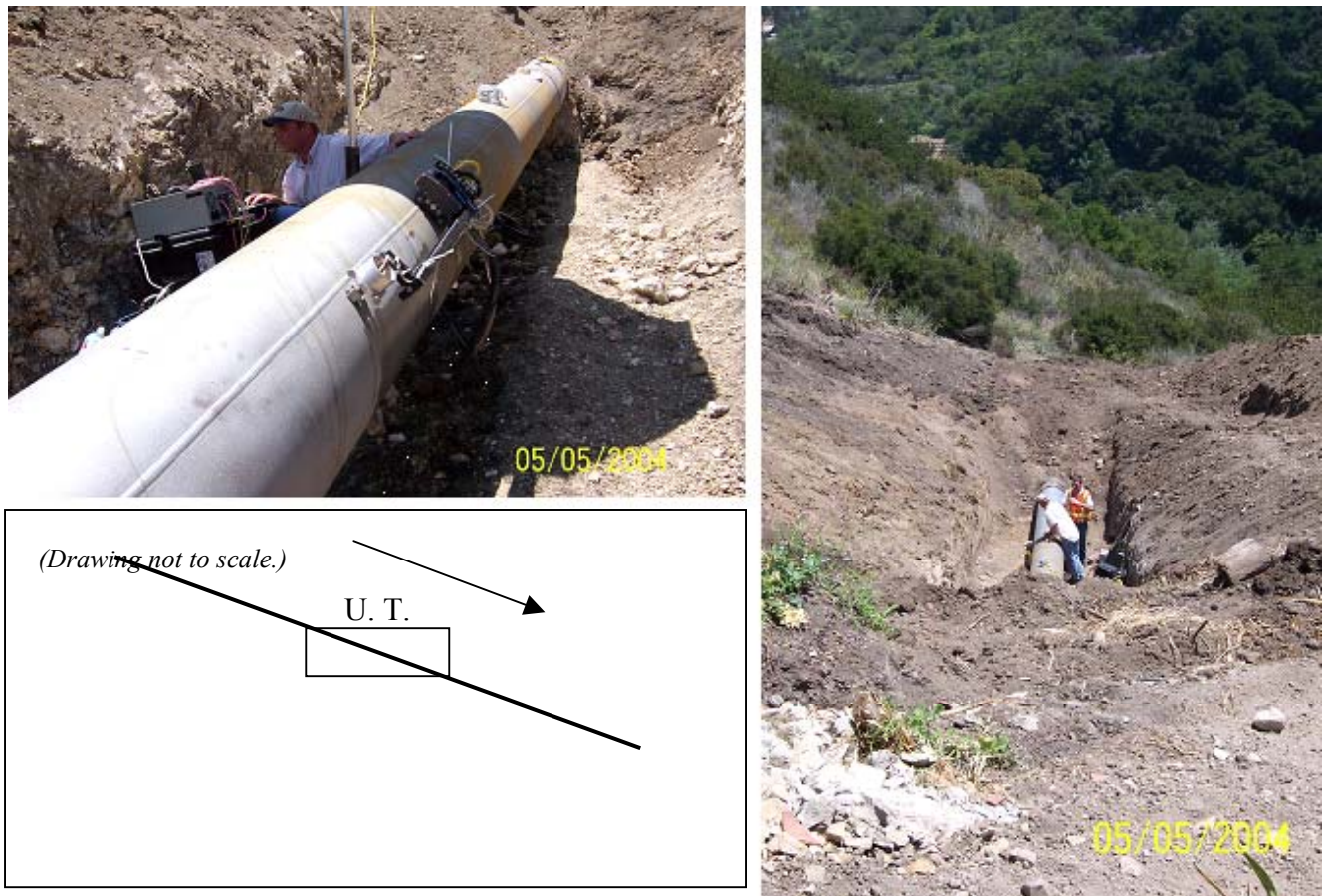


Figure 1-25. Pipeline C. MP 5.923: Location not predicted by ICDA dry gas model. Several ILI anomalies associated with this location. Direct examination and inspection revealed 10% depth of wall thickness internal anomalies found along the bottom of the line via ultrasonic transmission. Arrows indicate Region 1 gas flow direction. Lower left: Pipeline C. MP 5.923: Sketch of pipeline profile. Arrows indicates Region 1 gas flow direction.

1.6.5.2 Uncertainties

The effects of the reported sub-meter accuracy of GIS field measurements on the accuracies of the inclination angle calculations vary for different sets of GIS measurement points. In the case of two points separated by a short distance, the effect of accuracy on uncertainty of the inclination angle calculation may be very large, while it may be less severe for points separated by a longer distance. But concurrently, a longer distance between points increases the likelihood for missing a significant inclination. “High” and “Low” errors were calculated between each set of two points assuming sub-meter vertical and horizontal accuracy mean +/- 1m in horizontal and vertical directions. In fact, sub-meter accuracy refers typically

only to the horizontal positioning, and depending on the GIS tools used can mean more inaccuracy than it suggests. Depending on the survey-type used, horizontal stationing of “sub-meter” accuracy may mean accuracy is within +/- one meter but, more frequently, this is low, and actual uncertainty is much higher. Vertical stationing is usually twice as inaccurate and more. Therefore, these “error” calculations actually are better-case scenarios, where the actual uncertainty is greater.

For the calculations, the horizontal distance between points was shortened by two (2) meters (two points times one meter error per measurement point). The errors were approximated using this shortened distance and vertical deviation by positive (High) or negative (Low) two (2) meters. High and Low inclination angle ranges are shown plotted with inclination angles for each pair of GIS field data, in Figures 1-7, 1-9, 1-11, and 1-13. Some horizontal distance uncertainties are estimated in Table 1-28. (These are rough estimates only; as suggested above uncertainty is actually expected to be greater). Also sources of uncertainty are the possibilities that the 2001 flow rate and/ or pressure data used in the analysis do not accurately represent all flow rates and pressures for the duration of the pipeline history.

Table 1-28. Pipeline C: Estimated Horizontal Uncertainties

Regions	GIS Reported Accuracy (Sub-meter), miles (km)	GIS to Company Stationing (Estimated), miles (km)	ILI to Company Stationing (Estimated), miles (km)	National Map Accuracy Standards miles (km)
1 through 4	0.001 (0.0016)	0.015 (0.024)	0.015 (0.024)	0.0126 (0.02)

1.7 Pipeline D

1.7.1 Summary

General information about Pipeline D and typical conditions were supplied. Pipe outer diameter was 20 inches (51 cm). Wall thickness was 0.312 inches (0.79 cm) for most of the pipe length and was 0.25, 0.375, 0.437, and 0.5 inches (0.64, 0.95, 1.11, and 1.27 cm) for short portions of the pipe. Operating range reported was 500 to 600 psi (3.45 to 4.14 MPa), maximum operating pressure (MAOP) 800 psi (5.52 MPa). Gas flow has always been uni-directional, with maximum flow rate said to have averaged 40MMSCFD ($47.2 \times 10^3 \text{ m}^3/\text{h}$). There were several inlets and outlets; maximum flow rates for different regions of the pipe theoretically ranged 19 to 150 MMSCFD (22.4 to $176.9 \times 10^3 \text{ m}^3/\text{h}$), according to 2002 flow data. Gas was dry, although based on 2001-2002 gas quality data liquid upsets appear to have occurred.

A set of 2000 ILI anomaly information was provided for the Detailed Examination Step. Some information about an internal corrosion leak repair was available. Distance and elevation were obtained from computerized USGS maps, and the pipe depth was assumed constant.

Recent ILI, some detailed examination, all required and much recommended data were provided for Pipeline D. Therefore, Pipeline D is an ideal candidate for ICDA Validation and is ranked Category I (Ideal).

The ICDA Method predicted locations of internal corrosion in Pipeline D. Eighty-seven percent of ILI-identified internal anomalies showing greater than 30% depth of wall thickness were identified by the ICDA method when a horizontal uncertainty of +/- 200 ft (61 m) was employed, as shown in Tables 1-29 and 1-30 and in the overview summary, Table 1-4. Of the anomalies indicated as having greater than 30% depth of wall thickness, using the same uncertainty bounds, 79% of ILI-anomalies having length greater than ½-ft (15 cm) were predicted. Using the horizontal uncertainty of +/- 200 ft (61 m), 63% of all >15% depth of wall thickness internal call-outs having greater than ½-ft length were predicted; see Table 1-31. There was one known historical internal corrosion leak, and it was predicted by ICDA. The leak occurred in 1993 at ~MP 9.5 (15.3 km; lake crossing). The total pipe length evaluated by ICDA was 26.52 miles (42.7 km).

Table 1-29. Pipeline D: Summary of Results A) for Anomalies with >30% Percentage Depth of Wall Thickness and B) for Anomalies of > 1 Ft (0.305 M) Length

<i>Internal Anomaly Descriptions</i>	<i>Total Number of Sites Examined</i>	<i>% ILI Internal Anomalies Predicted by ICDA utilizing USGS/ ILI</i>	<i>% ILI Internal Anomalies Predicted by ICDA utilizing USGS/ ILI</i>
		<i>Uncertainty +/- 200ft (61 m)</i>	<i>Uncertainty +/- 100ft (30.5 m)</i>
>30% Depth Wall Thickness	69	87	71
> 1-ft (0.305 m) Length	147	63	50

Table 1-30. Pipeline D: Percentage of Tool-Identified Internal Anomalies Predicted by ICDA, by Percentage Depth of Wall Thickness

Validation Results based on Percentage Depth of Wall Thickness						
Error Bounds	no. of 30-39% depth	30-39% depth no. Predicted	30-39% depth % Predicted	no. of 40-49% depth	40-49% depth no. Predicted	40-49% depth % Predicted
If +/- 100ft	51	37	73	18	12	67
If +/- 200ft	51	46	90	18	14	78

TOTAL no.	Total no. Predicted	TOTAL % Predicted
69	49	71
69	60	87

Table 1-31. Pipeline D: Percentage of Tool-Identified Internal Anomalies Predicted by ICDA, by Anomaly Length (1. >30% Depth Of Wall Thickness, and 2. >15% Depth Internal Anomalies Considered)

ICDA Validation Results based on Anomaly Length (For anomalies having 30% Depth of Wall Thickness or Greater)
For Anomaly Length >1 ft, maximum length 3 ft.

Error Bounds	no. with Length 1-3 ft (max.) (0.3 - 0.91 m)	1-3 ft Length (0.3 - 0.91 m) no. Predicted	1-3 ft Length (0.3 - 0.91 m) % Predicted	no. with Length 6-12 in.	6-12 in. Length (0.15 - 0.3 m) no. Predicted	6-12 in. Length (0.15 - 0.3 m) % Predicted	TOTAL no.	Total no. Predicted	TOTAL % Predicted
If +/- 100ft	14	8	57	14	9	64	28	17	61
If +/- 200ft	14	10	71	14	12	86	28	22	79

ICDA Validation Results based on Anomaly Length (For ALL suspected internal corrosion anomalies)
For Anomaly Length >1 ft, maximum length 3 ft.

Error Bounds	no. with Length 1-3 ft (max.) (0.3 - 0.91 m)	1-3 ft Length (0.3 - 0.91 m) no. Predicted	30-39% depth (0.3 - 0.91 m) % Predicted	no. with Length 6-12 in.	6-12 in. Length (0.15 - 0.3 m) no. Predicted	6-12 in. Length (0.15 - 0.3 m) % Predicted	TOTAL no.	Total no. Predicted	TOTAL % Predicted
If +/- 100ft	54	27	50	93	44	47	147	71	48
If +/- 200ft	54	34	63	93	61	66	147	95	65

1.7.2 Step 1: Pre-Assessment (Pipeline D)

1.7.2.1 Collected Data and Feasibility Assessment

An internal corrosion leak was reported to have occurred at MP 9.5 (15.3 km) in 1993. The ILI tool run which was used in this analysis is from the year 2000.

Gas analyses were available for the period 2001-2002. The analyses show no evidence of presence of hydrogen sulfide. The maximum CO₂ content reported was 2.3%; CO₂ content typically ranged 1 to 1.9%. Maximum water content for the period 2001 to 2002 was not shown to exceed 6 lb/MMSCF (96 mg/m³) between MP 1.7 (2.7 km) and MP 15 (24.1 km). However, based on the same data it appears saturated gas existed for some durations between MPs 0 (0 km) and 1.7 (2.7 km) and between MPs 15 (24.1 km) and 32.16 (51.8 km), suggesting possible liquid upsets. Gas statistics for the different regions for 2001-2002 are shown in Table 1-32. Corrosion inhibitor was first used in, and is still in use as of, 1999. As ILI data was collected in 2000, the ICDA analysis addresses internal corrosion that occurred in the period prior to the introduction of corrosion inhibitor in 1999. Weight loss coupons have also been in use as of 1999.

Table1-32. Pipeline D: 2001-2002 Gas Analysis Statistics

Location miles (km)	Region	Maximum % CO ₂ measured	Maximum H ₂ O content measured lb/MMSCF (mg/m ³)
0 (0)	1	1.648	11.4 (183)
1.7 (2.74)	2	1.167	2 (32)
7.82 (12.59)	3	1.96	6 (96)
9.66 (15.55)	4	2.018	6 (96)
10.26 (16.51)	5	2.298	6 (96)
11 (17.7)	6	1.988	5 (80)
11.8 (19)	7	1.721	6 (96)
15 (24.14)	8	1.621	6 (96)
16.58 (26.68)	9	1.647	18 (288)
19.04 (30.64)	10	1.526	30 (481)
21.6 (34.76)	11	1.991	11.8 (189)

Pipeline D passed most of the criteria for assessment by ICDA (NACE International, 2005). There was insufficient information to judge on some of the criteria. Batch treatments were reportedly performed semi-annually; information on the duration this procedure had been in place was unavailable. It was also reported that approximately one drum of solids/ sludges was removed at the receiver with each batch treatment; it is unknown what significance if any these solids/sludges hold for ICDA. A third unknown is the frequency of liquid upsets. Lastly, a small number, 3%, of ILI-indicated internal anomalies were associated with the top of the pipeline; the source/validity of these is unknown.

1.7.2.2 ICDA Region Definition

Flow in the pipe has been in only one direction. Therefore it was necessary to define ICDA regions in only one direction. The pressure was not reduced or increased for different parts of the pipeline and therefore did not play a role in ICDA region definition. The flow rate, however, changed at inlets and outlets. ICDA regions were therefore defined based on inlets. The pipe length for ICDA validation was between MP 0 (0 km) and MP 32.06 (51.6 km). The pipeline was divided into eleven ICDA regions. Inlets and outlets are shown with Region definitions in Figure 1-26.

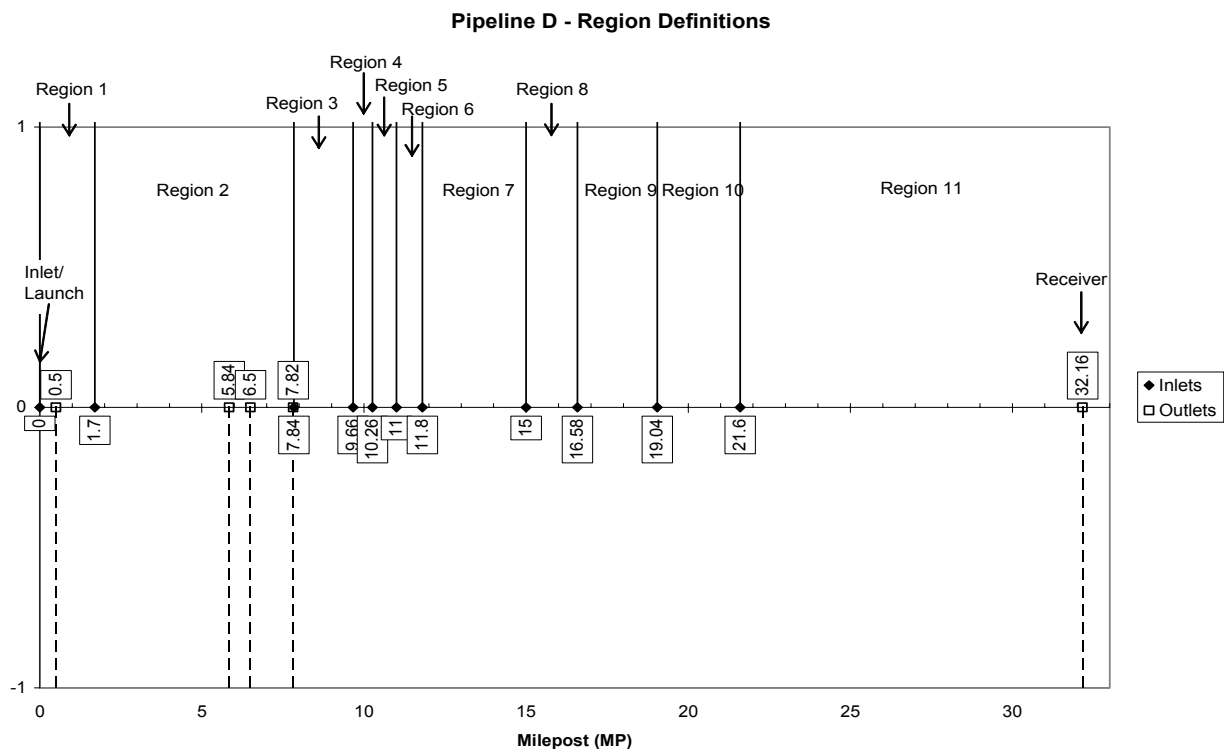


Figure 1-26. Pipeline D. ICDA regions based in inlet locations, uni-directional flow.

1.7.3 Step 2: Calculations and Initial ICDA Site Selections (Pipeline D)

1.7.3.1 ICDA Calculations

Each calculation of the maximum flow rate for any location on the pipeline assumed all inlets were at their maximum 2001 to 2002 flow rates and outlets were not in use. The low operating pressure of 500 psi (3.45 MPa), and inner diameter of 19.38 inches (49.2 cm) were used in the calculations of critical inclination angles. The results of the flow modeling for the variety of conditions are shown with the maximum flow rates in Table 1-33. Small differences in diameters (due to different wall thicknesses) present for short lengths of the pipeline were considered in the final analysis and found to be negligible in their effects.

Table 1-33. Pipeline D: Maximum Flow Rates and Critical Angles

Inner diameter = 19.38 inches (49.2 cm)

Temperature = 60 degrees F (16 degrees C)

Pressure = 500 psia (3.45 MPa)

<i>Region</i>	<i>Start</i> miles (km)	<i>End</i> miles (km)	<i>Start</i> <i>Description</i>	<i>Max Flowrates</i> MMSCFD (10 ³ m ³ /h)	<i>Critical Angle</i> degrees
1	0 (0)	0.5 (0.8)	inlet, launch	33.7 (39.8)	0.3
	0.5 (0.8)	1.7 (2.74)	outlet	18.8 (22.2)	0.3
2	1.7 (2.74)	5.84 (9.4)	inlet	68.9 (81.3)	0.9
	5.84 (9.4)	6.5 (10.46)	outlet	68.9 (81.3)	0.9
	6.5 (10.46)	7.82 (12.59)	outlet	68.8 (81.2)	0.9
	7.82 (12.59)	7.84 (12.62)	outlet	68.8 (81.2)	0.9
3	7.84 (12.62)	9.66 (15.55)	inlet	69 (81.4)	0.9
4	9.66 (15.55)	10.26 (16.51)	inlet	69.4 (81.9)	1
5	10.26 (16.51)	11 (17.7)	inlet	99.4 (117.3)	3
6	11 (17.7)	11.8 (19)	inlet	104.4 (123.1)	4
7	11.8 (19)	15 (24.14)	inlet	104.8 (123.6)	4
8	15 (24.14)	16.58 (26.68)	inlet	104.9 (123.7)	4
9	16.58 (26.68)	19.04 (30.64)	inlet	105.3 (124.2)	4
10	19.04 (30.64)	21.6 (34.76)	inlet	105.4 (124.3)	4
11	21.6 (34.76)	32.16 (51.76)	inlet	149.7 (176.6)	7

1.7.3.2 Initial Site Selections

Flow modeling results were integrated with the inclination profile, as shown in Figures 1-27 to 1-30, which also show elevation profile, internal anomalies, and road and water crossings. As flow was unidirectional, plots should be read from left to right (positive inclinations) only.

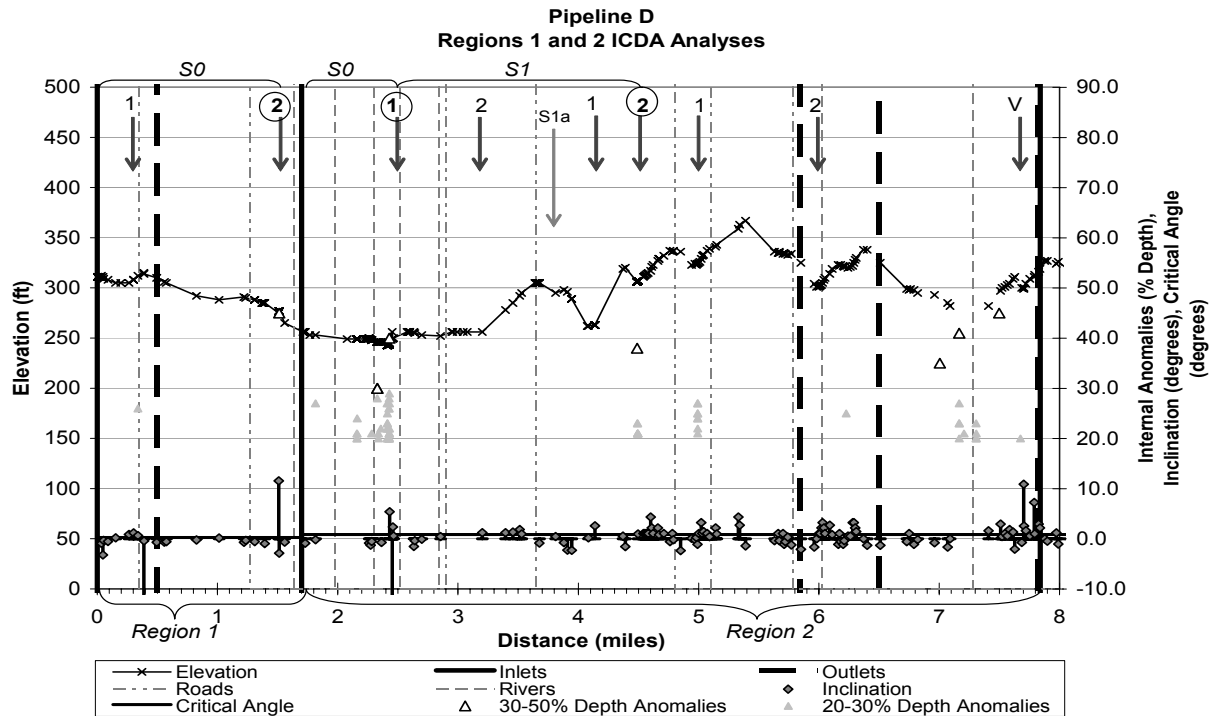


Figure 1-27. Pipeline D. Regions 1 and 2: ICDA predictions versus ILI anomalies.

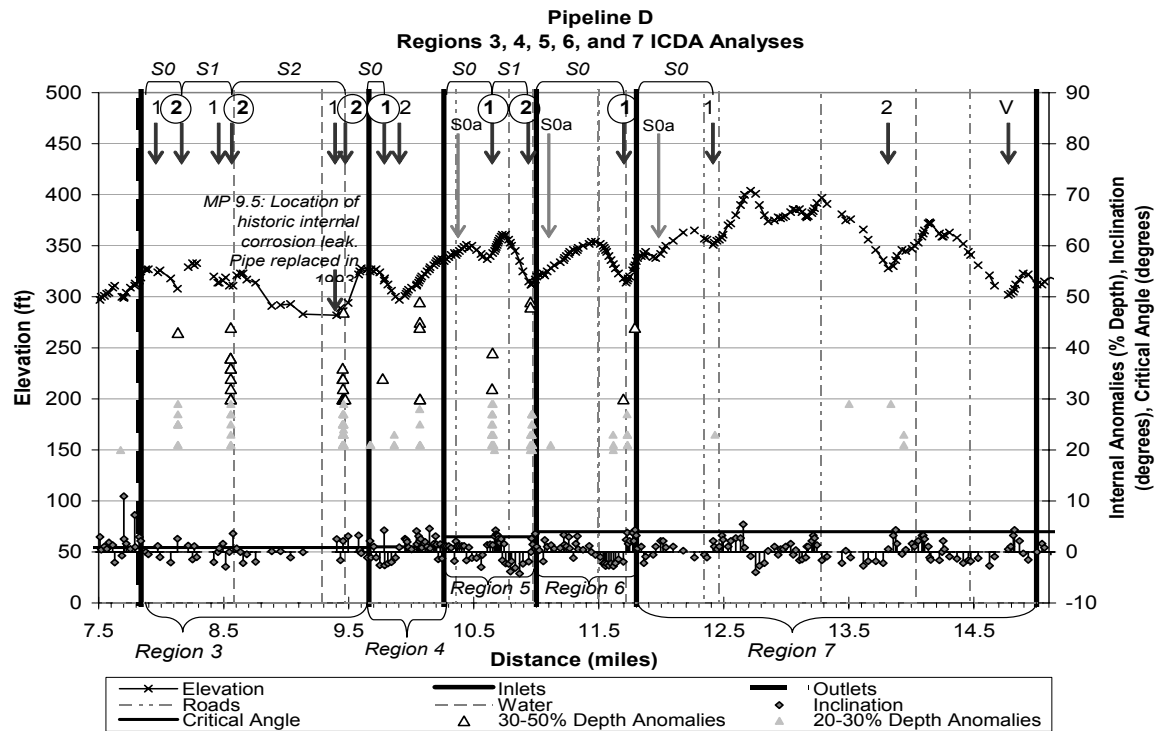


Figure 1-28. Pipeline D. Regions 3, 4, 5, 6, and 7: ICDA predictions versus ILI anomalies. Note location of historic leak at MP 9.5.

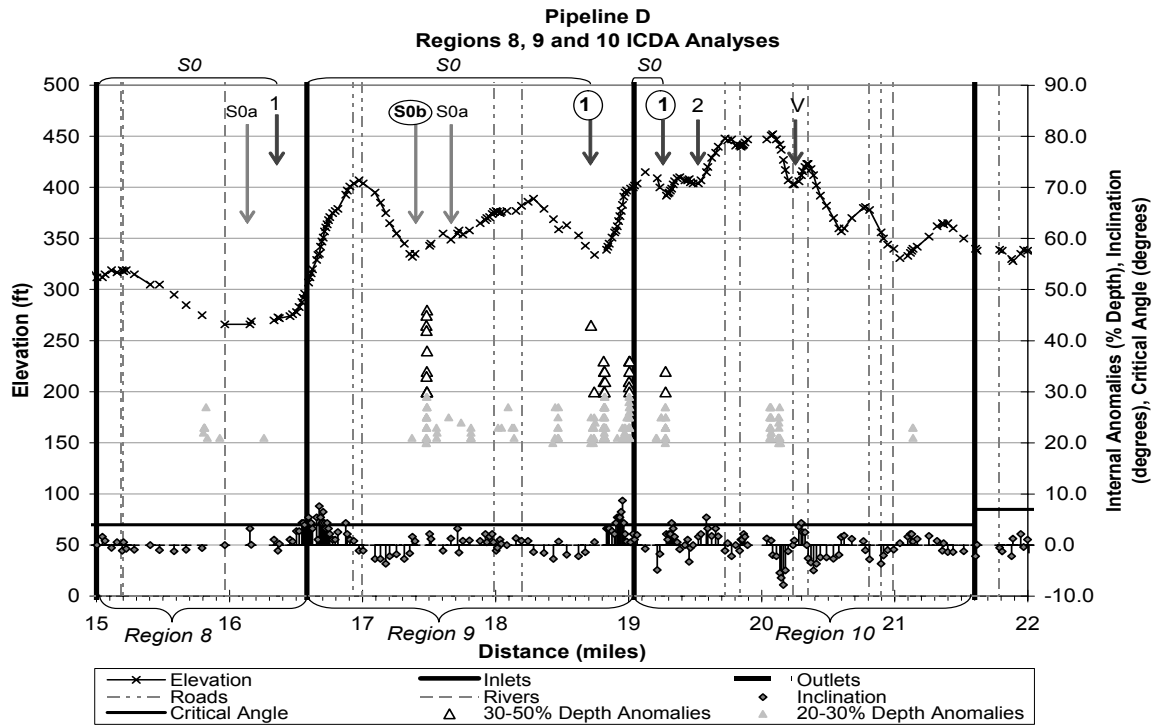


Figure 1-29. Pipeline D. Regions 8, 9, and 10: ICDA predictions versus ILI anomalies.

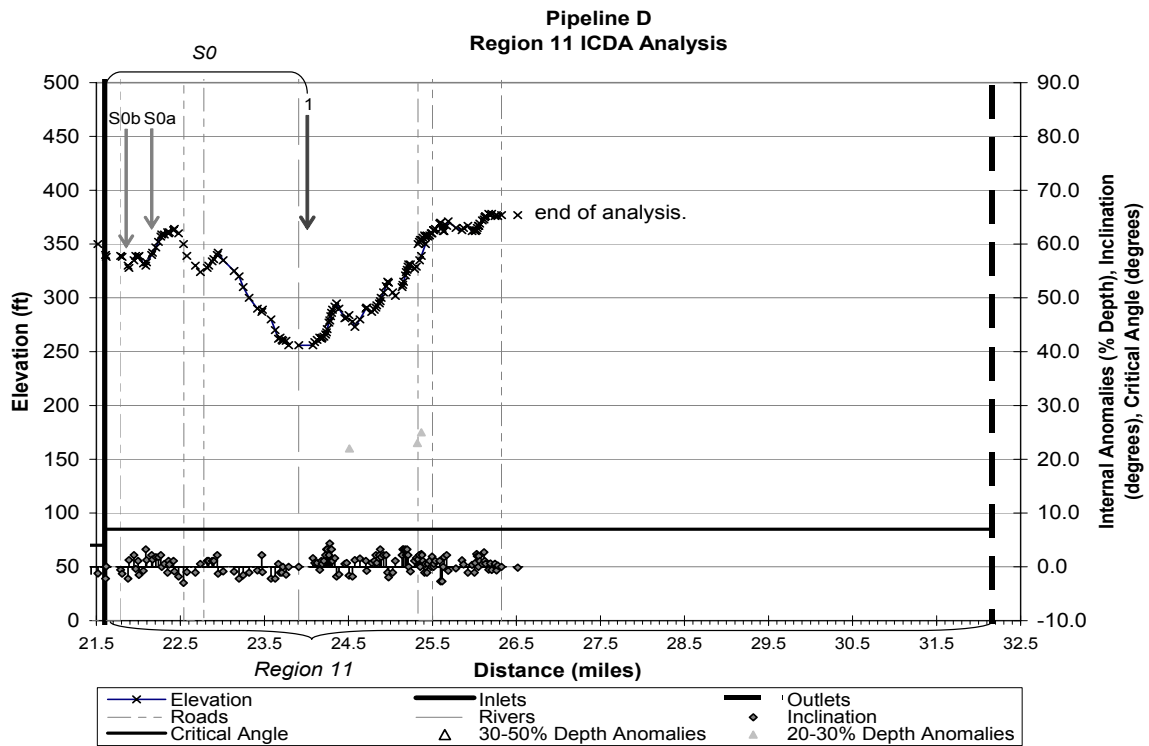


Figure 1-30. Pipeline D. Region 11: ICDA predictions versus ILI anomalies.

1.7.4 Step 3: Detailed Examination, Additional Site Selections (Pipeline D)

Pipeline D site selections are shown in Table 1-34. The examination followed the procedure described in the NACE draft standard (NACE International, 2005).

Table 1-34. Pipeline D: Sites Selected for Detailed Examination by The ICDA Method

Region Number (n)	First or Second Iteration, or Validation?	SubRegion (S*n) and Order of Inspection (a, b, c...)	inclination angle based on computerized USGS data (degrees)	START location of inclination angle (miles)	END location of inclination angle (miles)	Notes	Internal Anomaly?	Critical Angle (degrees)
1	1		1.2	0.264	0.302	1st site with inclination > than critical.	No	0.3
1	2		11.5	1.509	1.509	2nd Site with inclination > than critical.	Yes	0.3
2	1		5.4	2.43	2.43	1st site with inclination > than critical.	Yes	0.9
2	2		1.2	3.201	3.393	2nd site with inclination > than critical.	No	0.9
2	1		2.6	4.138	4.39	Next site with inclination > than critical.	No	0.9
2	2		4.3	4.495	4.6	Next site with inclination > than critical.	Yes	0.9
2	1		3.3	4.94	5.02	Next site with inclination > than critical.	No	0.9
2	2		3.3	5.98	6.01	Next site with inclination > than critical.	No	0.9
2	V		10.9	6.26	6.29	Next site with inclination > than previous inclinations.	No	0.9
2		S1a	2.6	3.81	3.909	Largest angle in Subregion 1 (S1).	No	0.9
3	1		1.2	7.972	7.99	1st site with inclination > than critical.	No	0.9
3	2		2.6	8.129	8.216	2nd Site with inclination > than critical.	Yes	0.9
3	1		1.6	8.494	8.514	Next site with inclination > than critical.	No	0.9
3	2		3.6	8.574	8.634	Next site with inclination > than critical.	Yes	0.9
3	1		2.5	9.404	9.457	Next site with inclination > than critical.	No	0.9
3	2		3.1	9.454	9.494	Next site with inclination > than critical.	Yes	0.9
4	1		4.2	9.782	9.788	1st site with inclination > than critical.	Yes	1
4	2		2	9.903	9.957	2nd site with inclination > than critical.	No	1
5	1		4.2	10.63	10.686	1st site with inclination > than critical.	Yes	3
5	2		4	10.957	11	2nd Site with inclination > than critical.	Yes	3
5		S0a	2.1	10.345	10.357	Largest angle in Subregion 0 (S0).	No	3
6	1		3.8	11.718	11.789	1st site with inclination > than critical.	Yes	4
6		S0a	3.4	11.068	11.086	Largest angle in Subregion 0 (S0).	No	4
7	1		5.4	12.424	12.654	1st site with inclination > than critical.	No	4
7	2		4.3	13.854	13.884	2nd site with inclination > than critical.	No	4
7	V		4.3	14.794	14.834	Next site with inclination > than previous inclinations.	No	4
7		S0a	2.2	11.954	12.034	Largest angle in Subregion 0 (S0).	No	4
8	1		4.3	16.374	16.554	1st site with inclination > than critical.	No	4
8		S0a	3.3	16.154	16.164	Largest angle in Subregion 0 (S0).	No	4
9	1		4.3	18.774	18.904	1st site with inclination > than critical.	Yes	4
9		S0a	3.3	17.664	17.724	Largest angle in Subregion 0 (S0).	No	4
9		S0b	2.2	17.394	17.514	Next largest angle in Subregion 0 (S0).	Yes	4
10	1		4.3	19.294	19.324	1st site with inclination > than critical.	Yes	4
10	2		5.4	19.524	19.584	2nd site with inclination > than critical.	No	4
10	V		4.3	20.245	20.298	Next site with inclination > than previous inclinations.	No	4
11	1		4.3	24.078	24.278	1st site with inclination > than critical.	No	7
11		S0a	3.3	22.088	22.098	Largest angle in Subregion 0 (S0).	No	7
11		S0b	2.2	21.888	22.088	Next largest angle in Subregion 0 (S0).	No	7

1.7.5 Step 4: Post-Assessment (Pipeline D)

1.7.5.1 Comparison of ILI with ICDA Results

If error bounds of +/- 200 ft are used the percentage of ILI-identified internal anomalies with >30% depth of wall thickness predicted by ICDA is 87%. With error bounds +/- 100 ft the percentage predicted is 71%, as shown in Table 1-30. The percentage of internal anomalies predicted based only on > 6 in. (15 cm.) anomaly length was 65% using +/- 200 ft, or 48% using +/- 100 ft (see Table 1-31).

Correlations of ILI with ICDA predictions are shown in Table 1-35. From this table it may be noticed that anomalies not identified by ICDA appear to correlate with low lying areas or “flat” locations on inclines (one exception was a case of obviously insufficient data). If these sites represent internal corrosion locations, one possible explanation is that there was not sufficient resolution in the USGS maps to show the maximum inclination angles and/or low points for these anomaly locations. Several anomalies also appear as if they might correlate with the inlet at MP 19.04 (30.64 km) or perhaps with an incline immediately after this inlet that was not resolved in the USGS maps.

Table 1-35. Pipeline D: ILI Tool Anomalies of > 30% Depth of Wall Thickness – Correlation with Sites Selected by ICDA Method

Location of Internal Anomaly miles (km)	Region nos.	% Depth of Wall Thickness	Length		Length (cm)	Orientation (clock)	Predicted by ICDA? If +/-100 ft (30.5 m)	Predicted by ICDA? If +/-200 ft (61 m)	Notes
			(ft.)	(in.)					
1.513 (2.434)	1	45		1.8	4.6	4:20	Yes	Yes	
2.328 (3.747)	2	30	2	10.2	25.9	6:00	No	No	Low lying area.
2.329 (3.748)	2	30		10	25.4	5:30	No	No	Low lying area.
2.428 (3.907)	2	40		1.8	4.6	5:40	Yes	Yes	
4.488 (7.223)	2	38		11.1	28.2	6:00	Yes	Yes	
7.004 (11.272)	2	35		0.9	2.3	11:30	No	No	Data appears sparse in vicinity of anomaly.
7.166 (11.533)	2	41		7.2	18.3	5:40	No	No	Low lying area.
7.498 (12.067)	2	45		1.6	4.1	5:30	No	No	Low lying area; inclination greater than critical.
8.133 (13.089)	3	43	1	2	5.1	5:00	Yes	Yes	
8.555 (13.768)	3	38	4	0.1	0.3	5:20	Yes	Yes	
8.556 (13.770)	3	38		9	22.9	6:20	Yes	Yes	
8.556 (13.770)	3	36		1.8	4.6	5:30	Yes	Yes	
8.556 (13.770)	3	32		4.3	10.9	5:30	Yes	Yes	
8.556 (13.770)	3	44		9.3	23.6	6:20	Yes	Yes	
8.556 (13.770)	3	30		1.2	3.0	5:20	Yes	Yes	
8.556 (13.770)	3	36		6.8	17.3	6:30	Yes	Yes	
8.556 (13.770)	3	34		4.2	10.7	5:20	Yes	Yes	
8.557 (13.771)	3	30		1.4	3.6	6:10	Yes	Yes	
9.451 (15.21)	3	36		9.9	25.1	5:40	Yes	Yes	
9.451 (15.21)	3	30		1.1	2.8	5:40	Yes	Yes	
9.451 (15.21)	3	34		4.8	12.2	5:40	Yes	Yes	
9.453 (15.213)	3	30		11.7	29.7	5:30	Yes	Yes	
9.454 (15.215)	3	34	4	3.1	7.9	5:40	Yes	Yes	
9.454 (15.215)	3	32	2	3.2	8.1	5:40	Yes	Yes	
9.455 (15.216)	3	30	1	1.1	2.8	5:50	Yes	Yes	
9.457 (15.22)	3	47		2.4	6.1	5:40	Yes	Yes	
9.458 (15.22)	3	30		7.9	20.1	5:40	Yes	Yes	
9.462 (15.228)	3	30		2.2	5.6	5:20	Yes	Yes	
9.471 (15.242)	3	30		0.5	1.3	11:50	Yes	Yes	Location of historic leak.
9.771 (15.725)	4	34		0.6	1.5	3:30	Yes	Yes	
10.067 (16.201)	4	49		1.2	3.0	5:50	No	No	Appears to correspond with flat spot on incline.
10.067 (16.201)	4	44	5	7.8	19.8	5:30	No	No	Appears to correspond with flat spot on incline.
10.068 (16.203)	4	45	3	11.5	29.2	6:00	No	No	Appears to correspond with flat spot on incline.
10.069 (16.204)	4	30		9.5	24.1	5:20	No	No	Appears to correspond with flat spot on incline.
10.069 (16.204)	4	30	3	10.9	27.7	5:40	No	No	Appears to correspond with flat spot on incline.
10.646 (17.133)	5	32		1.5	3.8	5:30	Yes	Yes	
10.649 (17.138)	5	39		0.8	2.0	6:00	Yes	Yes	
10.954 (17.629)	5	48	1	8.4	21.3	5:30	Yes	Yes	
10.954 (17.629)	5	49	3	0.1	0.3	5:50	Yes	Yes	
11.695 (18.821)	6	30		1.9	4.8	5:00	No	Yes	Low point.
11.787 (18.969)	6	44		1.9	4.8	5:40	Yes	Yes	
17.48 (28.13)	9	43		3	7.6	3:00	Yes	Yes	
17.481 (28.133)	9	45		1.6	4.1	5:40	Yes	Yes	
17.481 (28.133)	9	33		1	2.5	6:10	Yes	Yes	
17.482 (28.135)	9	42		1.8	4.6	5:40	Yes	Yes	
17.482 (28.135)	9	30		1.4	3.6	5:40	Yes	Yes	
17.484 (28.138)	9	34		1.2	3.0	5:50	Yes	Yes	
17.484 (28.138)	9	30		1.1	2.8	5:40	Yes	Yes	
17.484 (28.138)	9	46		1.1	2.8	5:40	Yes	Yes	
17.485 (28.139)	9	30		0.8	2.0	6:00	Yes	Yes	
17.485 (28.139)	9	38		1.2	3.0	6:10	Yes	Yes	
18.717 (30.122)	9	43		8.1	20.6	4:20	Yes	Yes	
18.742 (30.162)	9	30		7.2	18.3	6:10	Yes	Yes	
18.812 (30.275)	9	36		1	2.5	5:00	Yes	Yes	
18.813 (30.278)	9	30		3.6	9.1	5:00	Yes	Yes	
18.815 (30.28)	9	32		1	2.5	5:00	Yes	Yes	
18.815 (30.28)	9	34		9.4	23.9	5:00	Yes	Yes	
18.819 (30.286)	9	34	1	5.8	14.7	7:30	Yes	Yes	
18.819 (30.286)	9	30		2.3	5.8	7:20	Yes	Yes	
18.822 (30.29)	9	32		2.6	6.6	5:10	Yes	Yes	
19.002 (30.58)	9	32		4.2	10.7	8:10	No	Yes	~200 ft (61 m) from (upstream of) input at MP 19.04 (30.64 km)
19.002 (30.58)	9	32	1	9	22.9	3:20	No	Yes	~200 ft (61 m) from (upstream of) input at MP 19.04 (30.64 km)
19.003 (30.582)	9	31		6.1	15.5	7:00	No	Yes	~200 ft (61 m) from (upstream of) input at MP 19.04 (30.64 km)
19.005 (30.586)	9	36		5.6	14.2	3:40	No	Yes	~200 ft (61 m) from (upstream of) input at MP 19.04 (30.64 km)
19.006 (30.587)	9	30		9.8	24.9	8:10	No	Yes	~200 ft (61 m) from (upstream of) input at MP 19.04 (30.64 km)
19.007 (30.589)	9	34	1	3	7.6	3:40	No	Yes	~200 ft (61 m) from (upstream of) input at MP 19.04 (30.64 km)
19.007 (30.589)	9	36		2.1	5.3	4:50	No	Yes	~200 ft (61 m) from (upstream of) input at MP 19.04 (30.64 km)
19.277 (31.023)	9	30		1.8	4.6	5:50	Yes	Yes	
19.278 (31.025)	9	34		1.9	4.8	5:50	Yes	Yes	

1.7.5.2 Uncertainties

Some distance uncertainties were approximated in Table 1-36. Alignment of data was difficult beyond MP 22 (35.4 km) as scant feature data was available to coordinate ILI with USGS data for these locations. Due to unacceptable uncertainty with alignment beyond MP 26.5 (42.6 km), the analysis was stopped at this point. Analyses of Pipeline D considered two potential horizontal uncertainties bounds, +/-100ft (30.5 m) and +/-200ft (61 m). In general, interpolation accuracy between markers is best in the first 20 miles (32.2 km) of the pipeline.

Table 1-36. Pipeline D: Roughly Estimated Horizontal Uncertainties

Pipeline D	National Map Accuracy Standards miles (km)	ILI miles (km)	Interpolation miles (km)
	0.0126 (0.02)	0.019 (0.03)	0.038 (0.06)

A possibility exists that the 2001 to 2002 flow rate data used in the analysis does not accurately represent all flow rates for the duration of the pipe history. More detailed information on historical system pressures would also be beneficial.

2.0 WET GAS ICDA METHODOLOGY

2.1 Proposed Approach

Flow regimes typically found in wet gas systems are shown in Figure 2-1. For the purpose of wet gas ICDA, four flow regimes may be considered:

1. Stratified flow (i.e., fluids separated into layers, with lighter fluids flowing above heavier (i.e., higher density) fluids);
2. Stratified flow together with condensing water. The presence of condensing water in locations of high heat loss is considered an additional flow-related influence on corrosion when coinciding with stratified flow. The effects of condensation on top of line corrosion are considered less important for pipe containing slug or annular flow because the condensed water is contacted with transported liquids.
3. Slug flow, which includes all intermittent flows that episodically wet the entire pipe circumference; and
4. Annular flow, where liquid continuously wets the entire pipe circumference and mist can be carried down the center of the pipe with the gas.

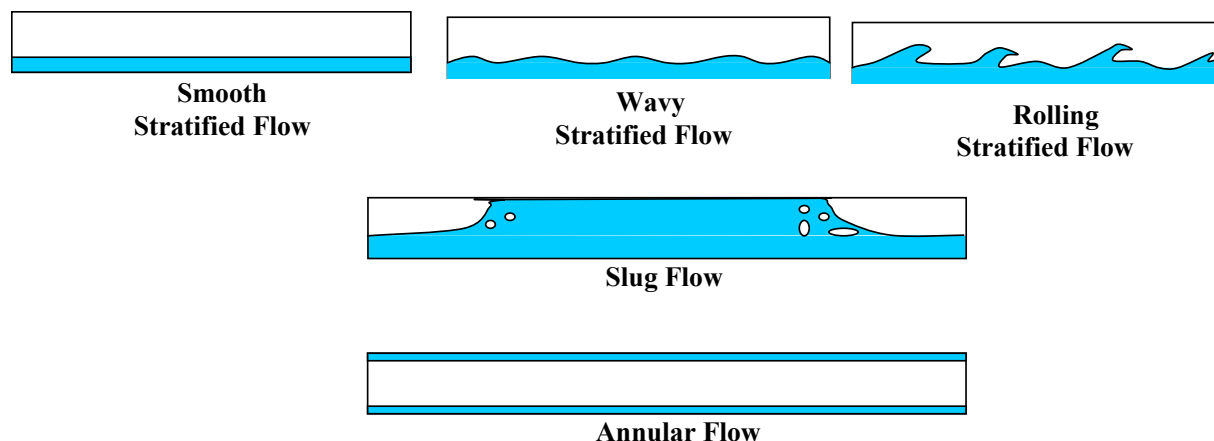


Figure 2-1. Flow Regimes Expected in Wet Gas Systems include stratified, slug and annular flow.

Although considered a secondary effect, it is recognized that flow effects on corrosion differ within a regime. For example, an area identified as slug flow does not reflect the secondary effects of slug frequency or severity. Similarly, defining an area as stratified does not discriminate between wavy and smooth. Defining an area as annular flow does not consider film velocity or amount of mist. One method to predict flow regimes is to perform detailed flow modeling on a pipeline (e.g., Shea et. al., 1997). A difficulty with this approach is that more input information might be required than what is available. In addition, this information needs to

be known over the period of operation for which the assessment is to be valid. That is, an initial assessment of a pipeline requires that the parameters for multiphase modeling be known over the life of the pipeline service. Since it is rare that a pipeline is operated under steady-state conditions (including flow rates and fluid properties) over its life, a series of flow model runs is required to consider the range of conditions.

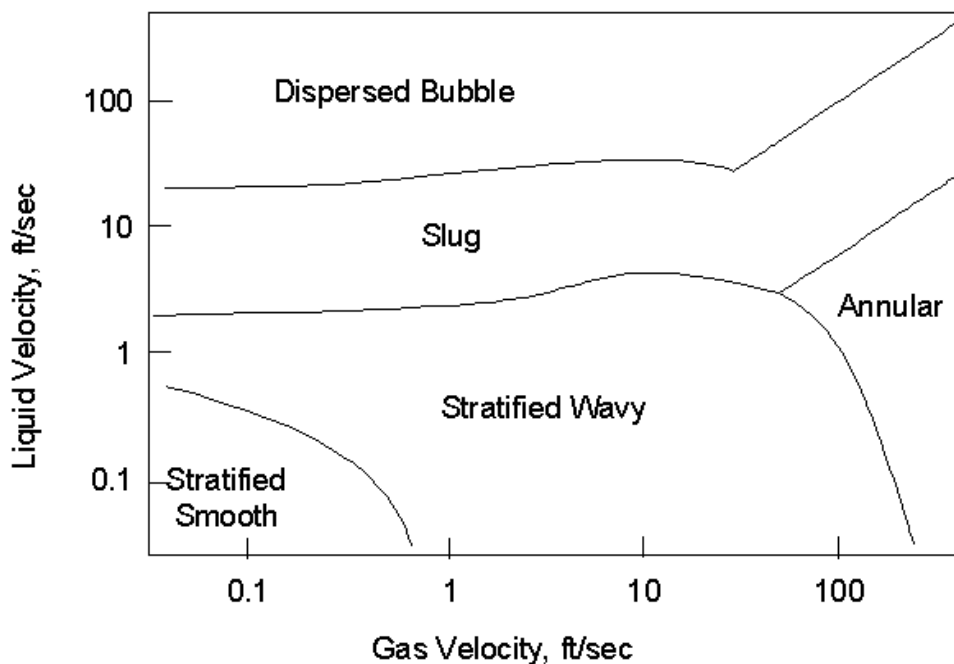


Figure 2-2. Example flow regime map for 24-inch I.D. horizontal pipe after Taitel and Dukler (1976).

A simple approach for predicting flow regimes is through the use of flow maps as shown in Figure 2-3 (Taitel and Dukler, 1976). Unfortunately, most of these flow maps are for horizontal (or near-horizontal) pipe. Ideally, a set of flow regime maps would be developed as a wet gas ICDA tool. Some hypothetical examples of flow regimes that might exist in a pipeline are shown in Figure 2-4. For the cases where the entire segment has the same flow regime (i.e., #1 and #2 of Figure 2-4), the effect of flow regime is disregarded. However, most pipelines are expected to 1) have sufficiently low liquid volumes and velocities to fall below annular flow regime criteria, and 2) have their flow regime influenced by topography. Because of this, a typical pipeline segment is expected to have portions of stratified and slug flow (i.e., #3 of Figure 2-4). In addition, the presence of condensation needs to be superimposed so its coincidence with stratified flow can be identified (i.e., #4 of Figure 2-4). Finally, it is expected that portions of the pipeline segment will have a flow regime that cannot be predicted (i.e., #5 of Figure 2-4). Each different flow regime with a given ICDA region will be considered as a separate subregion. One subregion may include non-continuous sections of the region. The use of such flow regime classification system in corrosion modeling may involve consideration of different models for corrosion. Additionally, the effect of certain factors that alter corrosion may also depend on the flow regime.

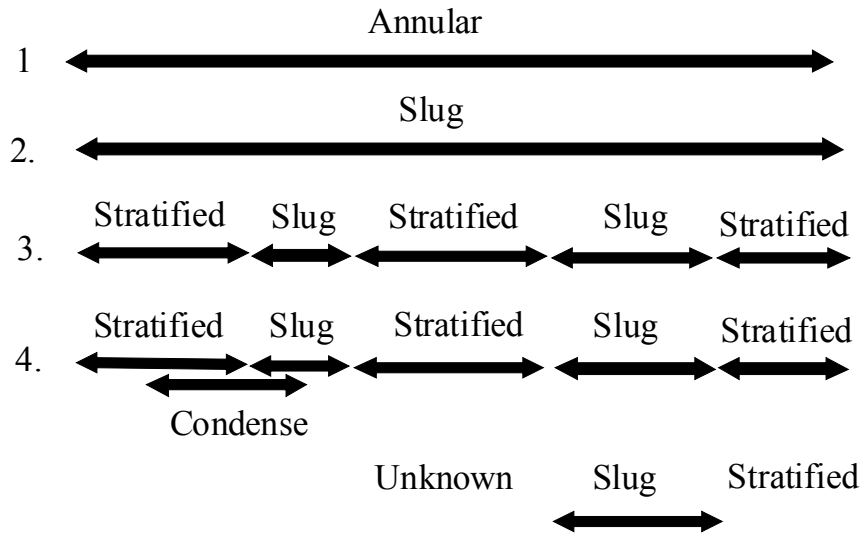


Figure 2-3. A schematic approach to classifying segments of a pipeline according to flow regimes

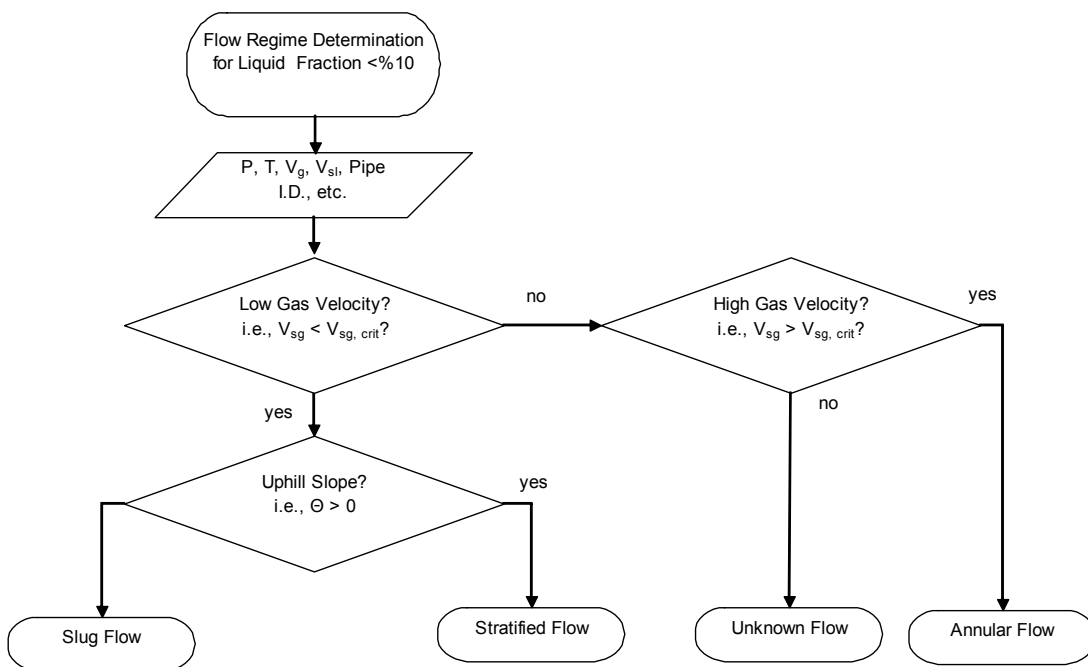


Figure 2-4. A simplified flow chart to classifying flow regimes.

At minimum, it is expected that areas of flow regime transition (e.g., from slugging to stratified) will have great uncertainty with respect to prediction of flow regime. It is also expected that the transition to annular flow will have high uncertainty, in part because of uncertainty with input parameters such as liquid fraction.

Prediction of flow regime would ideally take the form of a simple flow diagram as shown in Figure 2-4. For wet gas systems with low liquid throughput, it is expected that flow regime can be predicted with consideration of pressure, temperature, superficial gas and liquid velocities, and pipe diameter (along with some assumptions about gas and liquid properties). At low gas velocities (assuming low liquid fraction), uphill portions of a segment are expected to have slug flow and downhill portions are expected to be stratified. Additional work is required to better quantify the range of conditions for which this is valid and if a critical angle for uphill inclination is applicable. High velocities are expected to result in annular flow. However, the transition between stratified/slugging and annular flow has uncertainty so that accurate prediction of flow regime may not be possible. It should also be considered that most pipelines have had a range of operating conditions resulting in several different flow regime combinations within a pipeline segment.

2.2 Other Factors Affecting Corrosion

The corrosion rate depends primarily on gas quality, liquid chemistry, pressure, and temperature. However, the likelihood of finding corrosion damage at a particular location along a pipeline segment is influenced by a long list of additional factors, each of which needs to be considered in terms of its overall importance and effect on corrosion distribution.

2.2.1 Liquid Hydrocarbons

Liquid hydrocarbons can reduce corrosion by entraining water. If water is dispersed in the hydrocarbon phase, corrosion rate is expected to be lower than if it is directly in contact with the pipe wall.

If hydrocarbons are condensing along a pipeline segment resulting in an increase in the hydrocarbon/water ratio, it is possible that corrosion is less likely at downstream locations than upstream locations (i.e., the water cut is decreased). This is particularly true if liquid water dominates at upstream locations and hydrocarbon becomes the dominant liquid phase at downstream locations (Lotz et al., 1990).

Some hydrocarbons may also reduce corrosion rates through a corrosion inhibition mechanism similar to corrosion inhibitors, with efficiencies depending also on the water/hydrocarbon ratio (Mendez et al., 2001).

If water is emulsified in a continuous hydrocarbon phase, it is possible for this emulsion to break over distance. This would result in ‘free’ liquid water. If the flow regime is stratified, liquid water might drop to the bottom of the pipe resulting in increased likelihood of corrosion at downstream locations. If the flow regime is slugging or annular, this effect might be less because the liquid phases are mixed.

2.2.2 Corrosion Inhibition

The effectiveness of corrosion inhibitors can have a dependence on distance along a pipeline segment. This dependence is different for batch and continuously treated systems and is

influenced by the frequency of pigging. For batch treatment, corrosion might be more likely upstream than downstream. For continuous treatment, corrosion might more likely downstream than upstream.

Batch application of corrosion inhibitors have a treatment life where downstream pipe can remain inhibited longer than upstream portions (due to re-adsorption of inhibitor that desorbed from upstream locations) (Daugherty, 1987). The result is that batch treated systems have a higher likelihood of corrosion at upstream locations. This is especially true for systems whose batch frequency is determined by downstream coupon monitoring.

Pipelines where the inhibitor is continuously injected can also have effectiveness dependent on distance (Erikson et al., 1993). For pipelines with low liquid volume throughputs and high liquid volume holdup, frequent pigging (or sphering) can prevent an inhibitor (continuously injected at low volumes) from reaching downstream sections of the pipe. Removal of liquids from the pipe includes removal of the corrosion inhibitor, and the inhibitor only reaches downstream locations after upstream holdup locations are full. For some pipelines this process could take months.

It should be considered that the effectiveness of inhibitors intended to partition into the water phase is reduced over distance if the relative volumes of hydrocarbon and water increase over distance or if the degree of mixing (by emulsions or flow regime) decreases over distance.

Other factors may affect the effectiveness of inhibitors, so each combination of inhibitor type and process conditions should be evaluated to predict the impact on corrosion damage over distance.

2.2.3 Bacteria and Biocides

The effects of bacteria as a function of distance are difficult to predict, but the effectiveness of biocides over distance is expected to experience some of the same treatment effectiveness distributions as corrosion inhibition. A pipeline known to suffer from microbiologically influenced corrosion (MIC) is expected to have large uncertainty with respect to predicted severity over distance. A straightforward way to compensate for this uncertainty is to perform added excavations when MIC is considered an important mechanism.

2.2.4 Solids

Solids include both organic and inorganic materials that are carried into a pipeline segment, precipitate from the liquids, and/or grow on the pipe wall. Solids can have several effects on corrosion distribution. Scales primarily affect the transport of materials to (or from) the pipe wall or the kinetics of electrochemical reactions. If a sufficiently large volume of solids exist to reduce the effective pipe diameter, it should be considered that flow characteristics can be affected. The effectiveness of cleaning pigs over distance should also be considered.

Sources of solids include corrosion products (e.g., iron carbonates, iron sulfides), other inorganic scales (e.g., calcium carbonate, barium sulfate), organic scales (e.g., paraffins,

asphaltenes), and carryover of solids into the pipeline segment, including silicates (e.g., formation sand).

The composition of corrosion products is important because it reflects the corrosion mechanism. It is especially important to determine if a change in mechanism (e.g., between carbonate and sulfide scale) occurs within a pipeline segment. This would likely guide the inspection of locations within each corrosion mechanism area.

The presence of corrosion products or other adherent scale can affect corrosion rate. A system with changing scaling tendency (perhaps from change in temperature or pressure) might have less corrosion damage where a protective scale has formed.

Loose solids within a pipe can create crevices resulting in under-deposit corrosion. For example, locations of stratified flow where entrained solids might be deposited have a higher probability of corrosion damage.

2.2.5 Other Products

The influence of other products in a specific pipeline segment must be considered. For example, glycol and methanol can reduce corrosion rates (van Bodegom et al., 1987). If these materials are distributed uniformly through the pipeline (or uniformly mixed with water in the pipeline), their effects can be ignored because the expected distribution of corrosion will not change. However, if a mechanism exists by which the concentrations of these materials differ over distance, the resulting effect on corrosion distribution needs to be superimposed on the other factors.

Other examples of products to consider include formation treating chemical (e.g., backflow of acid treatments) that could increase the likelihood of corrosion at upstream locations.

2.3 Example Application with Comparison to ILI Data

The principles of the wet gas ICDA (WG-ICDA) methodology were applied to a pipeline segment. The process was compared to the results of a tethered in-line inspection tool and internal corrosion examinations at excavation sites.

2.3.1 Pre-Assessment

Based on the available data, conditions that preclude the application of the WG-ICDA were not identified; the process was therefore initiated with the recognition that data may arise during implementation that would affect the validity or effectiveness of WG-ICDA. Ten WG-ICDA regions were identified on trunk line SP 6984, five for withdrawal flow, and five for injection flow; these were distinguished by five well line inputs and the station.

Trunk line Alpha is a 36 year-old, 5450 foot long, 12” diameter, pipeline that transports wet gas to and from eight natural storage wells. The line has five well-line tie-ins along its length (Table 2-1). No historical leaks, ruptures or repairs have occurred.

Table 2-1. WG-ICDA Region Definition

1	0	0.121	Withdrawal
2	0.121	0.293	Withdrawal
3	0.293	0.332	Withdrawal
4	0.332	0.524	Withdrawal
5	0.524	1.032	Withdrawal
6	1.032	0.524	Injection
7	0.524	0.332	Injection
8	0.332	0.293	Injection
9	0.293	0.121	Injection
10	0.121	0	Injection

Table 2-2. Rates for Each Region

Pressure = 336 psi					
INJECTION MAX	Region 1	Region 2	Region 3	Region 4	Region 5
Flow Rate (MMSCFD)	4.224	24.24	25.296	29.52	30.576
Velocity (m/s)	<0.6	~2.6	~2.6	~3.1	~3.1

Pressure = 500 psi					
WITHDRAWAL MAX	Region 6	Region 7	Region 8	Region 9	Region 10
Flow Rate (MMSCFD)	15.77	15.218	13.034	12.482	2.138
Velocity (m/s)	~2.4	~2.3	~2	~1.9	~0.3

Trunk line Alpha was installed in 1968 of new (1967) X42 seamless pipe. The outer diameter is 12.75 inches, and wall thickness is 0.312 inches. The pipeline maximum operating pressure (MAOP) is 970 psi, minimum operating pressure 210 psi (for the period 2000 to 2003), and maximum hoop stress at MAOP is 47.18% SMYS (Specified Maximum Yield Strength). A hydrotest to 2100 psi was performed in 1968 (following construction). The pipeline is buried and is exposed at three locations; there are no other pipelines, structures, high voltage electrical transmission lines or rail crossings in the immediate vicinity of the pipeline. A high resolution GIS survey including elevation profile and depth of cover, was conducted March 19, 2004. There are seven road and three water crossings on alpha.

Operation of the gas storage system is seasonal withdrawal and injection. Wet gas is typically withdrawn from the wells in late fall, winter and early spring, and injected in late spring, summer and early fall. Withdrawal temperature is about 49 °F (9 °C). Maximum injection gas flow rate for the period 2000 to 2003 was 19.76 MMSCFD, and maximum withdrawal flow rate was 34.29 MMSCFD (Table 2-2). Water production varied seasonally, with the majority of produced water entering the lines at the end of the withdrawal season, as well pressure decreased. No corrosion inhibitor or dehydration has been used on the pipeline, although there are methanol drips (i.e., injection) at the wells, which input into the trunk line.

The pipeline has no history of repairs, leaks, or ruptures. Starting May 2003, the operator started running a cup-type pig annually, and the pipeline has been pigged four times in the past two years (Table 2-3). Previous pigging prior to these runs was the early '70s. Two sets of coupon data (7 total coupons) from a separator at the receiving Station were available. Data was collected between January and March of 2003 (withdraw season) for 4 coupons exposed for 1-1/2 to 2 months inside gas (2 coupons) and liquid (2 coupons) vessels; all coupons were positioned outside the flow paths. Pit depth measurements indicated corrosion rates of 0.59 to 0.76 mpy in the gas vessel and 0.76 to 1.5 mpy in the liquid vessel. Scale was observed on 3 of the 4 coupons. Pitting and etching were noted on coupons in both the gas and liquid vessels. The presence of bacteria was noted on one of the liquid coupons, but corrosion was not considered accelerated due to bacteria. One of the liquid vessel coupons exhibited heavy deposits and patches of scale were associated with pits. Heavy deposits (but no corrosion) were observed on one of the gas coupons.

Table 2-3. Recent Pigging History

Time of Pigging	Quantity of Liquid Removed (gallons)
Spring 2003	3,000
Dec-03	1,300 including 25 gallons of hydrates
Spring 2004	670
Jun-04	691

On April 12, 2004 (injection season) 3 coupons were removed from the separator. The coupons were at the bottom (i.e., liquid environment), top (i.e., gas phase), and at an orifice plate. Pitting rates for the 60 day exposure were between 0.5 and 1mpy for all coupons. Brown scale was noted on all coupons. Thick scale and bacteria were identified on the coupon from the top of the separator. Bacteria were not detected in the other two coupons.

Gas sample analysis results indicate significant quantities of water in the gas: 11.25 lb/MMSCF in February of 2004 (withdrawal) and 40 lb/MMSCF in May 2004 (injection). The withdrawal gas sample also showed hydrogen sulfide (H₂S), 2 ppm. It was considered that the H₂S was either produced from 8 wells at 2 ppm, or the concentration might have been at higher concentration in one of more wells. The presence of H₂S in gas withdrawn from a field can indicate the activity of sulfate reducing bacteria, given that the injected gas does not contain H₂S.

2.3.2 Indirect Examination

The dominant factor used for internal corrosion prioritization was flow regime. The elevation profile was plotted, and subregions for slugging and stratified flow regimes were defined. Other factors were either not significant or could not be determined by historical data. The onset of slugging (i.e., liquid accumulation) at the bottom of a significant incline was considered representative of the most frequent (or severe) slugs. Representative sections of stratified flow were examined.

Most corrosion rate influencing factors were considered uniform along each pipeline region. Records indicate that neither corrosion inhibitor nor biocide treatments were used. Liquid hydrocarbons existed in the line, and some locations tested positive for bacteria, however the net effects of these factors could not be determined from available data. Their effects were therefore considered uniform. Records showed that scale and other deposits existed at many locations, but their influence on corrosion distributions could not be determined a priori. Methanol was continuously injected at the wells during the withdrawal season. It was considered that a higher volume of methanol would be present at upstream locations following initiation of withdrawal (or after a cleaning pig run). After an extended period of injection, the line would be uniformly filled with methanol. In the presence of water, methanol is expected to reduce corrosivity making corrosion more likely further downstream of a well input. Since the regions were short, the effect of methanol was not initially used to prioritize locations for examination.

A basic assumption of wet gas is that water is distributed throughout the pipeline length. Since it is known that slugging is more likely at the beginning of higher and longer inclines, locations that best represent slugging were chosen on this basis. It should be noted that during injection cycle, sites where during withdrawal slug flow may be expected exhibit stratified flow, and vice versa. For this reason, selected sites are duplicated in injection and withdrawal regions, and thus the total net number of excavations required was significantly reduced. Further reducing the total number of excavations is the fact that many selected sites are directly adjacent one another (i.e., stratified and slug flow sub-region sites can be inspected with the same excavation).

First priority WG-ICDA locations are listed in Table 2-4. These locations are intended to represent conditions of stratified and slug flow for each region (as defined by well line inputs). The locations are also marked graphically in Figure 2-5, where secondary locations are also identified. Note that the secondary locations are not identified in Table 2-4. Depending on future WG-ICDA industry experience, the secondary locations would either be required or be conditional upon finding corrosion at the primary locations.

Table 2-4. First Priority Sites as Determined by The WG-ICDA Method. STF is Stratified Flow, and SLG is Slug Flow

<i>MP</i>	<i>Region</i>	<i>Expected Flow</i>	<i>Notes</i>
0.10	1	STF, SLG	Both sides of low-point
	10	STF, SLG	
0.12	2	SLG	Uphill
	9	STF	Downhill (reverse flow)
0.29	2	STF	Downhill
	9	SLG	Uphill (reverse flow)
0.33	3	STF, SLG	Both sides of road-crossing
	8	STF, SLG	
0.44	4	STF	Downhill
	7	SLG	Uphill (reverse flow)
0.49	4	SLG	Uphill
	7	STF	Downhill (reverse flow)
0.84	5	STF, SLG	Both sides of creek-crossing
	6	SLG, STF	

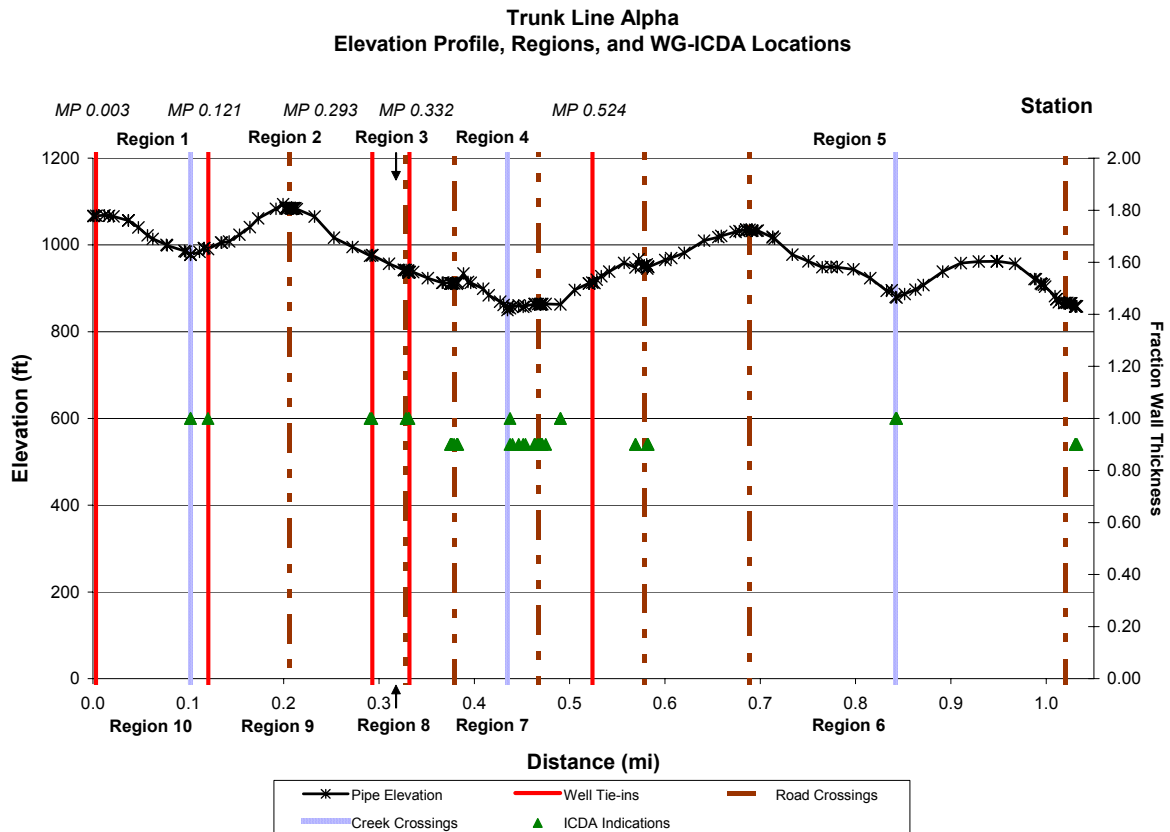


Figure 2-5. Elevation profile with regions defined by well line inputs. Green triangles at locations in Table 2-4 are primary WG-ICDA indications. Triangles at other locations in the figure are secondary indications.

2.3.3 Direct Examination and Comparison to ILI Data

The results of a tethered ILI tool were used in place of WG-ICDA excavations for the purpose of determining if the WG-ICDA process would guide an operator to locations of damage. A summary of the comparison is shown in Figure 2-6. Excavations were not performed at WG-ICDA indications, but a series of excavations were performed for the purpose of validating the ILI results. These excavations revealed uncertainties in the ILI data that prevented quantitative comparison of WG-ICDA with the ILI assessment. However, the comparison showed that WG-ICDA indications tended to align with internal corrosion flaws as identified by ILI.

Excavations to verify the ILI results revealed significant uncertainty. The results of 8 excavations are shown in Table 2-5. All excavations with inspections that indicated internal corrosion were cut out and directly examined. An example of a cut-out is shown in Figures 2-7, 2-8, and 2-9; direct examination allowed accurate evaluation of internal corrosion damage and root-cause analysis. Excavations where internal corrosion anomalies were not identified included those where external corrosion was identified. In those cases, a flaw was detected but not correctly identified. A graph of actual internal corrosion damage (as measured by direct examination) versus the anomaly sized by ILI is shown in Figure 2-10. Anomalies either not detected or identified as internal corrosion are plotted as zero depth. For ILI to be 100% accurate, all data points would fall on the diagonal line. A quantitative comparison between WG-ICDA and the ILI data was considered inappropriate because the uncertainty in ILI detection, identification, and/or sizing would be greater than the desired uncertainty of correlation between WG-ICDA and ILI. However, a qualitative comparison of the two data sets supported the validity of WG-ICDA principle.

The pipeline information including ILI anomalies (>20% wall thickness) is shown in Figure 2-6. From the ILI data, it can be seen that Regions 1, 4, and 5 have significant internal corrosion damage (corresponding to Regions 10, 7, and 6 in the reverse gas flow direction) while Regions 2 and 3 (corresponding to Regions 9 and 8) have few corrosion spots greater than 20% of wall thickness in depth.

Comparing the first priority WG-ICDA indications with ILI results shows that regions of significant corrosion could be identified.

- Region 1: The WG-ICDA indication aligns with corrosion as indicated by ILI. However, almost any excavation in region 1 would show significant corrosion. Consecutive excavations through the WG-ICDA process would show that an alternative integrity assessment would be more cost effective since an operator would need to excavation nearly the entire region to complete a WG-ICDA assessment.
- Region 2: The WG-ICDA indication is not associated with an ILI anomaly. This represents the overall condition of the region because ILI did not identify anomalies significantly greater than 20% of wall thickness.
- Region 3: The WG-ICDA indication is not associated with an ILI anomaly. This represents the overall condition of the region because two ILI anomalies existed, one

that is near 20% and another that was 15% by direct examination (reduced from 37%).

- Region 4: The WG-ICDA indication aligns with corrosion as indicated by ILI. However, almost any excavation in region 4 would show significant corrosion. Consecutive excavations through the WG-ICDA process would show that an alternative integrity assessment would be more cost effective since an operator would need to excavation nearly the entire region to complete a WG-ICDA assessment.
- Region 5: The first priority WG-ICDA indication aligned with the most severe location within Region 5 (at a creek crossing). This outcome was significant because the ILI data shows severe corrosion at this location surrounded by pipe without any indications greater than 20%. In addition, the second priority WG-ICDA indications align with damage at MP 0.565. However, the 72% ILI anomaly was found to actually be 23% following direct examination.

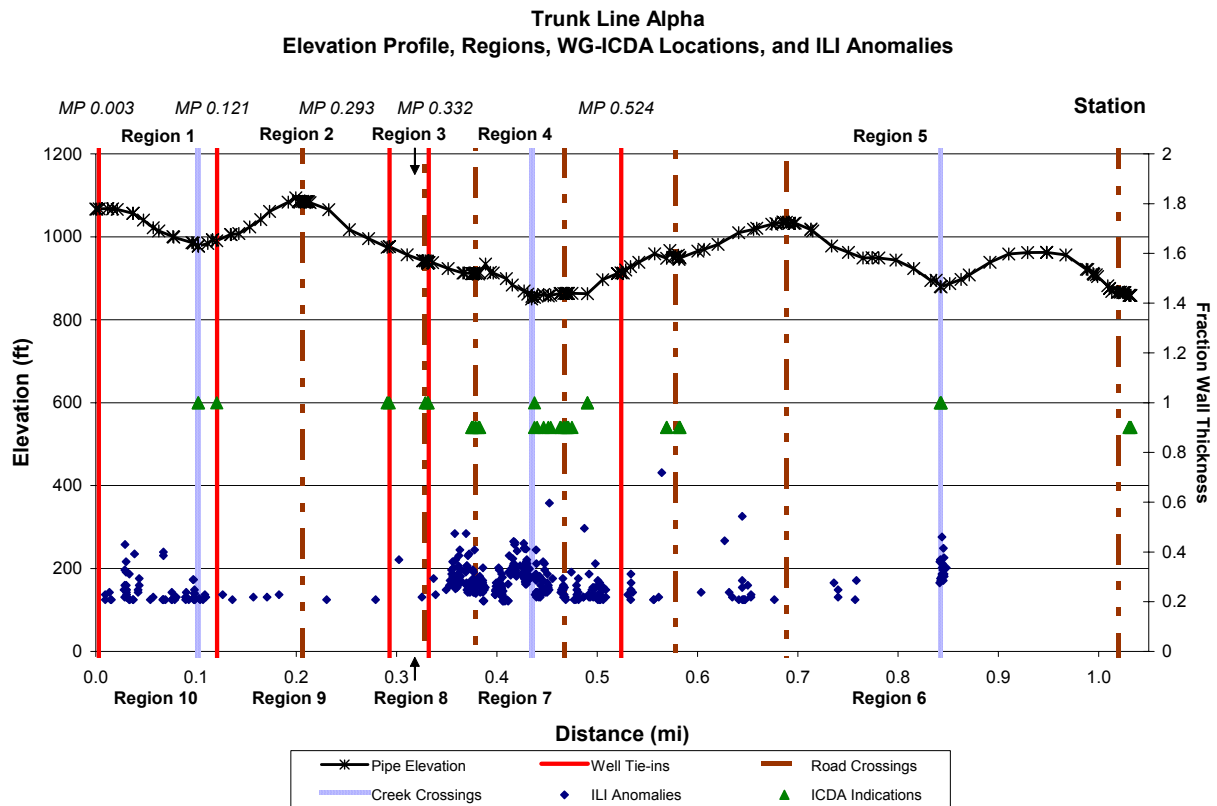


Figure 2-6. Trunk line alpha is divided into 10 regions (5 each for gas injection and withdrawal). ILI anomalies (>20%) are plotted by size according to the right hand axis. First priority ICDA indications are marked at 100% wall thickness (i.e., '1'), and second priority are marked at 0.8.



Figure 2-7. Cutout of trunk line alpha at MP 0.456.

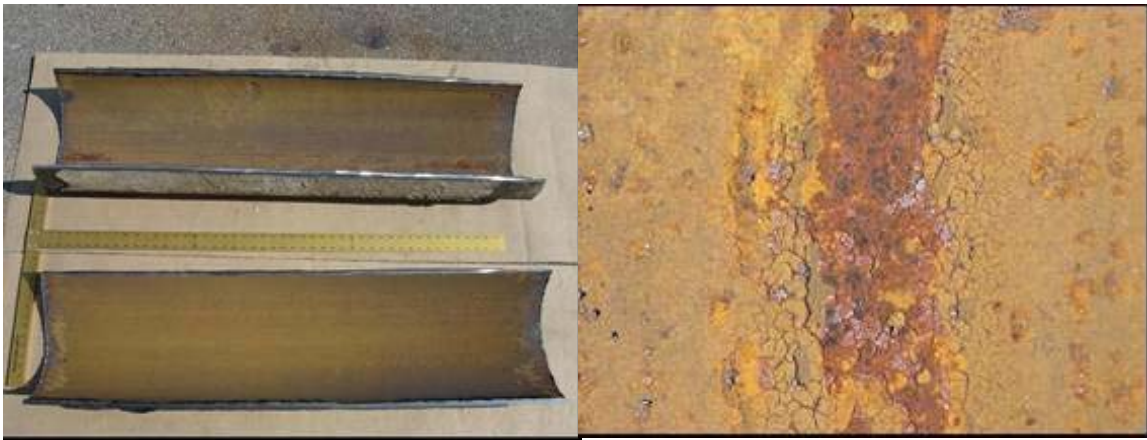


Figure 2-8. Deposits on pipe at MP 0.456. Top section of pipe on left hand photo is top-of-pipe.



Figure 2-9. Cleaned pipe at MP 0.456. Top section of pipe on left hand photo is top-of-pipe.

Table 2-5. Locations of Excavation Based on ILI Anomalies. Locations where No Internal Diameter Anomalies were Identified were Excavation for Other Reasons (e.g., External Diameter Anomalies). Locations with Internal Corrosion were Cut Out and Examined

Location of Excavation	ILI Maximum Depth (% of Wall)	Actual Deepest Internal Corrosion (% of Wall)	Pipe Sample Cut Out?
MP 0.257	Internal Anomaly not Identified	24	Yes
MP 0.303	37	15	Yes
MP 0.399	25	30	Yes
MP 0.456	29	39	Yes
MP 0.524	Internal Anomaly not Identified	0	No
MP 0.565	72	23	Yes
MP 0.636	22	34	Yes
MP 0.930	Internal Anomaly not Identified	30	Yes

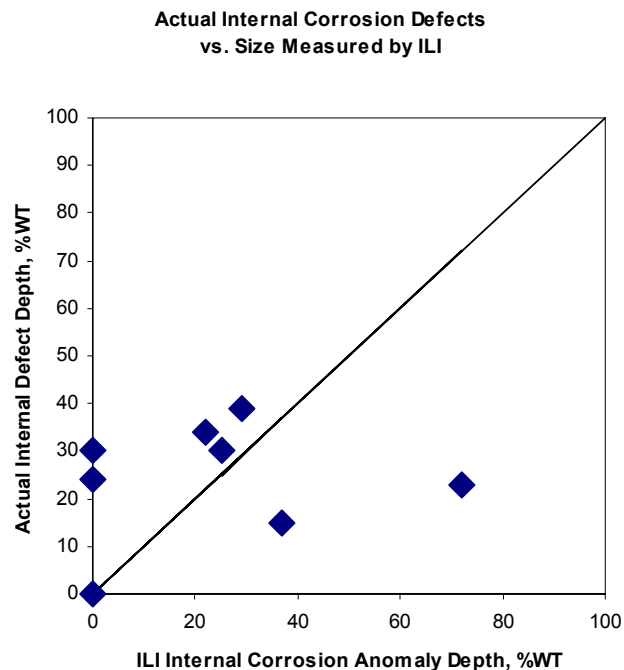


Figure 2-10. Comparison of ILI internal corrosion anomalies with actual examination of the pipe surface. ILI anomaly depth of zero indicates that internal corrosion was not identified.

2.3.4 Post Assessment

This step includes judging the overall effectiveness of the WG-ICDA process and determining a reassessment interval.

The analysis of WG-ICDA data supports the validity of the approach because the prioritization of corrosion likelihood was consistent with the damage found by ILI and direct examinations at excavation sites. However, the effectiveness of this particular application of WG-ICDA to trunk line alpha could not be verified because insufficient ICDA-selected excavations were performed.

The WG-ICDA process identified that extensive internal corrosion existed in the pipeline. For pipelines with extensive corrosion, WG-ICDA is not expected to be the most cost-effective approach for finding all corrosion damage.

Locations predicted by WG-ICDA to have the highest likelihood of corrosion were verified by ILI anomalies and/or inspections at excavation sites. This included detection of internal corrosion not identified by ILI. However, quantitative comparison of WG-ICDA performance and ILI was not possible because of large uncertainties in both the WG-ICDA influencing factors and the ILI anomalies.

A reassessment interval was not determined. Calculation of reassessment interval requires knowledge about the worst remaining flaws and future growth rates. Uncertainty about the worst remaining flaw was considered large, and it is recommended that future growth rates in this pipeline be determined by coupons located in locations known to accumulate water.

3.0 PROBABILISTIC ANALYSIS OF ICDA LOCATIONS

3.1 Introduction

Each of the steps involved in ICDA introduces uncertainties into the overall assessment. The pipeline inclination profile has several sources of error related to errors in the digital elevation maps of the pipeline terrain and uncertainties in the pipeline mapping tools. The flow modeling has uncertainties related to flow parameters. The detailed examination methods may detect pipe wall-loss that may not be related to internal corrosion. There is also uncertainty in the distance along the pipeline from a critical location at which internal corrosion may be found. The last uncertainty determines the extent of excavation one has to perform for detailed examination.

Probabilistic analysis can be used to incorporate uncertainty in data and obtain the relative likelihood of failure in a pipeline subjected to corrosion growth. Here the model parameters are represented as random variables, each with a probability distribution. The state of failure is represented by the probability that the corrosion depth will exceed a critical amount at a specified location and time of operation of the pipeline. The combination of physics-based modeling, associated parameter and model uncertainties, and inspection-based model updating provides a more rational framework for making inspect/repair/replace decisions than does traditional deterministic analysis. An example application of probabilistic analysis to the prediction of life governed by mechanical failure in gas distribution pipelines is given in Thacker et al. (1992).

Muhlbauer (1996) developed a risk indexing system that relies on establishing subjective weighing factors derived from judgment of the corrosivity of the product and presence/absence of mitigation methods (monitoring coupons, ILI, inhibitor injection, gas treatment, and internal coating). Other risk assessment methods use a fault-tree/event-tree approach but assign subjective probabilities to various processes leading to a leak. These approaches are limited by the fact these indices or probabilities are fixed, subjective, and do not allow updated pipeline information.

Ahammed and Melchers (1995) used the First Order Reliability Method (FORM) to predict the pipe leak probability at a single location subjected to pitting corrosion. Ahammed and Melchers (1997) and Ahammed (1998) performed reliability analysis to incorporate uncertainty in data and obtain failure probability of a single section of pipe subjected to widespread corrosion growth. Ahammed (1998) and Caley et al. (2002), assumed that the number and location of defective sites were known and used a probabilistic approach to compute the reliability of a pipeline segment subjected to corrosion growth in the presence of multiple defects. Vinod et al. (2003), used Markov chains and FORM to estimate inspection time for a pipe segment for maintaining a specified probability of failure. They used the erosion-corrosion growth model to estimate the time required for corrosion depth to exceed a critical depth. Hong (1999) also used Markov chains to develop a method for obtaining optimum inspection time for a pipeline subjected to corrosion growth including generation of new defects during the service life of a pipeline. All of these methods are based on calculating the reliability estimate of a single section of pipe, which is assumed to govern the overall structural integrity of the

pipeline. Consequently, they provide no framework to identify the critical location in the pipeline itself. Gartland et al. (2003) developed a model to predict the corrosion profile throughout the length of a pipeline. The model combines pipeline profile and flow information into multiphase flow modeling software to obtain water wetting factors at different locations along pipe length. This is combined with a point corrosion model and inhibitor effect to estimate CO₂ corrosion along the pipe length. They also developed a framework to combine the model predictions with inspection and monitoring data to obtain updated estimates. However they did not account for uncertainty in pipeline profile information in calculating water wetting factors. Also their results are conditioned upon predictions of a single model, which may not be suitable for all conditions in pipelines.

The proposed approach is aimed at developing a probabilistic model for assessing the extent of internal corrosion along the length of a pipeline. The probabilistic model can incorporate inspection data, so the model as well as the results can reflect observational data. The probabilistic model uses either Monte Carlo simulation or an approximate FORM solution to perform the probability integration. A Bayesian approach is used to update the model prediction with field data. Because the “true” corrosion rate model is unknown, three candidate corrosion rate models are used to obtain the probability estimate. The corrosion rate models are combined as a weighted average, where the weight factors are updated using the corrosion depth measured from inspection data.

3.2 Sources of Uncertainty

3.2.1 Flow Modeling Uncertainties

For the case of dry gas ICDA (Moghissi et al., 2002, 2003), calculations were performed using OLGA-S (steady-state) model and the results were abstracted in terms of a Froude number for different pipeline inclination angle regimes. A similar procedure was attempted for wet gas lines by assuming different amounts of input water (Figure 3-1). The water loading (input water) was varied by varying the superficial water velocity (in feet per second), which is defined as the volumetric flow rate of water divided by the total pipeline cross-section area. Then the water drop out, defined as the fraction of the cross-section area of the pipe occupied by water was calculated as a function of superficial gas velocity (volumetric flow rate of gas divided by the total pipeline cross-section area) and angle of inclination of the pipe. The parameters that were held constant for these calculations were the total gas pressure (700 psig), pipe diameter (19.25 inches I.D.), and temperature (60°F).

As shown in Figure 3-1, for low water loading (superficial water velocity less than about 0.01 ft/s, there is a sharp transition in the fraction of water hold-up with gas velocity for any given pipeline inclination. This is the result that enabled the use of a single Froude number to estimate the critical angle for water hold-up and incorporation of the critical angle in the dry-gas ICDA approach. Below the sharp transition superficial gas velocity, the flow regime is predicted to change from stratified flow to slug flow. However, as the water loading is increased, OLGA-S predicts that the hold-up fraction decreases gradually with increase in superficial gas velocity. This means that there is no single critical angle for water hold-up and a broad range of critical angles may need to be considered.

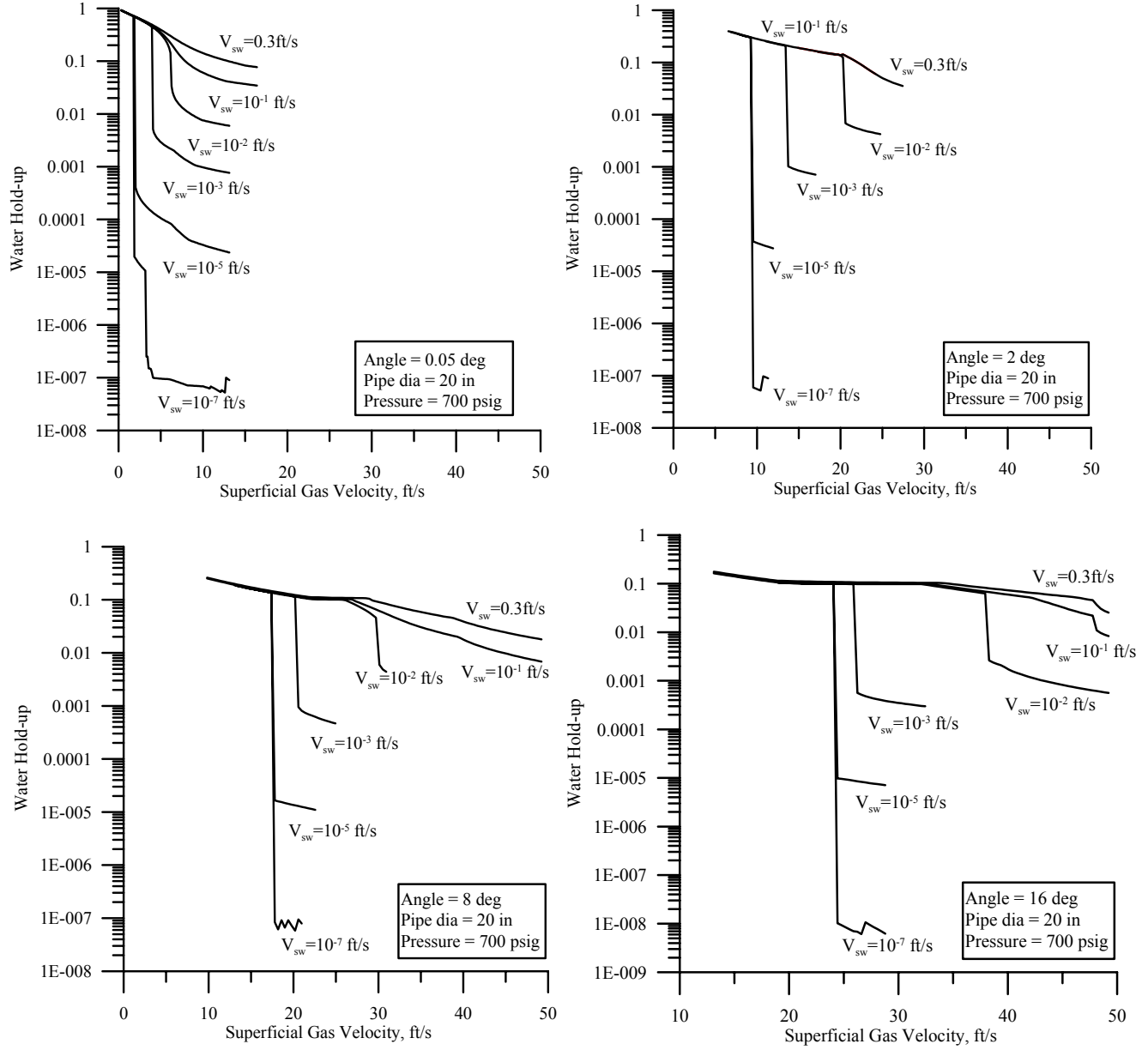


Figure 3-1. OLGA-S calculations of water hold-up fraction as a function of different water loading (as superficial water velocity) and pipe inclination angles.

3.3 Proposed Methodology

3.3.1 Water Accumulation

As discussed in the previous section, for water loading below a certain value, water hold-up occurs at all pipeline inclination angles greater than critical angle. The critical angle, α , is given by:

$$\alpha = \sin^{-1} \left(\frac{F \rho_g V_g^2}{(\rho_l - \rho_g) g D_i} \right) \quad (3-1)$$

where

$$V_g = \frac{4H_p}{\pi D_i^2}$$

$$H_p = \frac{S_p \times T \times Z \times 101325}{P \times 273}$$

$$\rho_g = \frac{P \times MW}{R \times T \times Z}$$

where F is the Froude number, ρ_g is the gas density, V_g is the gas velocity, ρ_l is water density, g is acceleration due to gravity, D_i is internal diameter of pipe, H_p is high-pressure flow rate, S_p is flow rate at standard temperature and pressure, Z is compressibility factor, MW is molecular weight of gas and R is universal gas constant. Typical values of these constants are given in Table 3-1.

Table 3-1. Typical Wet Gas Pipeline Flow Parameters

Constant	Value
ρ_l	1000 kg / m^3
G	9.81 m / s^2
D_i	0.559 m
S_p	136.111 m / s^2
Z	0.83
MW	0.015 $kg / mole$
R	8.314 $J / K / mole$
Froude number, F	0.56 ($\theta > 2$ deg), 0.35 ($\theta < 2$ deg)
	0.140 + 0.28 (0.5 < θ < 2 deg)
Pipe thickness	8.33 mm

For wet gas systems with high water loading, the uncertainty in the critical angles arises not from parameter uncertainty, but from the smeared out value of hold-up angle or velocity (Figure 3-1). This distributed value of critical angles cannot be considered in terms of Equation (3-1) because there is no unique Froude number in the case of high water loading.

3.3.2 Corrosion Rate Model

The nature of corrosion growth largely depends on the presence of electrolyte such as water, concentration of species such as CO_2 , O_2 , H_2S , pH, and flow parameters such as

temperature, pressure and velocity. Here we focus on the internal region of a pipeline where the presence of widespread corrosion is prominent. Various empirical equations are available to represent the corrosion rate as a function of aforementioned parameters. Three candidate models were selected.

M₁: de Waard-Milliams (1975)

$$\text{Corrosion rate, } \frac{mm}{year} : \frac{da}{dt} = k \times C_I \times 10^{\left(5.8 - \frac{1710}{T} + 0.67 \log_{10}(pCO_2)\right)} \quad (3-2)$$

M₂: de Waard-Lotz (1993)

$$\text{Corrosion rate, } \frac{mm}{year} : \frac{da}{dt} = k \times C_I \times CF \times 10^{\left(5.8 - \frac{1710}{T} + 0.67 \log_{10}(pCO_2)\right)} \quad (3-3)$$

Where,

$$CF = \begin{cases} 10^{\left(-6.7 + \frac{2400}{T} - 0.6 \log_{10}(pCO_2)\right)}, & \frac{2400}{(6.7 + 0.6 \log_{10}(pCO_2))} < T \\ 1, & \text{otherwise} \end{cases}$$

M₃: SwRI[®] (Sridhar et al., 2001)

$$\begin{aligned} &\text{Corrosion rate, } \frac{mm}{year} : \\ \frac{da}{dt} &= k \times C_I \times 0.0254 \times \left(\begin{aligned} &8.7 + 9.86 \times 10^{-3}(O_2) - 1.48 \times 10^{-7}(O_2)^2 - 1.31(pH) + \\ &4.93 \times 10^{-2}(pCO_2)(pH_2S) - 4.82 \times 10^{-5}(pCO_2)(O_2) - \\ &2.37 \times 10^{-3}(pH_2S)(O_2) - 1.11 \times 10^{-3}(O_2)(pH) \end{aligned} \right) \end{aligned} \quad (3-4)$$

These three models are referred to as DM, DL, and SwRI, respectively. In the Equations (3-2)-(3-4), a, is the corrosion depth, t is time, T is temperature, pCO₂ partial pressure of CO₂ in the mixture, pH₂S is partial pressure of H₂S in the mixture, O₂ is the concentration of O₂ in parts per million, k is the modeling error, CI is inhibitor correction factor, and CF is the temperature correction factor.

Corrosion inhibitors can be added to the inlet of a pipeline to reduce the corrosion rate. Since the effect of inhibitor will diminish as a function of distance from the injection point, an exponential model is assumed to represent the reduction in corrosion rate with distance along pipe length. The inhibitor correction factor is represented by the following equation

$$C_I = 1 - e^{\left(-A \frac{L}{L_0}\right)} \quad (3-5)$$

where A , is the model parameter, L is the distance along the pipe length, and L_0 is the characteristic length to describe the effect of inhibitor. The effect of continuous inhibitor injection on corrosion in multiphase flow system was examined by Erickson et al. (1993). Their modeling showed that the inhibitor effectiveness in a condensate pipeline is a complex function of gas and liquid flow rate and pipeline elevation profile. However, they made a general observation that increasing condensation occurs as a function of distance away from the inlet end. Because the inhibitor does not partition to the condensed phase, the concentration of inhibitor decreases as the liquid flow increases due to condensation. The result is that the inhibitor effectiveness decreases as a function of distance away from the inlet end. The decay distance is a function of condensation and gas flow rates.

3.4 Probabilistic Model

3.4.1 Corrosion Damage

The probability of corrosion damage at a specific location is the probability of corrosion depth exceeding a critical value times the probability that water is present at that location. The likelihood of water formation at a location is given by

$$P_w = P(\theta \geq \alpha) \quad (3-6)$$

where θ is inclination at a particular location. Figure 3-2 illustrates that there will always be some probability that the inclination angle will exceed the critical angle. The uncertain inclination angle arises from uncertainties in mapping measurements, cover depth and axial location (discussed later in the paper). The uncertain critical angle arises from uncertainties in the flow velocity, pressure, temperature and pipe diameter.

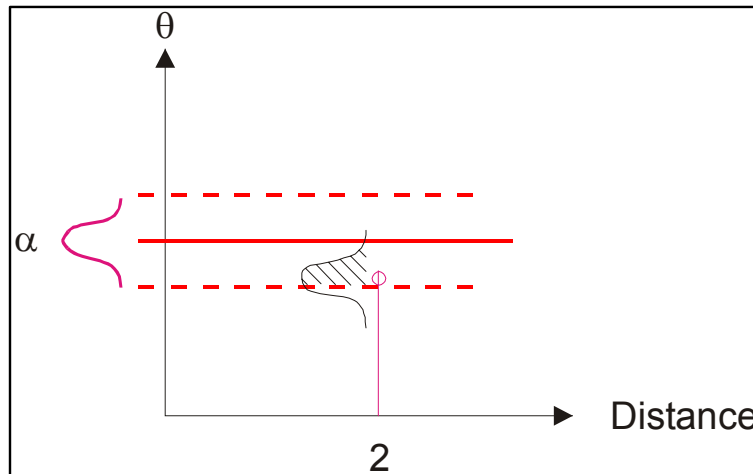


Figure 3-2. Uncertainty in inclination and critical angle.

The corrosion probability at a location is calculated by using three candidate models

$$P_{cr} = P(a_{M1} \geq a_c)W_1 + P(a_{M2} \geq a_c)W_2 + P(a_{M3} \geq a_c)W_3 \quad (3-7)$$

where a_c is the critical corrosion depth, a_{Mi} is the corrosion depth predicted by i^{th} model, W_i is the weight factor for the i^{th} model, and $P(a_{Mi} \geq a_c)$ is the probability of exceeding the critical corrosion depth for the i^{th} model. For oil and gas lines the critical corrosion depth has been assumed to be 80% of wall thickness (Caleyo et al. 2002, Vinod et al. 2003).

The total corrosion probability at a location given that water is present at that location is given by

$$P_{tot} = P_w P_{cr} \quad (3-8)$$

3.5 Input Uncertainties

Safety measures such as inspections and repairs are scheduled to reduce the chance of leaks and structural failure in face of uncertainties. These uncertainties include parameters affecting, for example, corrosion growth, water flow and elevation data. These uncertainties should be accounted for by assessing the extent of corrosion damage at given location along pipe length and scheduling excavation and repairs. Probabilistic analysis can be used to account for randomness in these parameters. Table 3-2 presents random variables and their associated probability distributions for a demonstrative pipeline scenario.

Table 3-2. Typical Wet Gas Pipeline Corrosion Growth Parameters

Random Variable (units)	Distribution Type	Mean	Standard deviation
T (degree K)	Normal	289	28.9
% CO ₂ (mole)	Lognormal	5	1
O ₂ (ppm)	Lognormal	5000	1500
PH	Lognormal	6	1
% H ₂ S (mole)	Lognormal	0.05	0.005
P, (Pascal)	Lognormal	4080000	808000
k , Corrosion Model error	Lognormal	1.0	0.5
A , Inhibitor factor	Lognormal	1.0	0.5

3.6 Mapping Uncertainty

The uncertainty in pipeline inclination data occurs because of inaccuracies in elevation data present in digital maps and uncertainties in pipeline burial depth. The mapping inaccuracies are location specific and there is substantial evidence to suggest that it is positively

correlated to the ruggedness of terrain (Riley et al. 1998, Sakude et al., Holmes et al. 2000 and Tang et al. 2002, Weng 2002). A linear equation between the terrain ruggedness index (TRI) and the accuracy in elevation can be obtained by a regression analysis on data from Tang (2002). Weng (2002) used the USGS database to obtain the maximum error of 11 meters and minimum error of three meters in the elevation data obtained from digital maps. The elevation data is used to calculate the terrain ruggedness index (this is the root mean square error between the elevation at a location and eight neighboring locations (Riley et al., 1998) for each location along the pipe. The regression equation developed above was used to obtain an estimate of elevation error at each location. The following equations are used:

$$TRI = \sqrt{\frac{\sum_{j=i-4}^{j=i+4} (y_i - y_j)^2}{8}} \quad (3-9)$$

$$\varepsilon_y = C_1 \times TRI + C_2 \quad (3-10)$$

where TRI is terrain ruggedness index, ε_y is the error in elevation, and C_1 and C_2 are regression constants. The error ε_y is used to calculate maximum and minimum inclination angles at these locations. We further assume that the inclination angle follows a normal distribution with a 6σ range between the maximum and minimum inclination angles (this was chosen to capture the majority of the data).

3.7 Inspection Updating

There will be uncertainty in our initial prediction because of lack of accurate information on model weights, physics considered (or neglected) in competing models, and the assumed distribution of random variables. Data collected from inspections can be used to update the reliability estimate. Bayesian updating provides a systematic method for incorporating measured data with prior information to estimate future outcome (Rajasankar et al. 2003, Simola et al. 1998 and Zhang et al. 2000). The underlying assumption in the approach taken is that the correct form of the corrosion rate model is unknown. Consequently, and as a demonstration of the methodology, three candidate models are considered. Based on inspection data, the weight factors are adjusted to reflect this additional information in the next prediction. We have used the reliability-updating model developed by Zhang (2000). We further assume that there is no uncertainty in the detection process so that the detected damage is the actual damage at a location. The event of damage detected with size a_d is expressed as

$$D_A = a_{M_i} - a_d \quad (3-11)$$

where a_{M_i} is the corrosion depth predicted by i^{th} model. The updated model weight and reliability in the event of a detected corrosion depth a_d can be expressed as

$$W_i | D_A = \frac{W_i \times \frac{\partial P_i(a_{M_i} - a_d \leq 0)}{\partial a_{M_i}} \big|_{a_{M_i}=a_d}}{\sum_{i=1}^3 W_i \times \frac{\partial P_i(a_{M_i} - a_d \leq 0)}{\partial a_{M_i}} \big|_{a_{M_i}=a_d}} \quad (3-12)$$

$$P_{Updated} = \sum_{i=1}^3 \frac{\frac{\partial P_i(a_{M_i} \geq a_c \cap a_{M_i} - a_d \leq 0)}{\partial a_{M_i}} \big|_{a_{M_i}=a_d}}{\frac{\partial P_i(a_{M_i} - a_d \leq 0)}{\partial a_{M_i}} \big|_{a_{M_i}=a_d}} \quad (3-13)$$

Note that the updating only affects the component weighting of the component models. No adjustment to the probability distribution of the component models is performed.

3.7.1 Example 1: Determination of Critical Location Prior to Inspection

A typical gas transmission pipeline was chosen for demonstrating the proposed methodology. The pipeline elevation data at 1000 locations was used to calculate the inclination angles and the associated uncertainties in them. These are actual elevation data from which company-specific geographic information has been removed. The probability of water formation is obtained from Equation 7 and the probability of corrosion damage is obtained from Equation 8 using inputs in Tables 3-1 and 3-2 after a time period of 10 years. As a first illustration, we demonstrate the methodology by calculating the corrosion probability at each of the 1,000 locations.

Figure 3-3 shows that the probability of water formation is at a maximum at location 971. Figure 3-4 shows that the probability of corrosion depth exceeding critical depth increases monotonically with pipe length. This is because the corrosion inhibitor reduces the corrosion rate in the beginning and its effectiveness diminishes with pipe length.

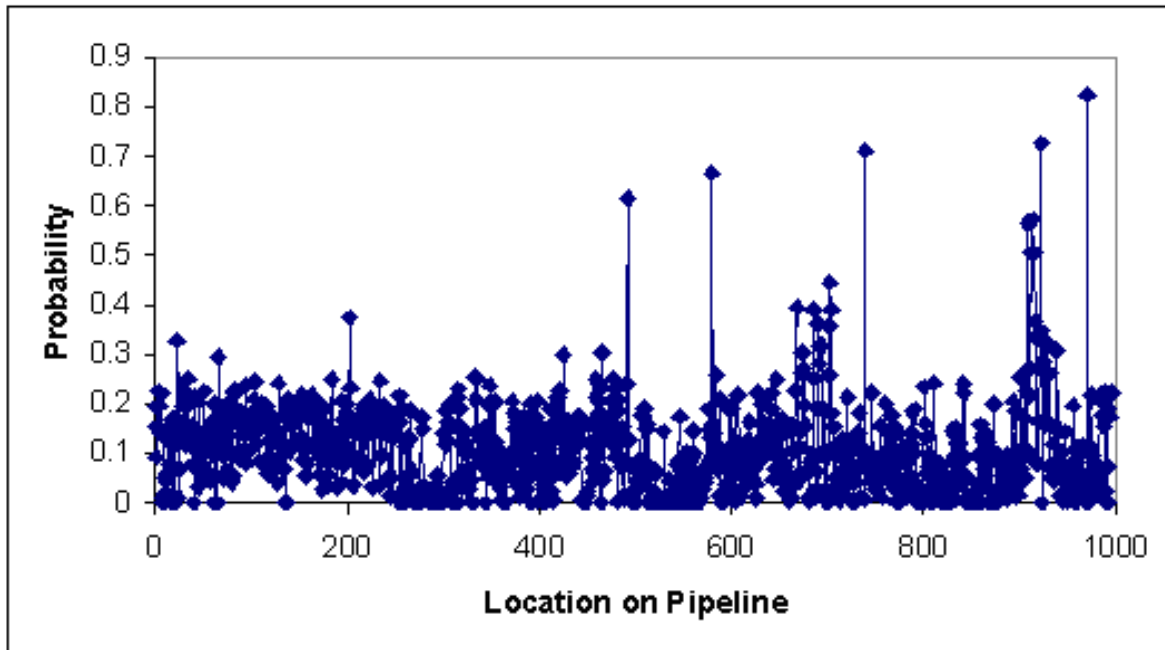


Figure 3-3. Probability of water formation along pipe length with highest probability observed at location 971.

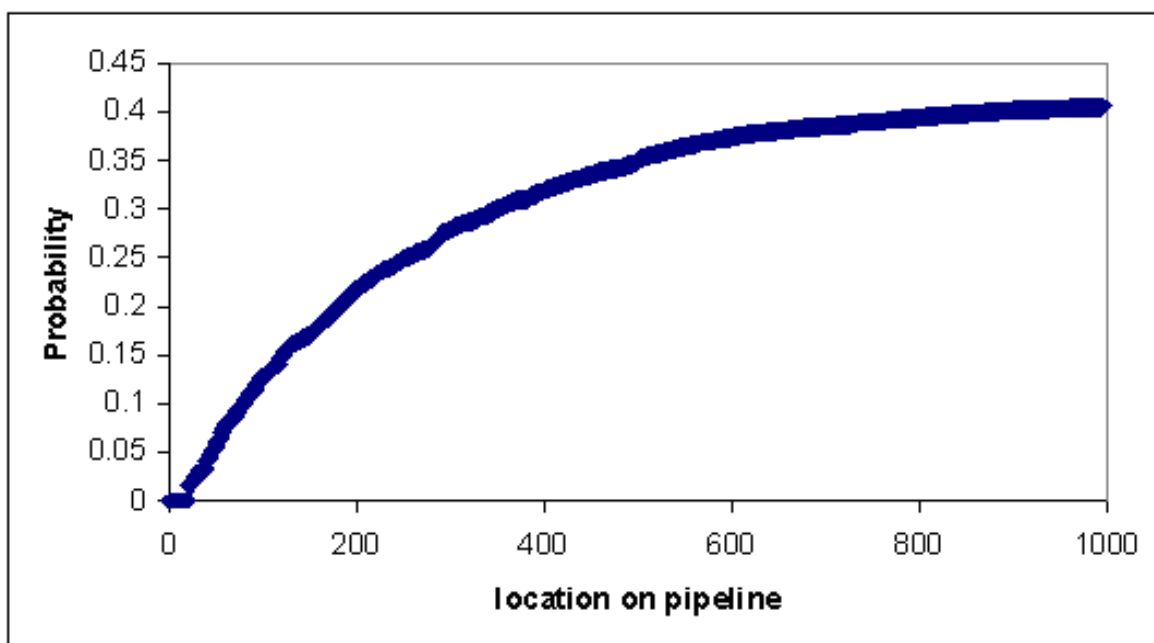


Figure 3-4. Probability of Corrosion depth exceeding critical depth along pipe length assuming water is present at all locations.

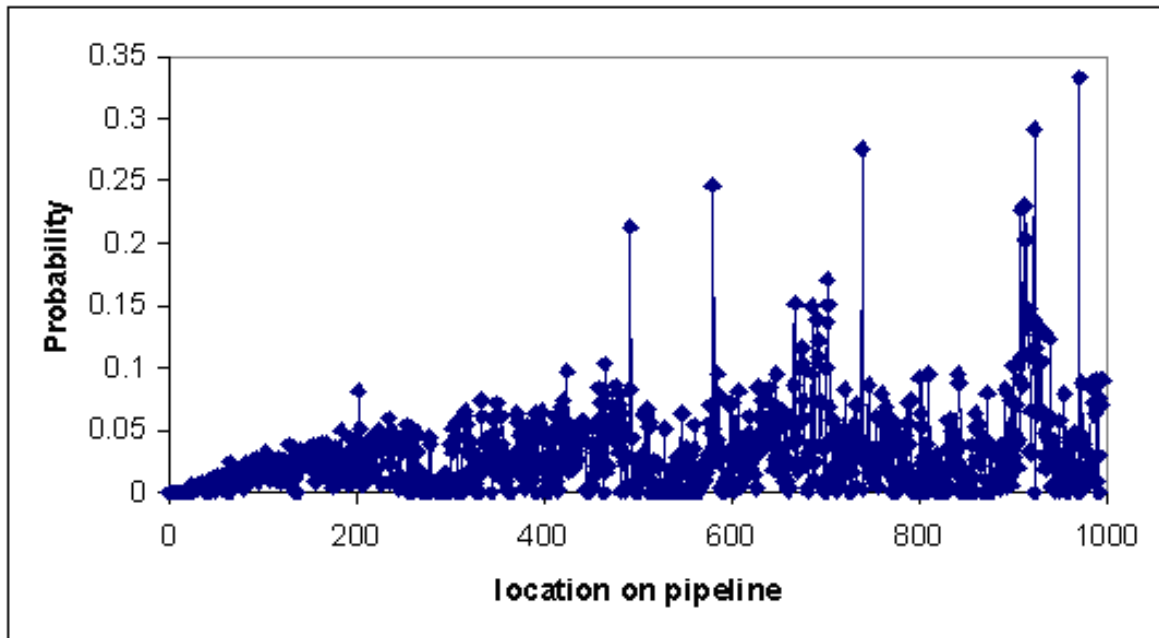


Figure 3-5. Total probability of corrosion exceeding critical depth along pipe length.

As we can see from Figure 3-5, the probability of corrosion is maximum at Location 971 (highest probability of water formation and far from the corrosion inhibitor injection). Consequently excavation and inspection is recommended at this location.

3.7.2 Example 2: Updating Corrosion Modeling with Inspection Data

In Example 1, three different corrosion models with equal model weights were used because there is no information regarding the accuracy of individual model prediction in a typical pipeline setting. The DM and DL models (derived for production systems) estimate corrosion rates that are higher than those obtained from the SwRI model. Also each model is based on different uncertain parameters. Inspections can be done to repair the damaged part of a pipeline with the data collected subsequently utilized with Bayesian analysis technique to improve reliability estimates. As more information from inspections becomes available, accuracy should improve as the most appropriate model or weighting of the three models is modified from the initial prediction.

An example of the updating process is provided in Table 3-3 to show how several observations affect the model weights.

Table 3-3. Updating of Model Weights Given Assumed Observations Corresponding to Input Component Models

Observed corrosion depth, mm	Observation derived from	Model weight W1 (DM)	Model weight W2 (DL)	Model weight W3 (SwRI)
0.05	SwRI	0.104	0.104	0.792
0.07	SwRI	0.019	0.019	0.962
0.11	SwRI	0.003	0.003	0.994
0.13	SwRI	0.0003	0.0003	0.9994
5.12	DM	0.500	0.500	0.000

The observations were made so that they corresponded to either the SwRI model (first four samples) or the DM model (last sample) at a given location. The analysis began with an equal weighting of 0.3333 for all three models. For the first four observations derived from the SwRI corrosion model, it is clear that the model weights rapidly approach 0.0 for both the DM and DL models while the SwRI goes to 1.0. The reason for this is the large disparity in the predictions between the competing models resulting from the differing intended applications for each model. The last observation corresponds to the DM model and there is no gradual transition in the weight factors. The reason for this is the probability associated with the SwRI model generating a 5.12 mm crack are exceptionally small compared to DM and DL. As such, the Bayesian updating immediately removes the SwRI model from active consideration in order to reflect the latest observation. Since the DM and DL models are equivalent for the conditions being considered, their corresponding weights each go to 0.50.

Typically pipelines are hundreds of miles long and excavating the entire length is impractical and uneconomical. Excavations can be scheduled at locations where the probability of corrosion is highest. Data obtained from each excavation can be used to update the reliability along the pipe length and to predict the next excavation location. This can continue until a specified level of reliability at each location on the pipeline is obtained. Here we assume that if corrosion is detected at a location, it is repaired or replaced such that the location becomes defect free.

Table 3-4 shows the results of a series of inspections and model updates. Only a few locations are illustrated in the table. Additionally, the method outlined below is one approach for updating. Depending on the inspection methods and procedures, other types of updating can be performed. In the illustrative example shown in Table 3-4, the following sequence of steps are performed:

- 1) Before any inspections are performed, location 971 is predicted to have the highest probability with other locations up and downstream from it having a lower probability of corrosion exceeding certain depth.
- 2) An inspection at location 971 is performed and the depth of corrosion is found to be 8.2 mm. Based on the predicted and detected corrosion depth at location 971, the

model is updated and the next location of maximum probability is predicted to be location 923.

- 3) An inspection is then performed at location 923, a defect depth of 7.5 mm is measured. This is then compared to model prediction and the model updated again. This updating then modifies the probabilities of corrosion downstream and upstream from this location.
- 4) This process is repeated at the next highest probability location until all the highest probability locations upstream and downstream from 739 are inspected. Note that as the model is updated based on inspections, the previously inspected location probabilities will change. However, since they would have been inspected already and mitigation measures adopted, the purpose of this assessment is considered to be fulfilled.

Table 3-4. Inspection Locations Along Pipeline

Location of Inspection	Detected Corrosion Depth (mm)	Maximum Updated Probability	Location of Maximum Updated Probability
971	8.2	0.7247	923
923	7.5	0.7100	739
739	5.1	0.6662	580
⋮	⋮	⋮	⋮

Note that updating procedure may be modified to suite individual pipeline needs. Furthermore, modeling and updating may be adopted such that a certain proportion of pipeline is inspected in detail and downstream from these inspections, the updated model is used for locating further examinations.

3.8 Sensitivity Analysis

The probabilistic analysis method also enables one to perform sensitivity analysis. In this case, the effect of one of the factors on the predicted outcome is examined when all other factors are held at their assumed range of values. The sensitivity analyses can be performed in terms of either the sensitivity to mean value of a parameter or to its standard deviation. In the former case, the mean value of a parameter is changed while all the distributions of the parameters are maintained constant. In the latter case, the mean values and distributions are held constant for all parameters except one. The standard deviation of the distribution of the desired parameter is then varied while keeping the mean value constant.

For example, from Equation (3-1), it is clear that gas pressure affects critical angle in terms of its effect on gas density and flow rate. The sensitivity of calculated probability of water hold up to pressure is only through the critical angle because the actual pipeline angle is not expected to be affected by gas pressure. The probability of water holdup increases with gas

pressure is shown in Figure 3-6. Also shown is the total probability of corrosion penetration, including corrosion model uncertainties. The probability of water hold-up decreases with increasing temperature (Figure 3-7). However, the probability of corrosion penetration increases with temperature because of its effect on corrosion rate. Further, the probability calculations are relatively insensitive to standard deviation in pressures (i.e. the assumed width of the distribution in pressure values), as shown in Figure 3-8. As described before, the actual pipeline angle is one of the most important parameter in determining the probability of water holdup given a range of other parameters (Figure 3-9). As the inclination angle increase beyond a certain value, the probability of holdup increases dramatically to 1. However, there is a small probability of water hold up at even small negative inclination angles (i.e. downward slope of pipeline in the direction of gas flow) because of the uncertainties associated with actual elevation angle. It should be noted that as the distribution of the pipeline angle becomes broader, the probability of water hold up decreases, as indicated by the sensitivity analysis with respect to standard deviation of pipeline angle (Figure 3-9). This is because even at high mean values of pipeline elevation, lower angles can exist due to the broad uncertainty band of elevation angles.

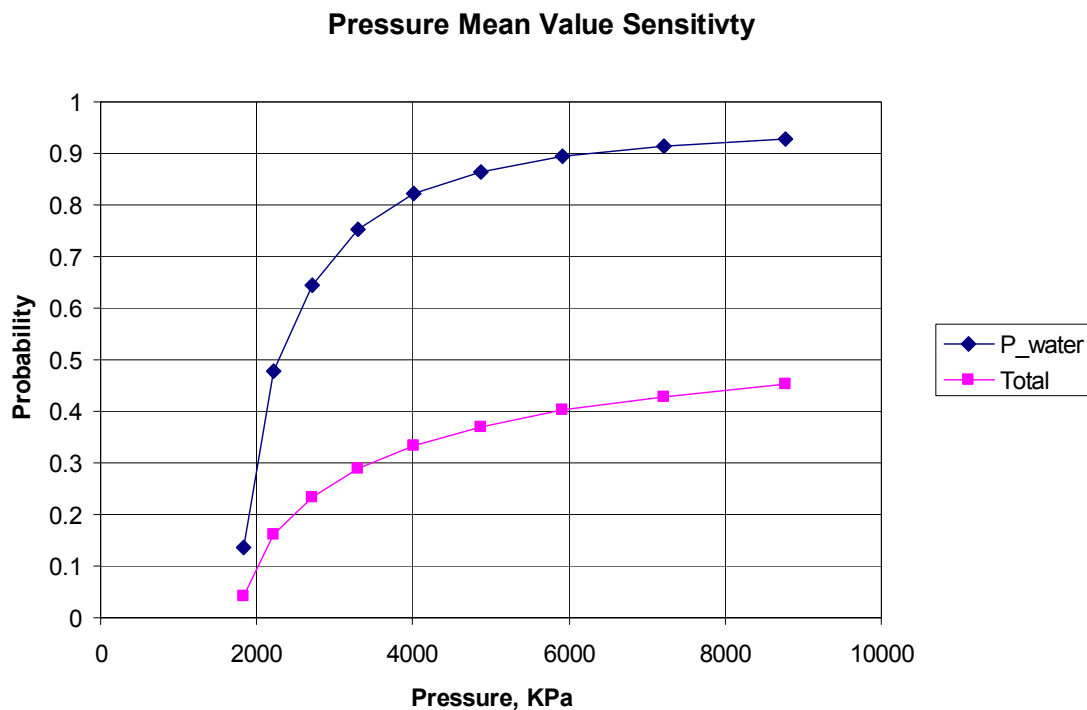


Figure 3-6. Sensitivity of the calculated probability of water hold-up given all other uncertainties in the parameters to the mean value of gas pressure.

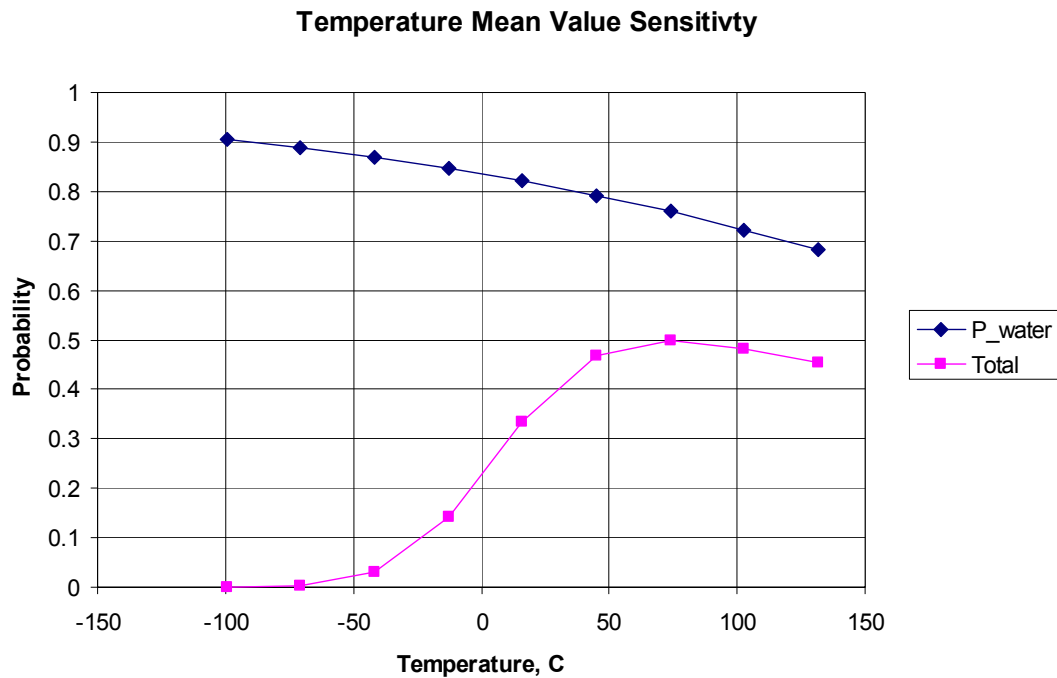


Figure 3-7. Sensitivity of the calculated probability of water hold-up given all other uncertainties in the parameters to the mean value of gas temperature.

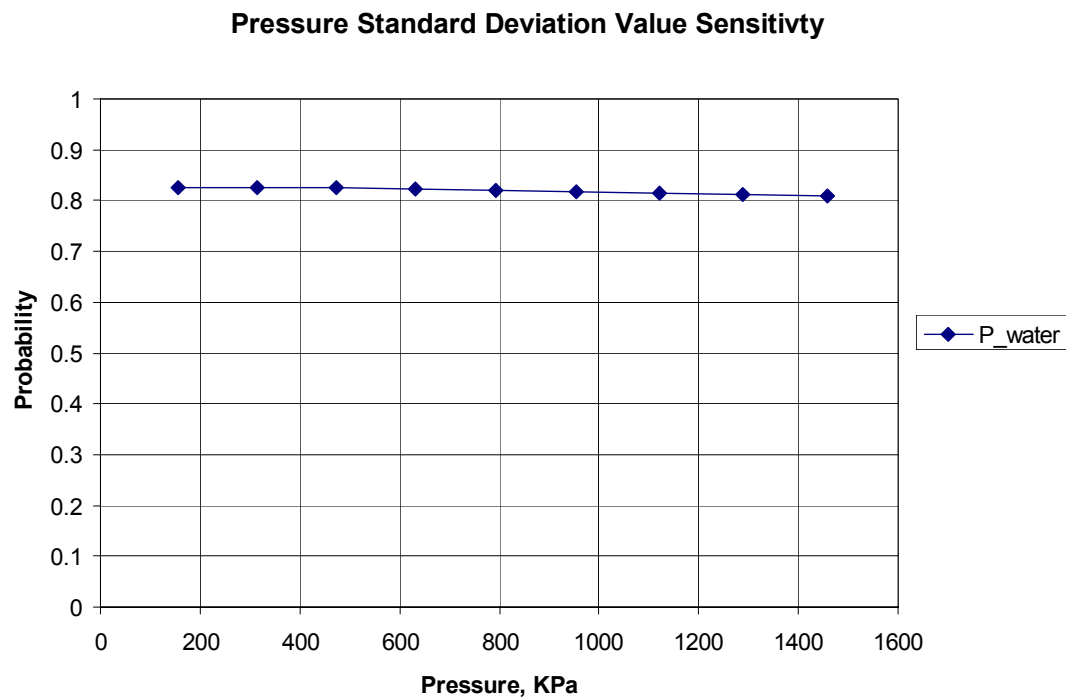


Figure 3-8. Sensitivity of calculated probability of water holdup to standard deviation in pressure (i.e., width of assumed pressure distribution) given all other uncertainties.

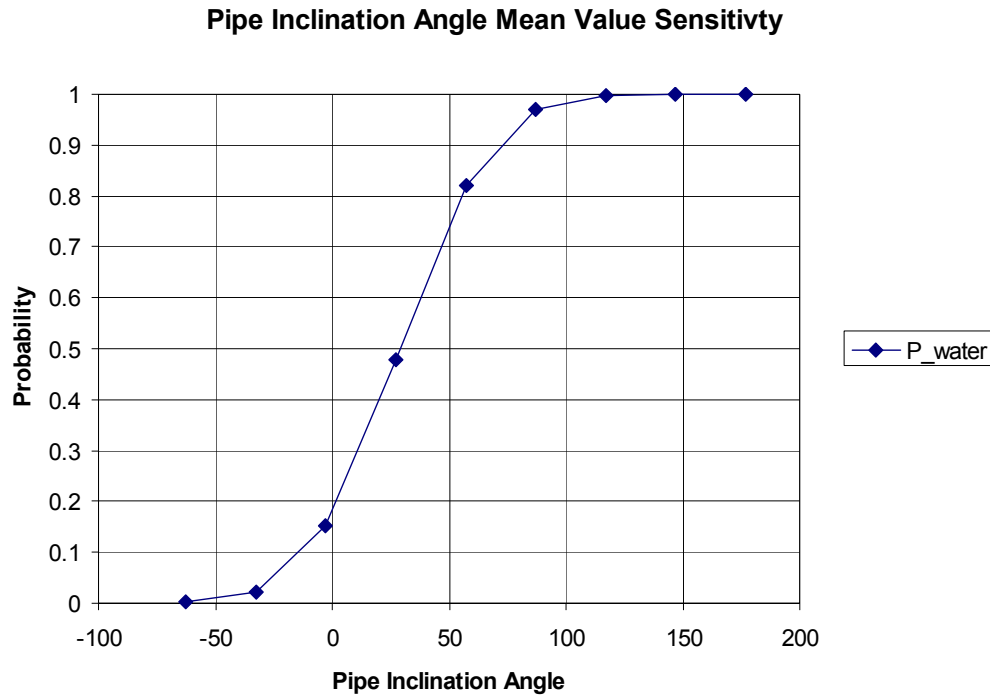


Figure 3-9. Sensitivity of the calculated probability of water hold-up given all other uncertainties in the parameters to the mean value of pipe angle.

3.9 Discussion

It must be emphasized that the probabilistic analysis of ICDA does not mean that inaccurate data can be compensated by uncertainty analysis. Rather, the probabilistic analysis recognizes that there are practical limitations to the accuracy and extent of data gathering, especially for older pipelines and provides a quantitative method for assessing the effect of these uncertainties. The probability of water holdup, combined with corrosion penetration and an updating method using detailed inspection data (Kale et al., 2004) can yield better insights into prioritizing excavation and inspection.

In conducting excavation and detailed inspection, it is often necessary to determine the location along a pipeline where detailed inspection should be performed. In a long, sloping pipeline section the water can contact the pipeline surface over a certain distance from the lowest elevation point. Therefore, it is not sufficient to examine only the lowest elevation point. Guided wave inspection can provide a method to inspect up and down stream from the sensor location. However, the maximum distance of such inspection is limited and these methods cannot at present resolve small penetrations due to pitting. Another approach is to perform detailed fluid dynamics modeling to determine how far up a pipe slope can the water be propagated by the gas.

3.9.1 Multiphase Fluid Dynamics Calculation

For this analysis, a 20" (50.8 cm) inside diameter pipe was assumed to be conforming to a rolling terrain where the elevation could be approximated by a sinusoidal description of the form shown in Figure 3-10. The slope of the terrain at the quarter period is specified as θ . For the analysis described here, an assumed rolling terrain configuration with a period of 0.5 mile (0.8 km) and a $\frac{1}{4}$ period slope of 20 degrees is used (Figure 3-10). To simplify the analysis, only the downstream half period ($\frac{1}{2} B$) is modeled. The velocity and phase stratification is specified at the $\frac{1}{2}$ period location, while a pressure outlet boundary is specified at the top of the hill or full period location. The Computational Fluid Dynamics (CFD) analysis was conducted using FLUENT 6.1, a CFD computer program. The Implicit VOF model is used both in steady and unsteady modes. The steady mode is used to calculate flow field variables for use as initial conditions in the unsteady solver. The unsteady solver is used to model the transient behavior of the water's trailing edge when it can no longer be moved up the hill by the gas. For simplicity, a 2D model is used. The fluid domain is meshed with quad fluid cells. The mesh has a vertical (across section of pipe) mesh spacing of 2" (5 cm) and a horizontal (along pipe flow direction) mesh spacing of 12" (30 cm), which results in 3,171 fluid cells. This is a rather coarse mesh, however this analysis is intended to demonstrate the methodology. The inlet velocity is specified as 57.3 ft/s (17.5 m/s) and the fraction of water is 10% and is considered completely segregated to the lower region of the pipe (i.e., the lowest 10 percent of the pipe cross-section is completely covered by water at the inlet end and the rest of the pipe cross-section is occupied by gas). The outlet pressure was held at 514.7 psia (3.55 MPa).

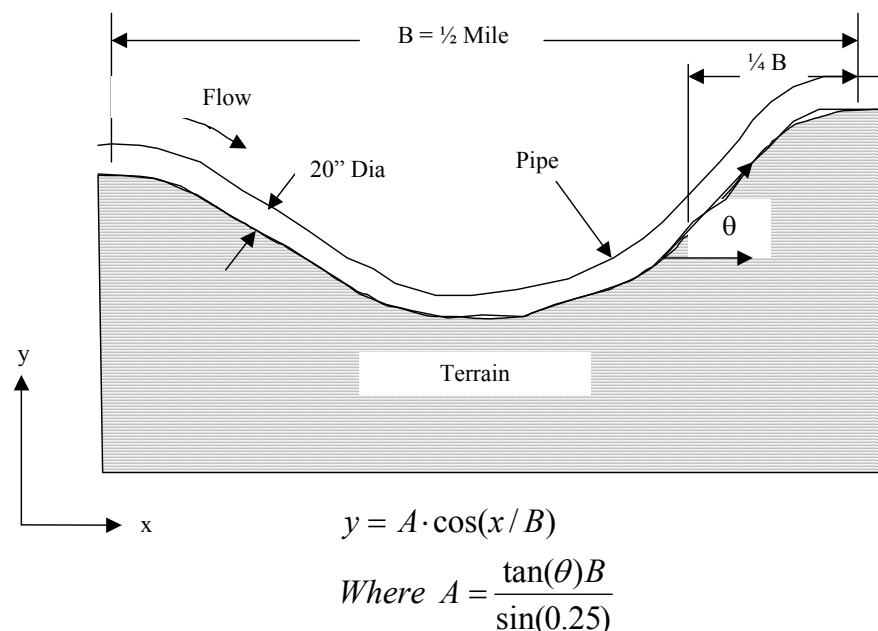


Figure 3-10. The simplified pipe segment used to perform detailed fluid dynamics calculation of water flow.

Figure 3-11 shows the liquid water phase volume fraction along the lower surface of the pipe. At the inlet, the lower surface is covered with water as expected (water volume fraction is 1). The water volume fraction only refers to the volume fraction in the lower part of the pipe section (up to 10 percent of the cross section from the bottom). It does not mean that the water fills the whole pipe section. The combined effects of the water inlet velocity and the “pushing” action of the overflowing methane transport the liquid water up the slope about 0.07 miles (43.8 m) in the horizontal direction and about 50ft (15.2 m) in the vertical direction. Then, gravity and viscous forces begin to take over and the liquid water slows down which reduces the phase concentration (0.07 – 0.1) mile. A slight resurgence of water is seen near the 0.08-mile position. This is the region of unsteady flow and can be visualized as waves lapping the beach. The flowing methane pushes the water up the hill, then viscous and gravity forces begin to dominate and the water falls back down the slope. The pushing or “blowing” action of the methane causes the liquid water depth to increase as it traverses up the slope. This in turn causes the available flow area for methane to decrease which increases the methane velocity. The increase in methane velocity enables the methane to push harder, until a point when gravity and viscous forces over rule. At that point, a gulping action takes place that further magnifies the wave action at the trailing edge of the water pool. For these specific conditions, the water was never able to make it over the hill. A slight change in inlet conditions could potentially cause this to happen, especially if the gulping action at the trailing edge of the water becomes high enough to block or nearly block the flow of methane.

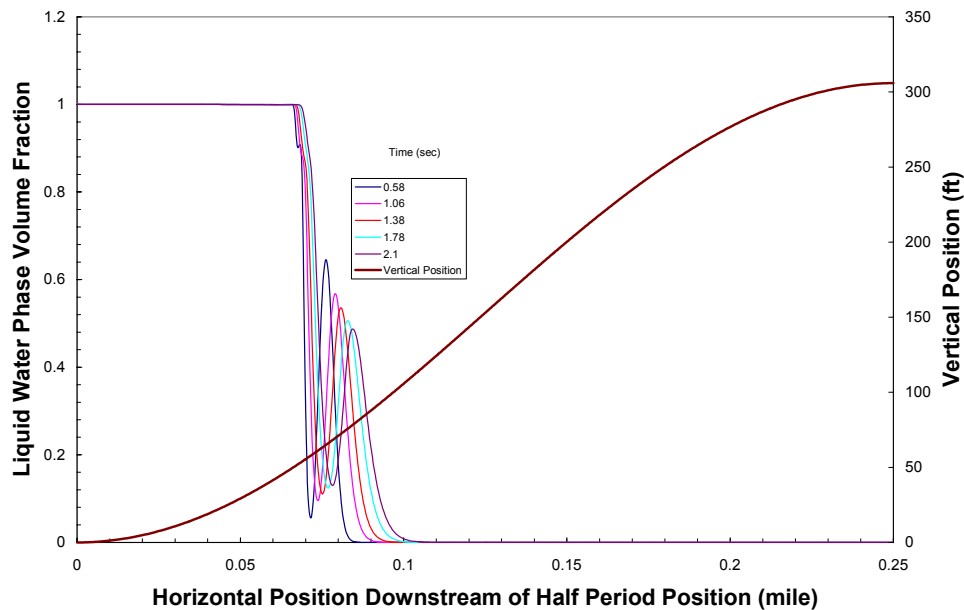


Figure 3-11. Liquid water buildup on the bottom 10 percent of pipe cross section in the upslope from the water and gas entry point indicating that water location point a significant distance from the bottom of a critical angle.

Figure 3-11 shows that detailed examination of the pipe should be performed to about 0.08 miles from the lowest point in the example indicated. It is possible that the corrosion

is most severe at the edge of this water hold up region because here the water film is thinnest and access of the gas constituents to the steel surface is the easiest.

While detailed CFD modeling indicates one approach to determining the distance along the pipe for detailed examination, this type of modeling is computationally intensive for realistic geometries and conditions. Therefore, an approach could be to perform a number of detailed calculations and derive an approximate number (for example distance in terms of pipe diameters or fraction of the slope length) for water accumulation.

4.0 CONCLUSIONS AND RECOMMENDATIONS

The results of this work confirm the validity of the dry gas ICDA approach. It was found that one important limitation for implementation of ICDA is accuracy in the elevation profile. Improvements in locating, elevation measurements, and data alignment are expected to result in greater confidence for selecting excavation locations. Recommendations for further investigations include: 1) development of appropriate procedures for pipeline elevation profile mapping with sufficient accuracy for ICDA; 2) development of an approach for precisely identifying the length of pipeline at inclinations to inspect; and 3) incorporation of probabilistic techniques in prioritizing inspection locations.

Four pipelines used in the ICDA for Dry Gas Pipeline Process Validation were studied. 85% of internal corrosion locations indicated by ILI in one pipeline were predicted by ICDA. An additional 5% of anomalies would likely have been identified if accurate elevation profiles were available (i.e., under road or stream crossings). The site of a leak was also successfully predicted by ICDA. ICDA correlated by 78% for the second pipeline. The uncertainty in flow, periods of stagnant conditions, and lack of corroboration of internal corrosion anomalies identified by ILI contributed significantly to uncertainty for identification of the locations of internal corrosion. In a third pipeline, 16 percent of ILI-indicated internal anomalies having greater than 30 percent depth of wall thickness were identified using GIS field data, while 53% of the internal anomalies were predicted using computerized USGS data. In this line, GIS survey data did not have sufficient resolution to detect many important inclinations. In addition, many of the ILI internal indications appeared to be at the top of the line, suggesting ICDA model premise may have been violated. Direct examination confirmed some of the ILI findings and highlighted some challenges in applying ICDA, as enumerated in the next paragraph. In the fourth pipeline, ICDA identified 87 percent of internal anomalies with greater than 30 percent depth of wall thickness; the site of a leak was also successfully predicted.

The validation activities also identified some of the practical difficulties in the application of ICDA. Apart from the uncertainties in elevation profiles, pipelines with a number of closely spaced input points or closely spaced locations of large elevation changes will require a large number of excavations and detailed examination. Such excavations may pose difficulties in terms of obtaining the necessary permits and the attendant costs, so that ICDA process may become impractical to implement. It must be noted that if detailed examination cannot be performed at an identified ICDA location or other methods to ascertain the presence or absence of internal corrosion cannot be implemented, the ICDA methodology cannot be fully implemented.

A preliminary methodology to predict the most probable corrosion damage location along a pipeline and update this prediction using inspection data has been developed for both dry and wet gas systems. The approach will:

1. Compute the probability of critical corrosion damage as a function of location along the pipeline using physical models for flow, corrosion rate, and inspection information as well as uncertainties in elevation data, pipeline geometry and flow characteristics. The probability of corrosion damage is computed as the probability

that the corrosion depth exceeds a critical depth given the presence of electrolytes such as water. Water is assumed to be present at locations where the pipeline inclination angle is greater than the critical angle. Three candidate corrosion rate models were employed to reduce the chance of selecting the incorrect model. Monte Carlo simulation and the first-order reliability method (FORM) implemented in a spreadsheet model were used to perform the probability integration. Bayesian updating was used to incorporate inspection information (e.g., in-line, excavation, etc.) and update the prediction of most probable damage location. This provides a systematic method for focusing costly inspections on only those locations with a high probability of damage and incorporating the results of the inspection in a manner that improves confidence in future predictions.

5.0 REFERENCES

- Ahammed M., Melchers R.E., 1995, "Probabilistic Analysis of Pipelines Subjected to Pitting Corrosion Leaks" *Engineering Structures*, **17**, (2).
- Ahammed M., Melcher R.E., 1997, "Probabilistic Analysis of Underground Pipelines Subjected to Combined Stresses and Corrosion" *Engineering Structures*, **19**, (12), 988-994.
- Ahammed M., 1998, "Probabilistic Estimation of Remaining Life of a Pipeline in the Presence of Active Corrosion Defects" *International Journal of Pressure Vessel and Piping* **75**, 321-329.
- Caleyo F., Gonzalez J.L., Hallen J.M., 2002, "A Study on the Reliability Assessment Methodology for Pipelines with Active Corrosion Defects" *International Journal of Pressure Vessels and Piping*, **79**, pp 77-86.
- de Waard, C. and Milliams, D.E., 1975, *Corrosion*, **31**, (5), 177-181.
- de Waard, C. and Lotz, U., 1993, "Prediction of CO₂ Corrosion of Carbon Steel" Corrosion/93, Paper 69, NACE International, Houston, TX.
- Doughtery, J., 1987, "Parameters Relating Corrosion Inhibitor Treatment Methods and Treatment Life Times," Corrosion/87, Paper 40, NACE International, Houston, TX.
- Erickson, D., Buck, E., and Kolts, J., 1993, "Corrosion Inhibitor Transport in a Wet-Gas Pipeline," Materials Performance, NACE International, September, Houston, TX.
- Erikson, D., Bucke, E., and Kolts, J., 1993, "Corrosion Inhibitor Transport in a Wet-gas Pipeline," Materials Performance, **32**, (9), 49.
- Gartland P.O., Johnsen, R., Ovstetun, I., 2003, "Application of Internal Corrosion Modeling in the Risk Assessment of Pipelines" Proc. Corrosion 2003, March 16–20, San Diego, CA.
- Holmes, K.W., Chadwick, O.A., Kyriakidis, P.C., 2000, "Error in USGS 30 – Meter Digital Elevation Model and Its Impact on Terrain Modeling" *Journal of Hydrology*, 154-173.
- Hong, H.P., 1999, "Inspection and Maintenance Planning of Pipeline under External Corrosion Considering Generation of New Defects" *Structural Safety*, **21**, 203-222.
- Kale, A., Thacker, B.H., Sridhard, N. and Waldhart, C., 2004, "A Probabilistic Model for Internal Corrosion of Gas Pipelines," IPC04-0483, ASME, International Pipeline Conference, Calgary, Canada.
- Lotz, U., van Bodegom, L., and Ouwehand, C., 1990, "The Effect of Oil or Gas Condensate on Carbonic Acid Corrosion," Paper 41, CORROSION/90, NACE International, Houston, TX.

- Mauney, D., Moghissi, O., and Sridhar, N., 2001, "Internal Corrosion Risk Assessment and Management of Steel Pipelines," PRCI Project PR 15-9808, Pipeline Research Council International, Houston, TX.
- Méndez, C., Duplat, S., Hernández, S., and Vera, J.R., 2001, "On the Mechanism of Corrosion Inhibition by Crude Oil," Paper 01030, CORROSION/2001, NACE International, Houston, TX.
- Moghissi, O.C., Norris, L., Dusek, P., Cookingham, B., and Sridhar, N., 2002a, "Internal Corrosion Direct Assessment of Gas Transmission Pipelines - Methodology," GTI Final Report #GRI-02/0057, Gas Technology Institute, Des Plaines, IL.
- Moghissi, O.C., Norris, L., Dusek, P., and Cookingham, B., 2002b, "Internal Corrosion Direct Assessment of Gas Transmission Pipelines," CORROSION/2002, Paper 02087, NACE International, Houston, TX.
- Moghissi, O.C., Perry, L., Cookingham, B., and Sridhar, N., 2003, "Internal Corrosion Direct Assessment of Gas Transmission Pipelines – Application," CORROSION/2003, Paper 03204, NACE International, Houston, TX.
- Muhlbauer, W.K., 1996, "Pipeline Risk Management Manual," 2nd Ed., Gulf Publishing Co., Houston, TX.
- NACE International, "Internal Corrosion Direct Assessment (ICDA) Methodology for Pipelines Carrying Normally Dry Natural Gas," TG 293 Draft NACE Standard, NACE International, Houston, TX (Expected to be Published in 2005).
- NACE International, Standard RP0502, "Pipeline External Corrosion Direct Assessment Methodology" Houston, TX, NACE, 2003.
- NMAS, United States National Map Accuracy Standards, U.S. Bureau of Budget, 1947.
- Rajasankar J., Iyer N.R., AppaRao, T.V.S.R., 2003, "Structural Integrity Assessment of Offshore Tubular Joints Based on Reliability Analysis," *International Journal of Fatigue*, **25**, 609-619.
- Riley, S.J., DeGloria, S.D., Elliot, R., 1999, "A Terrain Ruggedness Index that Quantifies Topographic Heterogeneity," *Intermountain Journal of Sciences*, **5**, 23-27.
- Sakude M.T., Schiavone, G., Morelos-Borja, H., Martin, G., and Cortes. A., "Recent Advances on Terrain Database Correlation Testing" Institute for Simulation and Training, University of Central Florida, Orlando FL, USA
- Shea, R., Rasmussen, J., Hedne, P., and Malnes, D., 1997, "Holdup Predictions for Wet-gas Pipelines Compared," *Oil & Gas Journal*, May 19.
- Simola K., and Pulkkinen, U., 1998, "Models for Non-destructive Inspection Data," *Reliability Engineering and Systems Safety*, **60**, 1-12.

- Sridhar, N., Thacker, B., Burwell, D., and Moghissi, O., 2004, "Internal Corrosion Direct Assessment Of Dry Gas Pipelines – Validation," May 14 SwRI Report 18.06484-30.
- Sridhar, N., Dunn, D.S., Anderko, A.M., Lencka, M.M., and Schutt, H.U., 2001, "Effect of Water and Gas Composition on the Internal Corrosion of Gas Pipelines-Modeling and Experimental Studies," *Corrosion*, **57**, (3).
- Taitel, Y., Dukler, A.E., 1976, "A Model for Predicting Flow Regime Transitions in Horizontal and Near Horizontal Gas-Liquid Flow," *AIChE Journal*, **22**, (1), 47.
- Tang G., Wenzhong, S., Mudan, Z., Zhang Y., "Modeling Slope Uncertainty Derived From DEMs: A Case Study in China Loess Plateau Area," National Nature Science Foundation of China, No. 49971065.
- Thacker, B.H., Popelar, C.F., and McClung, R.C., 1992, "A New Probabilistic Method for Predicting the Long Life Reliability of Pipelines," Proc. Int. Conf. on Pipeline Reliability, R.W. Revie and K.C. Wang (eds.), Calgary, Alberta, Canada.
- U.S. Department of Transportation, U.S. Code of Federal Regulations, 49 CFR Part 192, Pipeline Safety: Pipeline Integrity Management in High Consequence Areas (Gas Transmission Pipelines), 2004.
- van Bodegom, L., Van Gelder, K., Paksa, M.K.F., and van Raam, L., 1987, "Effect of Glycol and Methanol on CO₂ Corrosion of Carbon Steel," Paper 55, CORROSION/87, NACE International, Houston, TX.
- Vinod, G., Bidhar, S.K., Kushwaha, H.S., Verma, A.K., and Srividya, A., 2003, "A Comprehensive Framework for Evaluation of Piping Reliability Due to Erosion-Corrosion for Risk-informed In-service Inspection," *Reliability Engineering and Systems Safety*, **82**, 187-193.
- Weng, 2002, "Quantifying Uncertainty of Digital Elevation Models Derived from Topographic Maps," Department of Geography, Geology and Anthropology, Indiana State University, Terre Haute, Indiana – USA.
- Zhang, R., Mahadevan, S., 2000, "Model Uncertainty and Bayesian Updating in Reliability-based Inspection," *Structural Safety*, **22**, 145-160.*